Extensions and applications of the Virtual Reference Feedback Tuning

José David Rojas Fernández

PhD Thesis

Directed by
Ramón Vilanova Arbós, PhD

Departament de Telecomunicació i Enginyeria de Sistemes
Escola d'Enginyeria
Universitat Autònoma de Barcelona

2011

Abstract

In this work the data-driven control technique "Virtual Reference Feedback Tuning" is treated in different ways. In one hand, the capabilities of the method are extended with several proposed variations that allow a wider use of the method. An alternative two degrees of freedom control topology is considered, as well as its application to proportional-integral control. The multiple-inputs multiple-outputs case is also tackled, adding an automatic pairing selection between outputs and manipulated variables. The method is applied to the Internal Model Control topology in order to proposed a robust stability test based entirely on data.

All these extensions were applied to three important cases. In first place, the control of wastewater treatment plants is considered. The control objective in this case is to maintain the effluent of the plant with a low concentration of pollutants while trying to consume as less energy as possible. Both the multiple-inputs multiple-outputs and the decentralized case are used, yielding good results for this complex system. Second, the pairing selection is applied to a solid-oxide fuel cell plant. The output voltage and the oxygen excess is controlled by manipulating the fuel and the air flow rates. Finally the two degrees of freedom controllers are applied to a pH neutralization plant by controlling the acid flow rate.

Dr. **Ramón Vilanova i Arbós**, professor at Universitat Autònoma de Barcelona,

CERTIFIES

That the doctoral thesis entitled "**Extensions and applications of the Virtual Reference Feedback Tuning**" by José David Rojas Fernández, presented in partial fulfillment of the requirements for the degree of PhD, has been developed and written under his supervision.

Dr. Ramón Vilanova i Arbós

Bellaterra, July 2011

Contents

List of Figures

List of Tables

Acknowledgments

First, I want to thank my advisor, doctor Ramón Vilanova, for all the help and support along the development of this work, for the trust and the opportunity to participate on this project. Also, the financial support from Universitat Autònoma de Barcelona is acknowledged.

I also want to thank doctor Ulf Jeppsson and doctor Xavier Flores-Alsina for all the support and friendship they gave me during my time in Lund University in Sweden. The Simulink files of the BSM1 are acknowledged to the Division of Industrial Electrical Engineering and Automation at Lund University.

Even with this long distance, I have always counted with my friends in Costa Rica: Octavio Cruz, Marta Garro, Nathalia Martínez, Cristian Artavia, Chi-Lin Chen, Rodolfo Brenes, Josaha Chavarría, Miguel Aguilera, Alberto Salazar and Juan Morán. Thank you guys.

It has been four years now living in Spain. Sometimes it has been hard, but I'm happy to say that I have met people that have made it easier. I want to thank Adriana Ramírez, Catya Zúñiga, Rosa Herrero, Alejandra Ruvalcaba and Héctor Delgado for all the help, friendship and support I have received from them. Thank you for sharing this time with me.

Being here would have been impossible without my family. I know it has been hard for them, but I want to let them known that this thesis is for them. Thank you Ma, Pa, Ale, Luis, *abuelitos*, aunts, uncles and cousins.

And a really special mention goes for my beloved girlfriend Carolina Calvo. She has been always by my side, supporting me, giving me all her love. I don't know what would I have done without her. This thesis is yours.

Nomenclature

1DoF: One degree of freedom (controller)

2DoF: Two degrees of freedom (controller)

AE: Aeration Energy

ASM1: Activated Sludge Model 1

ASP: Activated Sludge Process

BOD: Biochemical Oxygen Demand

BSM1: Benchmark Simulation Model 1

CbT: Correlation based Tuning

COD: Chemical Oxygen Demand

CSTR: Continuous stirred-tank reactor

EC: Consumption of external carbon source

EQI: Effluent Quality Index

ETFE: Empirical Transfer Function Estimate

FRIT: Fictitious Reference Iterative Tuning

IAE: Integral of the Absolute Error

IEEE: Institute of Electrical and Electronics Engineers

IFT: Iterative Feedback Tuning

IMC: Internal Model Control

I/O data: Input-Output data

ISE: Integral of the Squared Error

K_La: Oxygen transfer coefficient

LTI: Linear Time Invariant

ME: Mixing Energy

MIMO: Multiple-Inputs Multiple-Outputs

MPC: Model Predictive Control

***M(z)*:** Complementary sensitivity function

OCI: Operational Cost Index

OE: Output Error (method)

PE: Pumping Energy

PID: Proportional-Integral-Derivative

PRBS: Pseudo Random Binary Signal

S_{NH}: Ammonia concentration

S_{NO}: Nitrate and nitrite concentration

S_O: Oxygen concentration

SOFC: Solid Oxide Fuel Cell

***S(z)*:** Sensitivity function

SP: Sludge Production to be disposed

TV: Total Variation

TITO: Two Inputs Two Outputs

VRFT: Virtual Reference Feedback Tuning

WWTP: Wastewater Treatment Plant

1. Introduction

1.1. Motivation

The motto of the IEEE Control System Society cannot be clearer: "Control Systems are ubiquitous". Industrial processes, transportation, medical application, even our own body is full of robust control loops that keep life going on. Maybe, control theory is one of the fields with more possible areas of application.

In the last century, technology and human development have grown in a pace not seen before. Certainly, control theory has helped to it and at the same time, has been adapting to the changes. Now, we humans, are reaching a point of no return, since our development is provoking catastrophic changes in the world. It is our turn to reverse the situation to a more sustainable state. And is just here where control theory can help. In this thesis, special attention is given to the control of wastewater treatment plants. This kind of process is complex and hard to control. Its performance is highly dependent on the correct control algorithm applied. One of the motivation for this work is to use an easy method to find this control.

That is the main reason why data-driven control was chosen as the control paradigm. Data driven control is a new trend in control theory where, using only data from the same plant, it is possible to directly find the right parameters of the controller in order to achieve certain desired behavior. Data-driven control methods allows the user to directly use data to transform the information of the plant into controllers. No modeling step is needed, only a set of data from the plant is enough to compute the controllers' parameters.

There are several data-driven methods in the literature. The basic characteristic that they share in common is that the parameters are found by solving an optimization problem. Depending on the performance index chosen, the problem can be solved using standard quadratic programming or using Newton-like techniques. Therefore, finding controllers for dynamical system reduce to solve an optimization with widely-available tools.

Another aspect of these new techniques is that a deep-knowledge of the plant is not necessary. The engineer can jump from pure data to controllers in a faster way. It does not mean that the engineer can blindly find the required controllers because any good control engineer will always have to understand the plant he or she is trying to control. This is something that cannot be skipped, but can be performed swiftly using data-driven techniques.

Along with waste management, energy sources are other important issue that has to be solved. In this sense, in this thesis the same algorithm is applied to the control of a solid oxide fuel cell, which produces electric energy from fuel without a combustion process, with just a reduced amount of CO_2 emissions to the atmosphere. Also, the method was further applied

in a pH neutralization process. It is known that this pH process is nonlinear and that its dynamics highly depends on the point in the titration curve of the process. But good results where obtained using data-driven control, showing the applicability of this new method on real-life problems.

Therefore the objective of this thesis is to extend the capabilities of data-driven control in order to apply them in these important problems. Today is the day, when humankind starts to fully realize the need to find real solution to pollution and energy production problems, and control theory is one of the tools that can help to solve them.

One of the anonymous reviewers of the papers derived from this thesis said: "*Be able of design a controller without the need of a controlled process model, with only open or closed-loop field test data, has been part of the wishes list of all control engineers*". The contribution of this thesis is to take those control engineers one step closer to fulfill this wish.

1.2. Contributions

The contribution of this thesis is twofold. In first place, *several extensions* to the Virtual Reference Feedback Tuning, a popular data-driven method, are proposed in order to use the virtual reference idea with different control topologies. Therefore, extending its possibilities of application. In the other hand, *three different applications* are presented where the suitability of the method is tested with good results.

This thesis has derived to the following papers:

- Conference Papers
  - J.D. Rojas and R. Vilanova. Model Driven Conceived / Data Driven Tuned Control Systems. *MATHMOD Vienna 09*. Vienna University of Technology. February 11-13, 2009.
  - J.D. Rojas and R. Vilanova. FeedForward based Two Degrees of Freedom formulation of the Virtual Reference Feedback Tuning approach. *European Control Conference 2009*. Budapest, Hungary. 23-26 August, 2009.
  - J.D. Rojas, and R. Vilanova, Guidelines for controller structure in the Two Degrees of Freedom VRFT framework based on a Correlation Test, *Emerging Technologies and Factory Automation, 2009. ETFA 2009. IEEE Conference on* pp.1-8, 22-25 Sept. 2009. Palma de Mallorca, Spain.
  - J.D. Rojas, F. Tadeo and R. Vilanova, Control of a pH neutralization plant using the VRFT framework. *Control Applications (CCA), 2010 IEEE International Conference on* , pp.926-931, 8-10 Sept. 2010. Yokohama, Japan.
  - J.D. Rojas, R. Vilanova and V.M. Alfaro, Application of the virtual reference feedback tuning on wastewater treatment plants: A simulation study, *Emerging Technologies and Factory Automation (ETFA), 2010 IEEE Conference on*, pp.1-8, 13-16 Sept. 2010. Bilbao, Spain.

  - J.D. Rojas, V.M. Alfaro and R. Vilanova, Control of an Activated Sludge Process using the Virtual Reference Approach. *International MultiConference of Engineers and Computer Scientists (IMECS) 2011*, pp. 902-907, 16-18 March 2011. Hong Kong.
  - J.D. Rojas, J.A. Baeza and R. Vilanova, Effect of the controller tuning on the performance of the BSM1 using a data driven approach, *Watermatex 2011*, June 20-22, San Sebastián, Spain.
  - J.D. Rojas, J.A. Baeza and R. Vilanova, Three degrees of freedom Virtual Reference Feedback Tuning design and its application to wastewater treatment plant control, *18th World Congress of the International Federation of Automatic Control*, August 28 - September 2, 2011. Milano, Italy.
  - J.D. Rojas and R. Vilanova, Internal Model Controller tuning using the Virtual Reference Approach with Robust Stability, *18th World Congress of the International Federation of Automatic Control*, August 28 - September 2, 2011. Milano, Italy.
  - J.D. Rojas and R. Vilanova, Controlling a Solid Oxide Fuel Cell using a multivariable data driven approach. *IV Seminar on Advanced Industrial Control Applications, SAICA, Escola Industrial, Barcelona Spain. November, 7-8, 2011.*

- Journal Papers
  - R. Vilanova, J.D. Rojas and V.M. Alfaro, Digital Control of a Waste Water Treatment Plant, *International Journal of Computers Communications & Control*, ISSN 1841-9836, 6(2):367-374, 2011.
  - J.D. Rojas and R. Vilanova, Data-Driven based IMC control. *International Journal of Innovative Computing, Information and Control*, 8(2) *In press*. 2012.
  - J.D. Rojas, X. Flores-Alsina, U. Jeppsson and R. Vilanova, Application of multivariate virtual reference feedback tuning for wastewater treatment plant control. *Submitted to Control Engineering Practice*.

- Book chapters
  - J.D. Rojas, V.M. Alfaro and R. Vilanova. Virtual Reference Approach applied to the control of an activated sludge wastewater treatment plant. *Submitted to the book Intelligent Control and Innovative Computing, Springer*.

1.3. Outline

The manuscript is divided in two parts. The first one is related with the extensions proposed to the VRFT. In chapter 2, an introduction to several data-driven control techniques is presented. In chapter 3 the contribution to the two degrees of freedom controllers are proposed: first an alternative structure which allows to completely separate the design and the response of the reference tracking and the disturbance rejection is adapted to the VRFT and compared with

traditional two degrees of freedom structures. Second, it was also found that, when using a PI controller with a two degrees of freedom structure, it was necessary to add a constraint in the optimization to guarantee a free steady-state error. The derivation of this constraint is presented in section 3.2. Finally, in section 3.3, an extra degree of freedom is added to the design by a feedforward controller, computed in conjunction with the two degrees of freedom case.

Chapter 4 contains the contribution to other advanced control structures. In section 4.1, some remarks about the parameterization and a reformulation of the performance criterion to take into account a weighting in the control effort is presented. The case of the multiple-input multiple-output strategy is presented in section 4.2. In this case, not only the controllers are tuned with a decoupling strategy, but also, in the decentralized case, the pairing selection of the input-output loops is chosen automatically within the optimization. An interesting approach to the tuning of model-free Internal Model Control (IMC) is presented in section 4.3. Taking advantage of the well-known robustness characteristics of IMC, a test is proposed to check the viability of the controllers once they have been computed.

The second part of the thesis presents three interesting cases where these extensions have been successfully applied. The first one is the application to a wastewater treatment plant. Using the world-wide known Benchmark Simulation Model 1, the VRFT is used in different scenarios and control configurations in chapter 5. A special preprocessing step is proposed and the performance of the controlled plant is issued.

In chapter 6 the MIMO approach is employed in a Solid Oxide Fuel Cell. In chapter 7, the VRFT is used in a pH neutralization process and tested in a bench plant, using real data and on-line control.

Part I.

Contribution to the Virtual Reference Feedback Tuning control method

2. Data-driven control: a new trend in control theory

In this introductory chapter, several Data-Based Control Approaches will be surveyed. Generally speaking, the control methodologies could be divided in two:

- Model-Based Control
- Data-Driven Control (or Data Based)

Model-Based Control refers to the methodologies which use information from the plant in the form of a model. For example, the classical tuning rules, may need a specific model of the plant in order to solve some optimization problem (Like minimizing an integral criteria or so). Also,the model could be used directly in the control law (many of them converges to the inversion of the minimum phase part of the model). The classical example of this kind of methodology is the Internal Model Control (IMC) (Morari and Zafirou, 1989)

On the other hand, *Data-Driven Control* never attempts to find the model of the plant: it uses the data of the plant directly to find a controller, which, generally, is meant to minimize some control performance criterion. In this work, the last methodology is the one that will be used. Firstly, an overview of some important examples of this approach are given.

Some of the most remarkable Data-Driven Methods are presented in this chapter, for instance, the Iterative Feedback Tuning (Hjalmarsson et al., 1998), the Correlation based Tuning (Karimi et al., 2007) the Virtual Reference Feedback Tuning (Campi et al., 2002) and the Fictitious Reference Feedback Tuning (Kaneko et al., 2005).

2.1. Iterative Feedback Tuning

Iterative Feedback Tuning (IFT) was born in the nineties as the result of joining the identification and the control problem for restricted complexity controllers. As its name suggests, the tuning of the parameters of the controllers is carried out by a series of iterations. In this case, each iteration attempts to minimize a certain control criterion, but each new iteration depends on the result of the last iteration, in order to improve the performance of the system. This overview is based on Hjalmarsson et al. (1998), Gevers (2002) and Lequin et al. (2003).

The method directly uses closed-loop data in order to improve the performance of the system. According to Gevers (2002), if the system is given as in fig. 2.1, where

- $C_r(z;\rho)$ and $C_y(z;\rho)$ are the parametrized reference and feedback controllers respec-

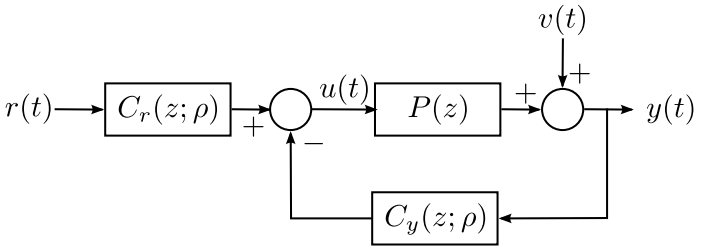

Figure 2.1: System structure for IFT.

tively, with parameters ρ.

- $P(z)$ is the unknown Linear Time Invariant (LTI) plant.

Then, the error between the desired and the achieved closed-loop response is given by

$$e(t) = \left(\frac{C_r(z;\rho)P(z)}{1 + C_y(z;\rho)P(z)} - T_d(z) \right) r(t) + \frac{1}{1 + C_y(z;\rho)P(z)} v(t) \tag{2.1}$$

Where $T_d(z)$ is the desired input-to-output Transfer Function.

Based on this expression, the performance criterion can be set as

$$J(\rho) = \frac{1}{2N} \mathrm{E} \left[\sum_{t=1}^{N} (e(t;\rho))^2 + \lambda \sum_{t=1}^{N} (u(t;\rho))^2 \right] \tag{2.2}$$

If $T_0(z;\rho) = \frac{C_r(z;\rho)P(z)}{1+C_y(z;\rho)P(z)}$ and $S_0(z;\rho) = \frac{1}{1+C_y(z;\rho)P(z)}$ are the achieved closed-loop response and sensitivity function with controller $\{C_r(z;\rho), C_y(z;\rho)\}$ and given the independence between $r(t)$ and $v(t)$ the performance criterion can be written as

$$\begin{aligned} J(\rho) = & \frac{1}{2N} \sum_{t=1}^{N} \left\{ \left(y^d(t) - T_0(z;\rho) r(t) \right) \right\}^2 + \frac{1}{2} \mathrm{E} \left[\left\{ S_0(z;\rho) v(t) \right\}^2 \right] \\ & + \lambda \frac{1}{2N} \mathrm{E} \left[\sum_{t=1}^{N} (u(t;\rho))^2 \right] \end{aligned} \tag{2.3}$$

where

- $v(t)$ is a quasi stationary noise.
- $r(t)$ is a external reference signal independent of $v(t)$
- $y^d(t)$ represents the desire response to the external signal $r(t)$ for the closed-loop system

To solve this optimization problem, an iterative algorithm is required. Three different experiments are performed on the closed loop system in order to find an unbiased estimated of the gradient of (2.3). The parameters of the controller are computed as:

$$\rho_{i+1} = \rho_i - \gamma_i R_i^{-1} \frac{\partial J}{\partial \rho} (\rho_i) \tag{2.4}$$

Where R_i is some positive definite matrix and the sequence γ_i obey some constraints so the algorithm can converge (Gevers, 2002) and

$$\frac{\partial J(\rho)}{\partial \rho} = \frac{1}{N}\mathrm{E}\left[\sum_{t=1}^{N} e(t;\rho)\frac{\partial e(t;\rho)}{\partial \rho} + \lambda \sum_{t=1}^{N} u(t;\rho)\frac{\partial u(t;\rho)}{\partial \rho}\right] \tag{2.5}$$

The three experiments are also presented by Gevers (2002). The first and the third are just normal operation collected data, while the second one requires to use the output of the first experiment as part of the input data. If the signals $\left\{r_i^j(t)\right\}$ are N-length reference signals for experiment $j = 1, 2, 3$ on iteration i (that is, while the controller $C(z;\rho_i) \triangleq \{C_r(z;\rho_i), C_y(z;\rho_i)\}$ is in the loop), the corresponding output signals are $\left\{y^j(t;\rho_i)\right\}$, for $j = 1, 2, 3$ and $r(t)$ is an arbitrary signal used to excite the closed-loop process, then:

$$\begin{aligned}
&r_i^1(t) = r(t) \text{ with output } y^1(t;\rho_i) = T_0(z;\rho_i)r(t) + S_0(z;\rho_i)v_i^1(t)\\
&r_i^2(t) = r(t) - y^1(t;\rho_i) \text{ with output } y^2(t;\rho_i) = T_0(z;\rho_i)(r(t) - y^1(t;\rho_i)) + S_0(z;\rho_i)v_i^2(t)\\
&r_i^3(t) = r(t) \text{ with output } y^3(t;\rho_i) = T_0(z;\rho_i)r(t) + S_0(z;\rho_i)v_i^3(t)
\end{aligned}$$

and corresponding control signals given by

$$\begin{aligned}
u^1(t;\rho_i) &= S_0(z;\rho_i)\left[C_r(z;\rho_i)r(t) - C_y(z;\rho_i)v_i^1(t)\right]\\
u^2(t;\rho_i) &= S_0(z;\rho_i)\left[C_r(z;\rho_i)(r(t) - y^1(t;\rho_i)) - C_y(z;\rho_i)v_i^2(t)\right]\\
u^3(t;\rho_i) &= S_0(z;\rho_i)\left[C_r(z;\rho_i)r(t) - C_y(z;\rho_i)v_i^3(t)\right]
\end{aligned}$$

Using these signals, in Hjalmarsson et al. (1998) is demonstrated that an unbiased estimation of the gradient can be found by

$$\widehat{\frac{\partial J(\rho_i)}{\partial \rho}} = \frac{1}{N}\sum_{t=1}^{N}\left(e(t;\rho_i)\widehat{\frac{\partial y(t;\rho_i)}{\partial \rho}} + \lambda u(t;\rho_i)\widehat{\frac{\partial u(t;\rho_i)}{\partial \rho}}\right) \tag{2.6}$$

with

$$\begin{aligned}
e(t;\rho_i) &= y^1(t;\rho_i) - y^d(t)\\
u(t;\rho_i) &= u^1(t;\rho_i)\\
\widehat{\frac{\partial y(t;\rho_i)}{\partial \rho}} &\triangleq \frac{1}{C_r(z;\rho_i)}\left[\left(\frac{\partial C_r(z;\rho_i)}{\partial \rho} - \frac{\partial C_y(t;\rho_i)}{\partial \rho}\right)y^3(t;\rho_i) + \frac{\partial C_y(z;\rho_i)}{\partial \rho}y^2(t;\rho_i)\right]\\
\widehat{\frac{\partial u(t;\rho_i)}{\partial \rho}} &\triangleq \frac{1}{C_r(z;\rho_i)}\left[\left(\frac{\partial C_r(z;\rho_i)}{\partial \rho} - \frac{\partial C_y(z;\rho_i)}{\partial \rho}\right)u^3(t;\rho_i) + \frac{\partial C_y(t;\rho_i)}{\partial \rho}u^2(t;\rho_i)\right]
\end{aligned}$$

The next controller is then computed by

$$\rho_{i+1} = \rho_i - \gamma_i R_i^{-1}\widehat{\frac{\partial J}{\partial \rho}}(\rho_i) \tag{2.7}$$

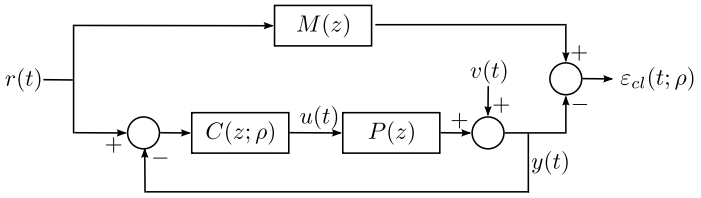

Figure 2.2: Correlations Based Tuning control problem.

2.2. Correlation based Tuning

In Karimi et al. (2007) the Correlation Based Tuning (CbT) is used to tune the parameters of a linear controller. The model reference control problem is given as in Fig. 2.2. The main idea is to find the controller's parameters in such a way that the signals $r(t)$ and ε_{cl} are uncorrelated. According to Karimi et al. (2007), one can say that

$$\begin{aligned}\varepsilon_{cl}(\rho,t) &= M(z)r(t) - (1-M(z))C(z;\rho)y(t) \\ &= [M(z) - P(z)(1-M(z))C(z;\rho)]r(t) - (1-M(z))C(z;\rho)v(t)\end{aligned} \tag{2.8}$$

if one is able to find the ideal controller $C(\rho^*)$ then the signal $\varepsilon_{cl}(t;\rho^*)$ will be independent of $r(t)$ since $v(t)$ and $r(t)$ are independent.

The optimization problem then, can be given by

$$J_c(\rho) = f^T(\rho)f(\rho) = \sum_{\tau=-l}^{l} R^2_{\varepsilon r_w}(\tau) \tag{2.9}$$

where

$$f(\rho) = \mathrm{E}\left\{\zeta_w(t)\varepsilon(\rho,t)\right\}$$

$$\zeta_w(t) = \left[r_w(t+l), r_w(t+l-1), \ldots, r_w(t), r_w(t-l), \ldots, r_w(t-l)\right]^T$$

$$\begin{aligned}R_{\varepsilon r_w}(\tau) &= \mathrm{E}\left\{\varepsilon(\rho,t)r_w(t-\tau)\right\} \\ &= \mathrm{E}\left\{\left[M(z) - P(z)(1-M(z))C(z;\rho)\right]r(t)W(z)r(t-\tau)\right\}\end{aligned}$$

with $r_w(t) = W(z)r(t)$ and l a sufficiently large integer. $W(z)$ is a weighting filter. $\zeta_w(t)$ is an instrumental variable correlated with r and $R_{\varepsilon r_w(\tau)}$ is the cross-correlation function between $r_w(t)$ and $\varepsilon(\rho,t)$.

If the controller is linear in the parameters, that is $C(\rho) = \beta^T(z)\rho$. The error then can be written as

$$\varepsilon(\rho,t) = y_d(t) - \phi^T(t)\rho \tag{2.10}$$

with

$$y_d(t) = M(z)r(t)$$

$$\phi(t) = \beta(z)(1-M(z))y(t)$$

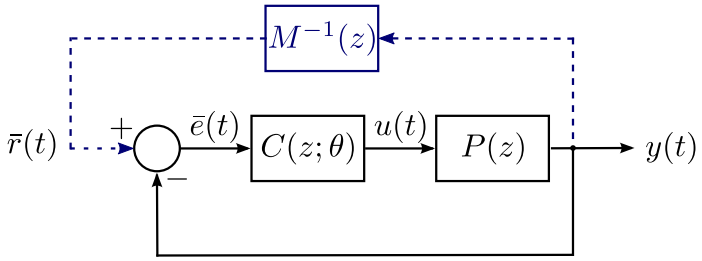

Figure 2.3: The VRFT set up. The dashed lines represent the "virtual" part of the method.

Then, for a finite number of data N, the criterion 2.9 can be estimated as $\hat{J}_c(\rho) = \hat{f}^T(\rho)\hat{f}(\rho)$ with

$$\hat{f}(\rho) = \frac{1}{N}\sum_{t=1}^{N}\zeta_w(t)\varepsilon(t,\rho) = \frac{1}{N}\sum_{t=1}^{N}\zeta_w(t)\left[y_d(t) - \phi^T(t)\rho\right]$$

2.3. Virtual Reference Feedback Tuning

The Virtual Reference Feedback Tuning (VRFT) is a one-shot data-based method for the design of feedback controllers. The original idea was presented in Guardabassi and Savaresi (2000), and then formalized by Lecchini, Campi, Savaresi and Guardabassi (Campi et al., 2002; Lecchini et al., 2002). In this section, both the one degree of freedom (1DoF) and the two degrees of freedom (2DoF) cases are presented.

In Campi et al. (2002), the method is presented for the tuning of a feedback controller. Suppose that the controller belongs to the controller class $\{C(z;\theta)\}$ given by $C(z;\theta) = \beta^T(z)\theta$, where $\beta(z) = [\beta_1(z)\ \cdots \beta_n(z)]^T$ is a known vector of transfer functions, and $\theta = [\theta_1\ \theta_2\ \cdots \theta_n]^T$ is the vector of parameters. The control objective is to minimize the model-reference criterion given by:

$$J_{MR}(\theta) = \left\| \left(\frac{P(z)C(z;\theta)}{1 + P(z)C(z;\theta)} - M(z) \right) W(z) \right\|_2^2 \tag{2.11}$$

The main idea of the method is that, given a set of input-output data from the plant in open-loop (i.e. $u(t)$ and $y(t)$ respectively), the designer should be able to minimize equation (2.11), without a model of the plant. This can be achieved by creating a "virtual" signal constructed from the open-loop data. If the real open-loop output ($y(t)$) had been taken in closed-loop and the closed-loop transfer function were $M(z)$, one can find a "virtual reference" $\bar{r}(t)$ that, if applied to the closed loop system, would yield $y(t)$ as the output. If the output of the plant is $y(t)$, then the output of the controller should be equal to $u(t)$. This controller can be found by *identifying* the transfer function which yields the output $u(t)$ when the input $\bar{r}(t) - y(t)$ is applied to the input as depicted in Fig. 2.3.

The original 1DoF VRFT algorithm, as presented by the authors in Campi et al. (2002), is given as follows: Given a set of measured I/O data $\{u(t), y(t)\}_{t=1,\ldots,N}$:

1. Compute:
   - a virtual reference $\bar{r}(t)$ such that $y(t) = M(z)\bar{r}(t)$, and
   - the corresponding tracking error $e(t) = \bar{r}(t) - y(t)$
2. Filter the signals $e(t)$ and $u(t)$ with a suitable filter $L(z)$:

$$e_L(t) = L(z)e(t)$$
$$u_L(t) = L(z)u(t)$$

3. Select the controller parameter vector, say, $\hat{\theta}_N$, that minimizes the following criterion:

$$J_{VR}^N(\theta) = \frac{1}{N}\sum_{t=1}^{N}\left(u_L(t) - C(z;\theta)e_L(t)\right)^2 \tag{2.12}$$

If $C(z;\theta) = \beta^T(z)\theta$, the criterion (2.12) can be given by

$$J_{VR}^N(\theta) = \frac{1}{N}\sum_{t=1}^{N}\left(u_L(t) - \varphi_L^T(t)\theta\right)^2 \tag{2.13}$$

with $\varphi_L(t) = \beta(z)e_L(t)$ and the parameter vector $\hat{\theta}_N$ is given by

$$\hat{\theta}_N = \left[\sum_{t=1}^{N}\varphi_L(t)\varphi_L(t)^T\right]^{-1}\sum_{t=1}^{N}\varphi_L(t)u_L(t) \tag{2.14}$$

The authors, also showed that, the filter $L(z)$ should be the one that approximates the criterion (2.12) to (2.11). This filter should holds:

$$|L(e^{\jmath\omega})|^2 = |1 - M(e^{\jmath\omega})|^2\,|M(e^{\jmath\omega})|\,|W(e^{\jmath\omega})|^2\,\frac{1}{\Phi_u(e^{\jmath\omega})} \tag{2.15}$$

where Φ_u is the spectral density of $u(t)$.

In the case of the 2DoF, the design methodology is presented in Lecchini et al. (2002) and an outline is also presented in this section. The steps are quite similar to the ones presented above for the 1DoF case. The control structure is presented in Fig. 2.4. The objective of this method is to minimize the criterion in (2.16).

$$\begin{aligned} J_{MR}(\theta_r,\theta_y) = &\|(\Psi_M(z;[\theta_r,\theta_y]) - M(z))W_M(z)\|_2^2 \\ &+ \|(\Psi_S(z;\theta_y) - S(z))W_s(z)\|_2^2 \end{aligned} \tag{2.16}$$

with

$$\Psi_M(z;[\theta_r,\theta_y]) = \frac{P(z)C_r(z;\theta_r)}{1 + P(z)C_y(z;\theta_y)}$$
$$\Psi_S(z;\theta_y) = \frac{1}{1 + P(z)C_y(z;\theta_y)}$$

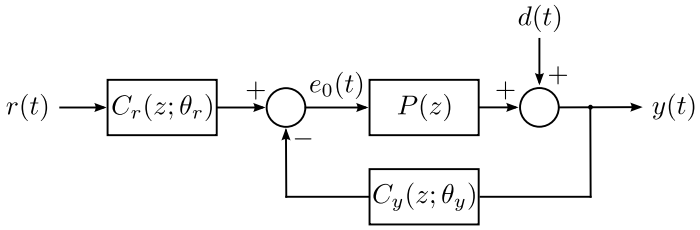

Figure 2.4: Two degrees of freedom structure.

and $M(z)$ being the target input-to-output transfer function and $S(z)$ the target sensitivity function. In order to find the parameters of the controllers (θ_r and θ_y) the signals $\bar{r}(t)$, $\bar{d}(t)$ and $\bar{y}(t)$ are defined. These are the "virtual" signal for the 2DoF case and are computed as:

$\bar{r}(t)$ is the virtual reference, so that $y(t) = M(z)\bar{r}(t)$

$\bar{d}(t)$ is the virtual disturbance, so that $y(t) + \bar{d}(t) = S(z)\bar{d}(t)$

$\bar{y}(t)$ is the virtual-disturbed output of the plant, so that $\bar{y}(t) = y(t) + \bar{d}(t)$

On the basis of these "virtual" signals the controller's parameters are found by minimizing the following alternative identification cost function:

$$\begin{aligned} J_{VR}^{N}(\theta_r, \theta_y) = & \frac{1}{N}\sum_{t=1}^{N}\left[\Gamma_M(t;[\theta_r,\theta_y])\right]^2 \\ & + \frac{1}{N}\sum_{t=1}^{N}\left[\Gamma_S(t;[\theta_r,\theta_y])\right]^2 \end{aligned} \tag{2.17}$$

where,

$$\begin{aligned} \Gamma_M(t;[\theta_r,\theta_y]) &= L_M(z)\left(u(t) - C_r(z;\theta_r)\bar{r}(t) + C_y(z;\theta_y)y(t)\right) \\ \Gamma_S(t;[\theta_r,\theta_y]) &= L_S(z)\left(u(t) + C_y(z;\theta_y)\bar{y}(t)\right) \end{aligned}$$

and $L_M(z)$ and $L_S(z)$ are appropriate filters to be chosen so (2.17) becomes an approximation to (2.16). If the controllers are linear in the parameter ($C_r(z;\theta_r) = \beta_r(z)^T\theta_r$ and $C_y(z;\theta_y) = \beta_y(z)^T\theta_y$) the cost criterion (2.17) becomes a standard quadratic optimization problem, and the solution is obtained by

$$\begin{bmatrix} \hat{\theta}_r^N \\ \hat{\theta}_y^N \end{bmatrix} = A_N^{-1}F_N \tag{2.18}$$

With

$$A_N = \frac{1}{N}\sum_{t=1}^{N}\left(\begin{bmatrix} \varphi^{\bar{r}}_{L_M}(t) \\ -\varphi^{y}_{L_M}(t) \end{bmatrix}\begin{bmatrix} \varphi^{\bar{r}}_{L_M}(t) \\ -\varphi^{y}_{L_M}(t) \end{bmatrix}^T\right) + \frac{1}{N}\sum_{t=1}^{N}\left(\begin{bmatrix} 0 \\ \varphi^{\bar{y}}_{L_S}(t) \end{bmatrix}\begin{bmatrix} 0 \\ \varphi^{\bar{y}}_{L_S}(t) \end{bmatrix}^T\right)$$

$$F_N = \frac{1}{N}\sum_{t=1}^{N}\left(\begin{bmatrix} \varphi^{\bar{r}}_{L_M}(t) \\ -\varphi^{y}_{L_M}(t) \end{bmatrix} u_{L_M}(t) - \begin{bmatrix} 0 \\ \varphi^{\bar{y}(t)}_{L_S} \end{bmatrix} u_{L_S}(t)\right)$$

where

$$\varphi^{\bar{r}}_{L_M}(t) = \beta_r(z)L_M(z)\bar{r}(t) \quad \varphi^{y}_{L_M}(t) = \beta_y(z)L_M(z)y(t)$$
$$\varphi^{\bar{y}}_{L_S}(t) = \beta_y(z)L_S(z)\bar{y}(t) \quad u_{L_M}(t) = L_M(z)u(t)$$
$$u_{L_S}(t) = L_S(z)u(t)$$

In Lecchini et al. (2002) the authors use the concept of "ideal controller" to derive the structure of this filter. The *ideal controller* C_{r0} and C_{y0} are the ones that, if used in the control loop, would solve (2.16) exactly, that is

$$C_{y0} = \frac{1-S}{SP} \tag{2.19}$$

$$C_{r0} = \frac{M}{SP} \tag{2.20}$$

When comparing (2.16) and (2.17) using the Parseval Theorem the expression of the filters $L_M(z)$ and $L_S(z)$ that must make the identification problem (2.17) match the control problem (2.16) are found to be:

$$|L_M(e^{\jmath\omega})|^2 = |M(e^{\jmath\omega})|^2|S(e^{\jmath\omega})|^2|W_M(e^{\jmath\omega})|^2\frac{1}{\Phi_u(e^{\jmath\omega})} \tag{2.21}$$

$$|L_S(e^{\jmath\omega})|^2 = |S(e^{\jmath\omega})-1|^2|S(e^{\jmath\omega})|^2|W_S(e^{\jmath\omega})|^2\frac{1}{\Phi_u(e^{\jmath\omega})} \tag{2.22}$$

One can see that if $C_{r0}(z)$ and $C_{y0}(z)$ are the ideal controllers, (2.16) can be written (dropping the frequency weights for simplicity) as follows

$$J_{MR}(\theta_r,\theta_y) = \left\| \frac{P(z)(C_r(z)-C_{r0}(z)) + P^2(z)(C_r(z)C_{yo}(z) - C_{ro}(z)C_y(z))}{(1+P(z)C_y(z))(1+P(z)C_{y0}(z))} \right\|_2^2 + \left\| \frac{P(z)(C_{yo}(z)-C_y(z))}{(1+P(z)C_y(z))(1+P(z)C_{y0}(z))} \right\|_2^2 \tag{2.23}$$

In the "tracking" part of the objective function (the first section), the reference tracking controller and the disturbance rejection controller, are both involved, so a compromise between both controllers will appear. Also, in (2.18) since the optimization involves both sets of parameters, the minimization of J^N_{VR} implies a compromise between both problems.

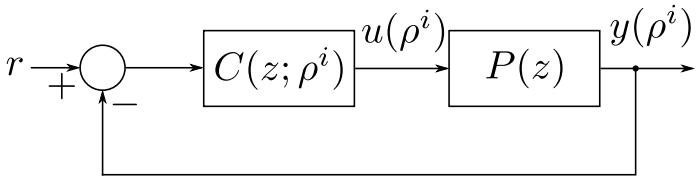

Figure 2.5: Feedback system using FRIT

2.4. Fictitious Reference Iterative Tuning

Other data-driven approach method is the Fictitious Reference Iterative Tuning (FRIT). As the name suggest, this method is similar to the VRFT and the IFT. At the beginning (Miyachi et al., 2006), in fact this was the case. Later a change in the definition of the problem yield to a more VRFT like method (Kaneko et al., 2006). In this section, both cases are shown.

Following Miyachi et al. (2006), if the controller $C(z;\rho^i)$ of Fig. 2.5 is given by

$$C(z;\rho^i) = \frac{\rho_1^i s^l + \cdots + \rho_l^i s + \rho_{l+1}^i}{s^k + \rho_{l+2}^i s^{k-1} + \cdots \rho_n^i} \tag{2.24}$$

where ρ^i are the parameter vector of the controller at iteration i, $u(t;\rho^i)$ and $y(t;\rho^i)$ are the input and output data collected in closed-loop with the controller $C(z;\rho^i)$ and $P(z)$ is the unknown plant. It is assumed that the original parameters of the controller ρ^0 stabilizes the plant, and that the desired closed-loop response is given by $T_d(z)$. The performance criterion that is intended to be minimized is given by

$$\begin{aligned} J(\rho^i) &= \frac{1}{2N}\sum_{t=1}^{N}\left(\bar{e}(t;\rho^i)\right)^2 \\ \bar{e}(t;\rho^i) &= \left(y(t;\rho^0) - T_d(z)\bar{r}(t;\rho^i)\right) \end{aligned} \tag{2.25}$$

The signal $\bar{r}(t;rho^i)$ is the fictitious reference at iteration i and given by

$$\bar{r}(t;\rho^i) = C^{-1}(z;\rho^i)u(t;\rho^0) + y(t;\rho^0) \tag{2.26}$$

where $C(z;\rho^i)$ is assumed to be invertible. The optimization problem:

$$\rho^* = \arg\max_{\rho}\ J(\rho) \tag{2.27}$$

can be solved by

$$\rho^{i+1} = \rho^i - \gamma R_i^{-1}\frac{\partial J(\rho)}{\partial \rho}\bigg|_{\rho^i} \tag{2.28}$$

where R_i is the Hessian matrix approximated by

$$R_i = \sum_{t=1}^{N}\left(\frac{\partial e(t;\rho)}{\partial \rho}\bigg|_{\rho^i}\right)^T\left(\frac{\partial e(t;\rho)}{\partial \rho}\bigg|_{\rho^i}\right) \tag{2.29}$$

The alternative definition of the problem starts with the same cost index as in (2.25). From this point, according to Kaneko et al. (2006), the fictitious error can be defined as:

$$e\left(\rho\right) = y(t;\rho^0) - T_d(q)\left(C(t;\rho,q)^{-1}u(t;\rho^0) + y(t;\rho^0)\right) \tag{2.30}$$

If the controller is given by

$$\begin{aligned} C(z;\rho) &= \frac{N(z;\alpha)}{D(z;\theta)} = \frac{\sum_{i=1}^{m}\alpha_i z^i + 1}{\sum_{i=0}^{n}\theta_i z^i} \\ \rho &= [\alpha_1 \cdots \alpha_m\, \theta_0 \cdots \theta_n] \end{aligned} \tag{2.31}$$

Then, in Kaneko et al. (2006), the following transformation is proposed

$$\begin{aligned} e'(t;\rho) &= N(z;\alpha)e(t;\rho) \\ &= N(z;\alpha)y(t;\rho^0) - D(z;\theta)T_d(z)u(t;\rho^0) - N(z;\alpha)T_d(z)y(t;\rho^0) \\ &= N(z;\alpha)Y_s(t) - D(z;\theta)U_T(t) \end{aligned} \tag{2.32}$$

with

$$\begin{aligned} S_d(z) &:= 1 - T_d(z) \\ Y_s(t) &:= S_d(z)y(t;\rho^0) \\ U_T(t) &:= T_d(z)u(t;\rho^0) \end{aligned}$$

Then, the new minimization problem becomes:

$$\hat{J}(\rho) = \sum_{t=1}^{N}\left(e'(t;\rho)\right)^2 \tag{2.33}$$

which, can be solved using least squares method. Therefore, the global optimum of the function can be guaranteed. In Kaneko et al. (2006) they show that the original $J(\rho)$ from (2.25) is equal to zero if and only if $\hat{J}(\rho)$ is equal to zero. This last problem statement makes the FRIT closer to the VRFT, with the difference that an initial controller is needed in order to compute the fictitious reference while for the VRFT no initial controller is needed.

2.5. Comparison of the methodologies

In this section, the different methods presented above are compared. In order to choose a methodology, it is important to take into account different factors as:

- Applicability of the method.
- Number of necessary experiments with the plant.
- Flexibility with different configurations.
- Applications

As seen above, all the presented methodologies have one characteristic in common: all of them can be seen as a way to define an optimization problem. In case of IFT, CbT and FRIT, the optimization problem that is solved tries to minimize the error between the output of the system and the expected output in closed-loop.

The differences are subtle but the resolution of the problem greatly varies. In both, the IFT and the FRIT, an iterative scheme is needed to solve the optimization problem. But the difference lies in the fact that, while in the IFT a series of experiments for each iteration are proposed, in the FRIT is the fictitious reference that is computed to find the needed data.

For the CbT, the error that is intended to minimize is the same as with the IFT and FRIT, but the difference is that what is minimized is the correlation between the error signal and the reference. When the controller is linear in the parameters, a least square method can be used.

In the other hand, the signal minimized with the VRFT is the difference between the expected input of the plant and the real input. Because of this, the VRFT method is said to transform a control problem into an identification problem.

Certainly, the IFT is the method that requires more computational effort. If for example, to solve the optimization problem, it requires 5 iterations, it means that 15 experiments are needed to be performed in the plant, since each iteration requires 3 different experiments.

Most of the methods are flexible in the sense that it is possible to use them in different control structures. For example, IFT has been used in a MIMO plant (Miskovic et al., 2007) and also extended to an IMC structure and an Smith predictor configuration (Bruyne, 2003). In a different direction, in Preitl and Precup (2006) the IFT is used to tune a two degrees of freedom controller that then is converted into a fuzzy controller. CbT has been also used to find a feedforward controller and a prefilter (Karimi et al., 2005), and multiple inputs multiple outputs strategies (Miskovic et al., 2007). However VRFT is the one that has attracted more attention in recent years.

Several different extension for the VRFT verifies the flexibility of the method. In Lecchini et al. (2001), the VRFT was used in a sensitivity shaping problem while in Lecchini et al. (2002) a two degrees of freedom controller was tuned using the methodology. The first multivariable approach was presented in Nakamoto (2004), where a matrix approach was taken. The control structure was a feedback compensator to decouple the loops along with a diagonal feedforward controller. In Sala and Esparza (2005a), a complete parameterization of the controller and the use of VRFT for feedforward control is first proposed. For non-minimum phase controllers, Sala and Esparza (2005b) propose to find an approximated model of the plant to identify the non-minimum phase zeros, while in Campestrini et al. (2011), a double optimization is proposed to firstly approximate the non-minimum phase zeros and then, use the result to include them in the desired closed-loop transfer function. Formentin et al. (2010) uses the VRFT to the tuning of IMC controllers for plants with important delays. The optimization problem they propose is a nonlinear optimization, which finds a model of the plant at the same time. An heuristic is needed to find the initial values of the parameters of the controller. The resulting controller is used for traction control in a two-wheeled vehicle. In Esparza et al. (2011), the VRFT is use to train neural networks in order to control a plant. An approximation of the plant using also neural networks is employed to compute the

backpropagation gradients to train the neural network controller.

All these methodologies have been used in a variety of processes. For example, the IFT was successfully applied in a chemical process where the parameters of PID controllers where updated with an important improvement in the performance (Gevers, 2002; Hjalmarsson et al., 1998), in Gunnarsson et al. (2003), a 2×2 IFT approach is applied to a two-link robotic arm, in Hamamoto et al. (2003) the IFT is applied to the control of a two-mass-spring system using a two-degrees of freedom controller, in a two-step procedure, while in Tay et al. (2006) is applied to the control of photoresist film thickness for the production of semiconductors as a supervisory algorithm to re-tune the controllers for each batch of production. The speed and position of a servo drive has been also an application of the IFT (Kissling et al., 2009). A three-tanks laboratory system was considered in Precup et al. (2010).

In the other hand, CbT has been applied to a magnetic suspension system (Karimi et al., 2003). In this case an iterative algorithm is used, because, originally, the CbT was seen as an extension to IFT that was later re-formulated to be used in a one-shot scheme. In van Heusden et al. (2010), the method is applied to a direct-drive pick-and-place robot. One of the interesting aspects of this last applications is that, a nonlinear constraint is applied in the optimization in order to guarantee closed-loop stability (see van Heusden et al. (2011) for a complete presentation in the subject).

Several applications have been presented for the VRFT. In Nakano et al. (2009), the VRFT is used to tune a decoupling MIMO controller in a two dimensional thermal process. It has also been used in the control of neuroprotheses (Previdi et al., 2004, 2005), for the velocity control of self-balancing industrial manipulators (Previdi et al., 2005), in a polymerization reaction (Kansha et al., 2008). In Formentin et al. (2010), the VRFT is used in an IMC structure to the traction control of a two-wheeled vehicle.

For this thesis, the VRFT was chosen as the work framework given its simplicity and flexibility. It was found that this method is suitable to control several non-linear processes with different control structures.

3. Virtual reference feedback tuning extensions for two degrees of freedom controllers

The Virtual Reference Feedback Tuning is very intuitive and it is easy to extend its capabilities to other controller structures. In this chapter, the extensions proposed for this methodology are discussed for the two degrees of freedom case. In the second part of this thesis, the extensions proposed are applied to several interesting cases as wastewater treatment plants, solid oxide fuel cells and pH neutralization process.

An alternative 2DoF tuning is proposed in section 3.1 which is useful to separate the reference tracking tuning from the disturbance rejection. If a 2DoF PI controller is used, it was found that a constraint in the optimization have to be included in order to obtain zero stationary error. This constraint is commented in section 3.2. The feedforward extension to the two degrees of freedom controller is studied in section 3.3.

3.1. Alternative 2DoF VRFT problem formulation

The 2DoF alternative structure under consideration is presented in Fig. 3.1. Originally, this structure was intended to be use in a model-based control, because the plant model should be factorized as $P(z) = N(z)D^{-1}(z)$ with $N(z)$ and $D(z)$ stable and proper transfer functions. It can be found that if $C_1(z) = D(z)Q(z)$ and $C_2(z) = N(z)Q(z)$, being $Q(z)$ a free stable transfer function parameter, the input-output transfer function becomes

$$y(t) = N(z)Q(z)r(t) \tag{3.1}$$

Of curse, the relation in (3.1) should be equal to M, the desired reference to output transfer

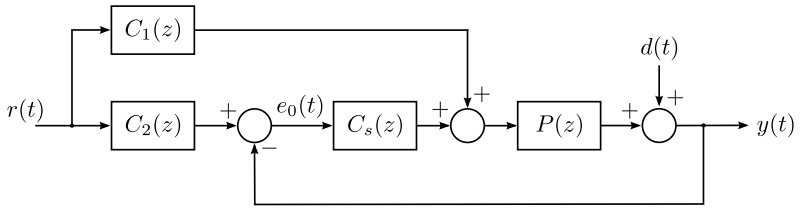

Figure 3.1: Alternative 2DoF controller with feedforward action.

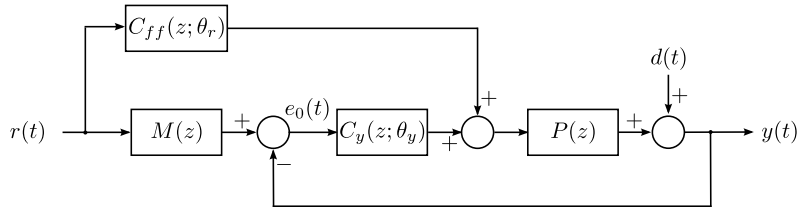

Figure 3.2: 2DoF structure, feedforward tracking controller for VRFT.

function, this leads to

$$Q(z) = N^{-1}(z)M(z) \tag{3.2}$$

The feedback controller $C_s(z)$ only acts if relation (3.2) ca not be fulfilled completely or in case of disturbance at the output of the plant. In other words, $C_s(z)$ is responsible of the stability of the closed-loop system and the disturbance rejection performance, which can be treated as a separate sensitivity shaping problem.

The separation between the sensitivity shaping problem and the complementary sensitivity shaping problem, leads to the idea of using this structure with alternative methods for controller design. The VRFT was found to be suitable for this. In fact, the separation property of this structure is an advantage since two different independent optimizations can be performed to achieve both shaping problems without the drawback of having a compromise between them. However, a reformulation will be needed as the design of $C_1(z)$ and $C_2(z)$ is model based, whereas within VRFT the plant model is not available.

In order to apply the VRFT's ideas on the above presented structure, let's redefine the blocks in Fig. 3.1. The prefilter block ($C_2(z)$) should represent the target complementary sensitivity transfer function. Thus, one can just define $C_2(z) = M(z)$. Then the feedforward controller ($C_1(z)$) has to provide the correct control input to the plant to achieve the tracking objective. Since this controller has to be determined, let's re-name it as $C_{ff}(z)$. The feedback controller $C_s(z)$ continues to be the responsible of the closed-loop as in the original model-based method. In Fig. 3.2 the structure for VRFT is shown. The goal then is to find the feedback, $C_s(z)$, and feedforward, $C_{ff}(z)$ controllers using only the available data. In what follows, the VRFT problem will be formulated first, followed by considerations on how to find $C_{ff}(z)$, $C_s(z)$ and some considerations with respect to the filters choice (as it is done on the original VRFT).

3.1.1. Formulation of the VRFT problem

Using this 2DoF structure, the VRFT cost function would be, as shown in (3.3)

$$\begin{aligned} J_{MR}(\theta_{ff}, \theta_s) = &\left\| \left(\Psi_M([\theta_{ff}, \theta_s]) - M(z)\right) W_M(z) \right\|_2^2 \\ &+ \left\| \left(\Psi_S([\theta_{ff}, \theta_s]) - S(z)\right) W_S(z) \right\|_2^2 \end{aligned} \tag{3.3}$$

with

$$\Psi_M([\theta_{ff},\theta_s]) = \frac{P(z)C_s(z;\theta_s)}{1+P(z)C_s(z;\theta_s)}\left(\frac{C_{ff}(z;\theta_{ff})}{C_s(z;\theta_s)} + M(z)\right)$$
$$\Psi_S([\theta_{ff},\theta_s]) = \frac{1}{1+P(z)C(z;\theta_s)}$$

Being $\Psi_M([\theta_{ff},\theta_s])$ and $\Psi_S([\theta_{ff},\theta_s])$ the achieved reference-to-output transfer function and the achieved sensitivity function, respectively [1]. As before, the idea of ideal controllers is introduced into (3.3). The ideal controllers $C_{ff0}(z)$ and $C_{s0}(z)$ for this alternate structure, are given by

$$\begin{aligned} C_{ff0}(z) &= P^{-1}(z)M(z) \\ C_{s0}(z) &= \frac{1-S(z)}{S(z)P(z)} \end{aligned} \tag{3.4}$$

With these ideal controllers, the signal $e_0(t)$ becomes the reference shaping error, since it reduces to $e_0(t) = S(z)d(t)$, and if there is no disturbance, $e_0(t) = 0$ for any value of $r(t)$. By introducing (3.4) into (3.3), it can be shown that (3.3) reduces to:

$$\begin{aligned} J_{MR}(\theta_{ff},\theta_s) = &\left\| \frac{P(z)\left(C_{ff}(z;\theta_{ff}) - C_{ff0}(z)\right)}{1+P(z)C_s(z;\theta_s)} W_M(z) \right\|_2^2 \\ &+ \left\| \frac{P(z)\left(C_{s0}(z) - C_s(z;\theta_s)\right)}{(1+P(z)C_s(z))(1+PC_{s0}(z))} W_S(z) \right\|_2^2 \end{aligned} \tag{3.5}$$

In Campi et al. (2002), to find the filter $L_M(z)$, the term $\frac{1}{1+P(z)C_s(z)}$ is approximated by $\frac{1}{1+P(z)C_s(z)} \approx S(z)$, which is a good approximation, since the solution of the right part of equation (3.3) looks for this condition. Since equation (3.5) is used only for the determination of the filters, as will be shown later, using this approximation, the equation can be written as:

$$\begin{aligned} J_{MR}(\theta_{ff},\theta_s) = &\left\| \left(C_{ff}(z;\theta_{ff}) - C_{ff0}(z)\right) P(z)S(z)W_M(z) \right\|_2^2 \\ &+ \left\| \frac{P(z)\left(C_{s0}(z) - C_s(z)\right)}{(1+P(z)C_s(z))(1+P(z)C_{s0}(z))} W_S(z) \right\|_2^2 \end{aligned} \tag{3.6}$$

The first term of 3.6 is used to find the controller $C_{ff}(z)$, while the second term is used to find $C_s(z)$. This control problem has to be translated into an identification problem to find the parameters of the controllers without the knowledge of any model for the plant. If the ideal controllers were found, the input to the feedback controller should always be zero if no disturbance is affecting the system. Therefore, using the ideas of the virtual signals of the VRFT, one is able to formulate an identification problem with the controllers $C_{ff}(z)$ and $C_s(z)$ also totally decoupled, and therefore it is possible to optimize each controller for the specific task it is intended to deal with ($C_{ff}(z)$ for tracking and $C_s(z)$ for disturbance rejection).

The design algorithm is analogous to that in Lecchini et al. (2002). Given the reference models $M(z)$ and $S(z)$, and the batch of data $\{u(t), y(t)\}_{t=1,\ldots,N}$:

[1] Now $\Psi_M([\theta_{ff},\theta_s])$ will not be the complementary sensitivity function as it will not be necessarily true that $\Psi_M + \Psi_S = 1$

- Construct the set of "virtual" data ($\bar{r}(t)$, $\bar{d}(t)$ and $\bar{y}(t)$), as in (2.17)
- Find the controller parameter vector ($\hat{\theta}_{ff}^N$, $\hat{\theta}_S^N$) that minimizes

$$\begin{aligned} J_{VR}^N = & \frac{1}{N}\sum_{t=1}^{N}\left[L_M(z)(u(t) - C_{ff}(z;\theta_{ff})\bar{r}(t))\right]^2 \\ & + \frac{1}{N}\sum_{t=1}^{N}\left[L_S(z)\left(u(t) + C_s(z,\theta_s)\bar{y}(t)\right)\right]^2 \end{aligned} \tag{3.7}$$

Since each part of (3.7) depends only on the parameters of one of the controllers, it can be solved separately. To check this, let us assume a general function $f(\theta_1, \theta_2)$ which is meant to be minimized. Supposing that $f(\theta_1, \theta_2) \geq 0$ and that it can be written as:

$$f(\theta_1, \theta_2) = f_1(\theta_1) + f_2(\theta_2) \tag{3.8}$$

with $f_1(\theta_1) \geq 0$ and $f_2(\theta_2) \geq 0$. Minimizing (3.8) implies

$$\begin{aligned} \frac{\partial f(\theta_1, \theta_2)}{\partial \theta_1} &= 0 \\ \frac{\partial f(\theta_1, \theta_2)}{\partial \theta_2} &= 0 \end{aligned} \tag{3.9}$$

but given (3.8), it is evident that

$$\begin{aligned} \frac{\partial f(\theta_1, \theta_2)}{\partial \theta_1} &= \frac{df_1(\theta_1)}{d\theta_1} \\ \frac{\partial f(\theta_1, \theta_2)}{\partial \theta_2} &= \frac{df_2(\theta_2)}{d\theta_2} \end{aligned} \tag{3.10}$$

therefore, minimizing $f(\theta_1, \theta_2)$ is the same as minimizing each single part individually, given this independence in the variables. For this reason, it is clear that (3.7) is totally decoupled. It is important to note that the original control criterion is not totally separated, as can be seen in (3.6). But using the adequate filters L_M and L_S, the decoupled identification criterion (3.7) can be used to find the controller parameters that approximate the desired control criterion, which is the standard procedure for the VRFT approach. The main advantage of applying this alternative two-degrees of freedom controller is that the controllers and the optimization to find each set of parameters are both independent. This independence allows the designer to use different optimization methods, data, or even only find one of the controllers if necessary. Below, the structure of suitable filters $L_M(z)$ and $L_S(z)$ is given.

3.1.2. Feedforward Controller Tuning

It is possible to *identify* the $C_{ff}(z)$ controller from the input/output data. It is desirable to find the best approximation of $Q(z)$ as given by (3.2), in that case, the ideal controller in

the feedforward path, should be given by $C_{ff}(z)$ as in (3.4) and, as in Fig. 3.2, the prefilter should be equal to $M(z)$.

So, if we introduce the signal $\bar{r}(t) = M^{-1}(z)y(t)$, the output of the feedforward controller should be $u(t)$. The direct consequence of this fact is that, one can use an identification method to determine $C_{ff}(z)$, using $\bar{r}(t)$ (the filtered version of $y(t)$ through $M^{-1}(z)$) as the input, and $u(t)$ as the output values.

This *identification problem* can also be derived using a VRFT approach: If the output data measured from the experiment performed on the plant (in open-loop) were taken in closed-loop with the ideal $C_{ff}(z)$ controller, then the error $e(t)$ should be always zero. In that case we should find a *virtual signal* $\bar{r}$ such that $y(t) = M(z)\bar{r}(t)$. Then the controller that one should identify is the one that, with an input signal $\bar{r}(t)$, should have an output $u(t)$ (since the error is always zero) So, the objective is to find $C_{ff}(z)$ as close as possible to $P^{-1}(z)M(z)$. The controller $C_s(z)$ is not involved in the $C_{ff}(z)$ optimization.

In the case of $C_{ff}(z)$, it is very important to have more freedom in the structure, since the advantage of the structure are strongly dependent on how good the controller is close of the ideal controller. For this reason it was decided to use an identification method (in this case, the Output Error Method (OE) see Ljung (1999)) to find the feedforward controller. The idea of using a different identification method to find the parameters of the controller and the idea of using the VRFT in a feedforward controller was first proposed in Sala and Esparza (2005a).

However, there is no inconvenience in trying to identify a linear-in-the-parameter controller for $C_{ff}(z)$. If $C_{ff}(z)$ is defined as $C_{ff}(z, \theta_{ff}) = \beta^T(z)\theta_{ff}$, (in the same way as in section 2.3) the performance criterion specifically for the tracking problem becomes:

$$J_{VR}^{N}(\theta_{ff}) = \frac{1}{N}\sum_{t=1}^{N}\left(u_L(t) - C_{ff}(z;\theta_{ff})\bar{r}_L(t)\right)^2 \tag{3.11}$$

The signals $u_L(t)$ and $\bar{r}_L(t)$ are the filtered versions of $u(t)$ and $\bar{r}(t)$ respectively filtered by $L_M(z)$. The parameters can be analytically obtained by

$$\begin{aligned} \hat{\theta}_{ff} &= a_N^{-1} f_N \\ a_N &= \frac{1}{N}\sum_{t=1}^{N}\varphi_L(t)\varphi_L(t)^T \\ f_N &= -\frac{1}{N}\sum_{t=1}^{N}\varphi_L(t)u_L(t) \end{aligned} \tag{3.12}$$

with

$$\varphi_L(t) = \beta(z)\bar{r}_L(t) \tag{3.13}$$

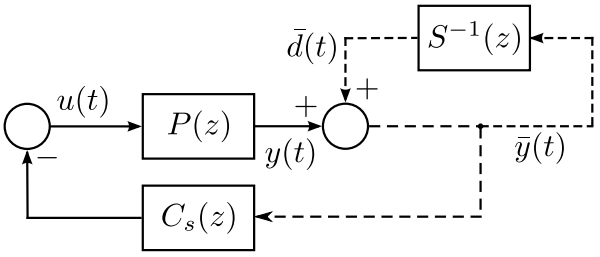

Figure 3.3: Structure to find the virtual signals, for the sensitivity shaping problem.

3.1.3. Feedback Controller Tuning

The $C_s(z)$ controller should be optimized to reject the disturbance, since $C_{ff}(z)$ was optimized to solve the tracking problem. In Lecchini et al. (2001) a method is presented in order to solve a *Sensitivity Shaping problem* based also in the VRFT formulation. Even though the authors use the controller in the feedback path, one can use the same method with the controller in the direct path, since the problem requires $r = 0$ and the result is independent from $C_{ff}(z)$. According to Lecchini et al. (2001), the structure to find the *virtual signals* is given as in Fig. 3.3. Once the virtual signals are calculated, the cost function is given by:

$$J_{VR}^{N}(\theta) = \frac{1}{N}\sum_{t=1}^{N}\left(u_L(t) + C_s(z;\theta_s)\bar{y}_L(t)\right)^2 \tag{3.14}$$

The signals $u_L(t)$ and $\bar{y}_L(t)$ are the filtered versions of $u(t)$ and $\bar{y}(t)$ respectively. According to the authors, the filter has to be given by $L_S(z)$ as shown below

If the controller is lineal in the parameters, the solution can be obtained analytical

$$\begin{aligned} \hat{\theta}_N &= a_N^{-1} f_N \\ a_N &= \frac{1}{N}\sum_{t=1}^{N}\varphi_L(t)\varphi_L(t)^T \\ f_N &= -\frac{1}{N}\sum_{t=1}^{N}\varphi_L(t)u_L(t) \end{aligned} \tag{3.15}$$

with

$$\varphi_L(t) = \beta(z)\bar{y}_L(t) \tag{3.16}$$

3.1.4. Filters Choice

The idea of filters $L_M(z)$ and $L_S(z)$ is to approximate the performance index (3.7) to the desired model reference criterion in (3.3). Applying the Parseval Theorem and (3.4), it is

found that (omitting the $e^{j\omega}$ term for simplicity)

$$\begin{aligned} J_{MR} = \frac{1}{2\pi}\int_{-\pi}^{\pi} \frac{|P|^2}{|1+PC_s(\theta_s)} \left|C_{ff}(\theta_{ff}) - C_{ff0}\right|^2 |W_M|^2 \,\mathrm{d}\omega \\ + \frac{1}{2\pi}\int_{-\pi}^{\pi} \frac{|P|^2|S|^2}{|1+PC_s(\theta_s)} \left|C_{s0} - C_s(\theta_S)\right|^2 |W_S|^2 \,\mathrm{d}\omega \end{aligned} \tag{3.17}$$

Now using the results in Campi et al. (2002), and considering $J_{VR}(\theta)$ as the asymptotic counterpart of $J_{VR}^N(\theta)$ as $N \to \infty$:

$$J_{VR}(\theta) = E[(u_L(t) - C(z;\theta)r_L(t))^2] \tag{3.18}$$

Again, applying the Parseval Theorem to J_{VR} (see (3.7)) it is found that

$$\begin{aligned} J_{VR}(\theta_{ff},\theta_S) = \frac{1}{2\pi}\int_{-\pi}^{\pi} |C_{ff0} - C_{ff}(\theta_{ff})|^2 \psi_M \mathrm{d}\omega \\ + \frac{1}{2\pi}\int_{-\pi}^{\pi} |-C_{s0} + C_s(\theta_s)|^2 \psi_S \mathrm{d}\omega \end{aligned} \tag{3.19}$$

with

$$\begin{aligned} \psi_M &= \frac{|P|^2}{|M|^2}|L_M|^2|\Phi_u|^2 \\ \psi_S &= \frac{|S|^2}{|S-1|^2}|P|^2|L_S|^2|\Phi_u|^2 \end{aligned}$$

To find the filters, one can compare (3.17) and (3.19). Since a plant model is not available, we can approximate the term $|1 + P(z)C_s(z;\theta_s)|^{-1}$ by $|S(z)|$ (that is, changing $C_s(z;\theta_s)$ by $C_{s0}(z)$). If done, the filters can be found to be:

$$|L_M|^2 = |M|^2|S|^2|W_M|\frac{1}{|\Phi_u|^2} \tag{3.20}$$

$$|L_S|^2 = |S-1|^2|S|^2|W_S|\frac{1}{|\Phi_u|^2} \tag{3.21}$$

Which turn out to be the same filters found in Lecchini et al. (2002).

3.2. The VRFT applied to the 2DoF PI controller

Data-Driven control has been used for the tuning of PID from the beginning. For example, in Gevers (2002) the IFT method is applied to a PID controller for a chemical industry process. VRFT has been also been applied to PID controllers as in Kansha et al. (2008). For the case of 2DoF PI controllers, it was found that some constraints has to be set, in order to have the same properties in the discrete time controller as in the continuous time version. Suppose a standard two degrees of freedom controller as in Fig. 3.4. The equations of this structure are given by:

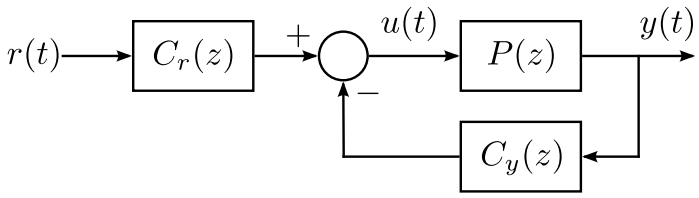

Figure 3.4: Two degrees of freedom PID controller.

$$\begin{aligned} u(s) &= C_r(s)r(s) - C_y(s)y(s) \\ C_r(s) &= K_c\left(\beta + \frac{1}{T_i s}\right) \\ C_y(s) &= K_c\left(1 + \frac{1}{T_i s}\right) \end{aligned} \tag{3.22}$$

After applying the bilinear transformation given by

$$s = \frac{2}{T_s}\frac{z-1}{z+1}$$

Where T_s is the sampling time, s is the Laplace variable and z^{-1} is the discrete unit delay. The discrete time version of the controllers are given by:

$$\begin{aligned} C_r(z) &= \frac{K_c\left(\beta + \frac{T_s}{2T_i}\right) + K_c\left(\frac{T_s}{2T_i} - \beta\right)z^{-1}}{1 - z^{-1}} \\ C_y(z) &= \frac{K_c\left(1 + \frac{T_s}{2T_i}\right) + K_c\left(\frac{T_s}{2T_i} - 1\right)z^{-1}}{1 - z^{-1}} \end{aligned} \tag{3.23}$$

This controller clearly is linear in the parameters, which is useful for the VRFT, since the optimization can be seen as a linear square problem and therefore, be solved by standard tools. If

$$\begin{aligned} C_r(z) &= \frac{\alpha_1 + \alpha_2 z^{-1}}{1 - z^{-1}} \\ C_y(z) &= \frac{\alpha_3 + \alpha_4 z^{-1}}{1 - z^{-1}} \end{aligned} \tag{3.24}$$

The output of the controller u is found to be

$$\begin{aligned} u &= \alpha_1 r - \alpha_3 y \\ &+ \frac{z^{-1}}{1 - z^{-1}}\left(\left(\alpha_1 + \alpha_2\right)r - \left(\alpha_3 + \alpha_4\right)y\right) \end{aligned} \tag{3.25}$$

From (3.23) and (3.24) it is clear that

$$\alpha_1 + \alpha_2 = \alpha_3 + \alpha_4 = K_c\frac{T_s}{T_i} \tag{3.26}$$

Then, in order to have a Two-degrees of freedom PI controller, tuned with the VRFT, it is necessary to add the constraint $\alpha_1 + \alpha_2 - \alpha_3 - \alpha_4 = 0$ to the optimization problem. Another interpretation of this constraint is that, in case that y and r have the same value, the integral factor (given by the term $z^{-1}/(1 - z^{-1})$) has to stop increasing since the error is zero. If this constraint is not accomplished, it may be possible to have an stationary error, even if the controller has integral action.

With this constraint, it may be possible to find the parameters of the PI in continuous time from the parameters obtained with the optimization:

$$\begin{aligned} K_c &= \alpha_3 - \frac{1}{2}(\alpha_1 + \alpha_2) \\ T_i &= Ts\left(\frac{\alpha_3}{\alpha_1 + \alpha_2} - \frac{1}{2}\right) \\ \beta &= \frac{\alpha_1 - \frac{1}{2}(\alpha_1 + \alpha_2)}{\alpha_3 - \frac{1}{2}(\alpha_1 + \alpha_2)} \end{aligned} \tag{3.27}$$

With this condition, it is guaranteed that only one integrator is needed for the implementation, a desirable condition as pointed out in Aström and Hägglund (2001).

3.3. VRFT approach to Feedforward control

A feedforward controller can be set using the VRFT. In Guardabassi and Savaresi (1997), the idea of using the VRFT controller was presented to be used in conjunction with a one-degree of freedom controller. The main difference is that it is assume that the disturbance is available for measurement and is used in the optimization problem.

This idea is extended here to a two degrees of freedom controller, in order to be used in the BSM1 problem. Suppose that the control system can be represented by the diagram in Fig. 3.5, where P_1 and P_2 represent the dynamic of the plant from the input u and the disturbance d to the output y. These three signals are measured from an open-loop experiment. $C_r(z)$, $C_y(z)$ and $C_f(z)$ are the controllers to be found. The "virtual" components and signals are:

- $M(z)$, which is the target closed-loop dynamics from the reference signal to the output of the controlled system.
- $S(z)$, is the target closed-loop dynamics from the unmeasured disturbance at the output to the output of the controlled system.
- $F(z)$, is the target closed-loop dynamics from the measured disturbance to the output.
- $\bar{r}_v(t)$, is the virtual reference computed from the data obtained from an open loop experiment and the closed-loop target functions.
- $\bar{p}(t)$, is an fictitious arbitrary signal that is added to the output of the experiment, and is considered as the unmeasured disturbance.

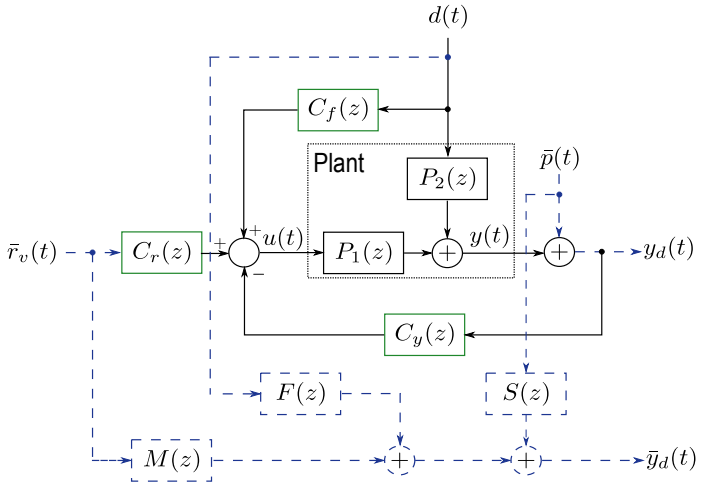

Figure 3.5: Virtual reference setup for feedforward plus 2doF controller. Solid lines are for "real" components and signals while dashed lines are for "virtual" components and signals.

- $d(t)$, is the measurable disturbances that is suppose to be available in open-loop experiment.
- $\bar{y}_d(t)$, is the result of the sum of the output of plant $y(t)$ and the fictitious disturbance $\bar{p}(t)$, that is $\bar{y}_d(t) = y(t) + \bar{p}(t)$

The virtual reference signal $\bar{r}_v$(t) has to be computed according to the ideal relationships and the measured and virtual signals:

$$\bar{y}_d(t) = M(z)\bar{r}_v(t) + F(z)d(t) + S(z)\bar{p}(t) \tag{3.28}$$

Then the virtual signal is computed from (3.28):

$$\begin{aligned} \bar{y}_d(t) &= y(t) + \bar{p}(t) \\ \bar{r}_v(t) &= M^{-1}(z)\left(\bar{y}_d(t) - F(z)d(t) - S(z)\bar{p}(t)\right) \end{aligned} \tag{3.29}$$

The output of the controlled system is

$$y_d(t) = \frac{P_1(z)C_r(z)}{1 + P_1(z)C_y(z)}r(t) + \frac{P_1(z)C_f(z) + P_2(z)}{1 + P_1(z)C_y(z)}d(t) + \frac{1}{1 + P_1(z)C_y(z)}p(t) \tag{3.30}$$

Note in (3.30), that the input signals do not have a bar, denoting that these signals are not virtual, but actually are entering to the system. When comparing (3.29) and (3.30), one is able to find the ideal controllers that would, theoretically, drive the system with the desired

dynamics (if the transfer functions of the plant were known):

$$\begin{aligned} C_{ro}(z) &= \frac{1}{P_1(z)}\left(\frac{M(z)}{S(z)}\right) \\ C_{yo}(z) &= \frac{1}{P_1(z)}\left(\frac{1}{S(z)} - 1\right) \\ C_{fo}(z) &= \frac{1}{P_1(z)}\left(\frac{F(z)}{S(z)} - P_2(z)\right) \end{aligned} \tag{3.31}$$

Then, following the paths in the diagram of Fig. 3.5 that lead from the measured and virtual inputs to the $u(t)$ signal, it is easy to find that the cost function to optimize is given by:

$$\begin{aligned} J(\theta) = &\frac{1}{N}\sum_{t=0}^{N-1}\left[u(t) - \left(C_r\left(z;\theta\right)\bar{r}_v(t)\right.\right. \\ &\left.\left. -C_y\left(z;\theta\right)y_d(t) + C_f\left(z;\theta\right)d(t)\right)\right]^2 \end{aligned} \tag{3.32}$$

Even more, if the controllers are linear in the parameters, that is $C_r(z) = \beta_r^T(z)\theta_r$, $C_y = \beta_y^T(z)\theta_y$ and $C_f(z) = \beta_f^T(z)\theta_f$, $J(\theta)$ can be rewritten as a standard least squares problem:

$$\hat{\theta} = \arg\min_{\theta} \frac{1}{N}\left|U - \Phi\cdot\theta\right|^2 \tag{3.33}$$

with

$$\begin{aligned} U &= \left[u(0), u(1), \ldots, u(N)\right]^T \\ \theta &= \left[\theta_r^T, \theta_y^T, \theta_f^T\right]^T \\ \Phi &= \left[\lambda_{\bar{r}_v}, \lambda_{y_d}, \lambda_d\right] \\ \lambda_{\bar{r}_v} &= \left[\beta_r^T(z^{-1})\bar{r}_v(0), \ldots, \beta_r^T(z^{-1})\bar{r}_v(N-1)\right]^T \\ \lambda_{y_d} &= -\left[\beta_y^T(z^{-1})y_d(0)\ , \ldots,\ \beta_y^T(z^{-1})y_d(N-1)\right]^T \\ \lambda_d &= \left[\beta_f^T(z^{-1})d(0), \ldots, \beta_f^T(z^{-1})d(N-1)\right]^T \end{aligned}$$

Solving this optimization problem, one is able to find directly the three controllers using only a batch of input-output data without any iterative scheme (one-shot).

Numerical Illustrative Example Suppose a discrete time plant as in Guardabassi and Savaresi (1997) given by $P_1(z) = \frac{1+0.4z^{-1}}{1-0.8z^{-1}}$ and $P_2(z) = \frac{1-0.3z^{-1}}{1-0.8z^{-1}}$. Suppose the target closed-loop response is given by

$$\bar{y}_d(t) = \frac{0.5}{1-0.5z^{-1}}r(z) + \frac{0.4-0.4z^{-1}}{1-0.4z^{-1}}p(z) + \frac{0.3-0.3z^{-1}}{1-0.3z^{-1}}d(z) \tag{3.34}$$

If the controllers are parameterized in such a way that the optimal controller belongs to the set of controllers and the input data of the open-loop experiment is rich enough, one is able

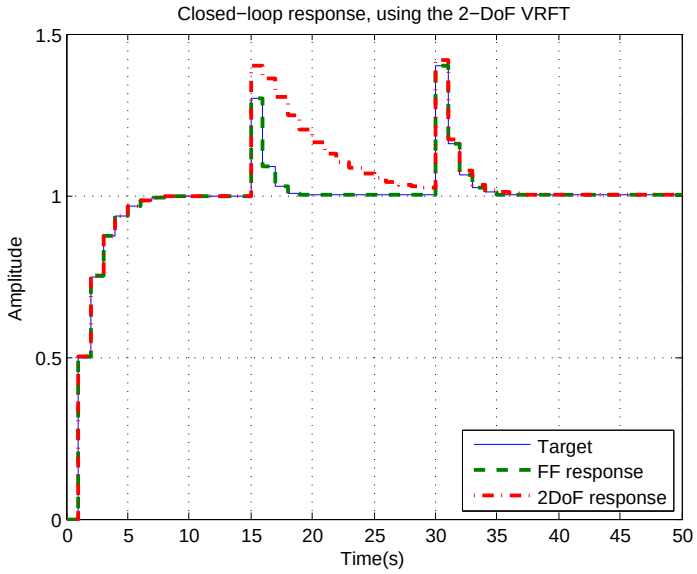

Figure 3.6: Response using the feedforward controller and the 2DoF controller. An measurable disturbance is applied at t= 15 s and a unmeasurable disturbance is applied at t= 30 s.

to find the ideal controllers using (3.33). The achieved controllers using a random uniform set of 1000 samples for $u(t)$, $d(t)$ and $p(t)$ are given by:

$$C_r(z) = \frac{1.25 - 1.5z^{-1} + 0.4z^{-2}}{1 - 1.1z^{-1} - 0.1z^{-2} + 0.2z^{-3}}$$
$$C_y(z) = \frac{1.5 - 1.2z^{-1}}{1 - 0.6z^{-1} - 0.4z^{-2}}$$
$$C_f(z) = \frac{-0.25 - 0.3z^{-1} + 0.15z^{-2}}{1 + 0.1z^{-1} - 0.12z^{-2}}$$

Using the VRFT with two degrees of freedom, but adding the unmeasured disturbance signal instead of calculating it as in (2.17), the result is as presented in Fig. 3.6. As expected, the response is seriously degraded because of the measurable disturbance, even if the controllers in the loop are equal to the ideal ones. The controller with the extra feedforward path perfectly achieves the desired closed-loop dynamics for a change in reference, the measurable disturbance and the unmeasurable disturbance. Also, finding the three degrees of freedom controllers does not add much more computational effort (in fact, one could say that it is almost the same).

How to choose the parametrization of the controllers and the target transfer functions are issues that still depend on the decisions of the designer and deserve more attention. For example, if the parametrization of the controller $C_r(z)$ has one parameter less than it is needed to achieve the perfect controller, the response degrades as shown in Fig. 3.7.

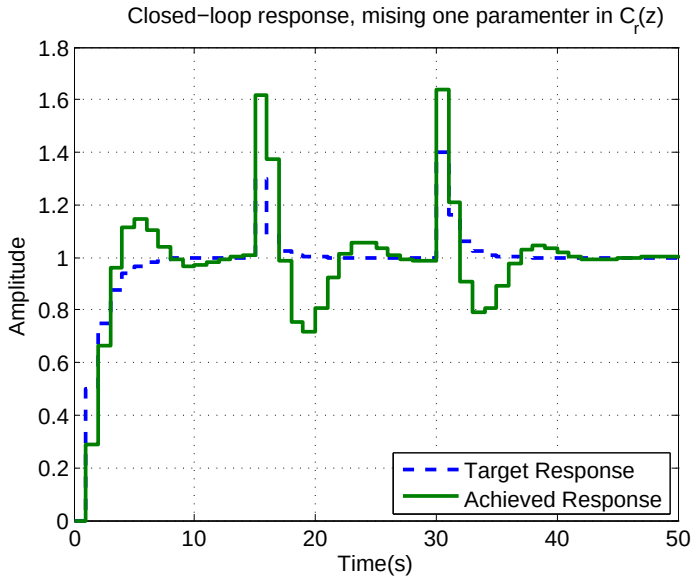

Figure 3.7: Response to a change in the reference, an unmeasurable disturbance (at t= 15 s) and a measurable disturbance (at t= 30 s), when the perfect controllers are not in the set of achievable controllers.

4. Virtual reference feedback tuning extensions for other advanced control structures

The versatility of the VRFT is once more tested under other control structures. First, some consideration are presented in section 4.1, regarding the parameterization of the controllers and the effect of including a weight to the input in the optimization. The application of the VRFT to the Multiple-Input Multiple-Output (MIMO) case is studied in section 4.2. in section 4.3 the VRFT is applied in an Internal Model Control (IMC) control structure which permits to obtain a robustness test to check if the control requirements can be safely achieved.

4.1. Parameterization of the controller and weighting of the input

In this section, some remarks are given about the parameterization of the controller and the weighting of the input signal during the optimization. The correct parameterization of the controller is fundamental while applying the VRFT. If the parameterization is not like the one of the ideal controller, it is impossible for the method to achieve the target function. In addition, if the plant is non-linear and continuous, this target function will likely to be not achievable with any parameterization. Therefore, to consider the control effort is important for robustness in those cases where the ideal controller is not achievable. The original VRFT control problem does not take into account the control effort, and therefore, the controllers tend to be aggressive, trying to achieve the target closed-loop transfer function.

4.1.1. Parameterization

As an example, lets considerer a second order plant P given by:

$$P(z) = \frac{a_0 z^{-1} + a_1 z^{-2}}{1 - a_2 z^{-1} + a_3 z^{-2}} \tag{4.1}$$

And lets suppose that the target closed-loop transfer function is given by:

$$M(z) = \frac{b_0 z^{-1}}{1 - (1 - b_0) z^{-1}} \tag{4.2}$$

With these conditions, the ideal controller is given by

$$C_{\text{ideal}}(z) = \frac{\frac{b_0}{a_0}\left(1 + a_2 z^{-1} + a_3 z^{-2}\right)}{\left(1 + \frac{a_1}{a_0} z^{-1}\right)\left(1 - z^{-1}\right)} \tag{4.3}$$

From (4.3), it is clear that a simple PI controller is not able to solve the problem. In fact, if the controller is parameterized as:

$$C(z, \theta) = \frac{F(z, \theta)}{1 - z^{-1}} \tag{4.4}$$

To achieve the ideal controller with a polynomial $F(z, \theta)$, an infinite number of parameters are needed. Therefore, even for a discrete time, noise free, linear invariant plant, achieving the desired response with a PI-like controller is not possible.

Two possible ways have been proposed to overcome this problem. The first one is having knowledge of the position of the zero of the plant and introduce it in the parameterization of the controller. In Campestrini et al. (2011), a two step optimization is proposed to first obtain an approximation of the plant zeros. This approach is very useful, despite the fact that some of the "model-free" aspect of the method is lost. The other one is to employ a full parameterized controller as pointed out in Sala and Esparza (2005a). However, this approach is very sensitive to under-parameterization, and the risk of obtaining an unstable closed-loop plant is higher.

Since in real case scenarios, the plants are not discrete and have other characteristics that can prevent the method to find the desired controller, some robustness consideration can be added in the optimization. The most basic consideration is to consider a weight in the control effort.

4.1.2. Control effort weight

It is possible to consider the control effort within the optimization problem. If a batch of N input-output data is available $\{u(t), y(t)\}|_N$, the performance criterion to be minimized can be extended to:

$$J(\theta) = \frac{1}{2} \sum_{t=1}^{N} \left(\left(u(t) - C(z, \theta) e_v(t)\right)^2 + \lambda \left(C(z, \theta) e_v(t)\right)^2 \right) \tag{4.5}$$

λ is the constant that is used to give more or less importance to the control effort weighting. If, as usual, the controller is linear in the parameters $C(z, \theta) = \beta^T(z)\theta$, (4.5) can be written in matrix form as:

$$J(\theta) = \frac{1}{2} \left(\|U - \Psi\theta\|_2^2 + \lambda \|\Psi\theta\|_2^2 \right) \tag{4.6}$$

with $U = [u(1), u(2), \ldots, u(N)]^T$, $\Psi = \beta^T(z) e_v$ and e_v is the virtual error. This equation can be written as a standard quadratic programming problem:

$$J(\theta) = \frac{1}{2} (1 + \lambda) \theta^T \Psi^T \Psi \theta + \left(-U^T \Psi\right) \theta + \frac{1}{2} U^T U \tag{4.7}$$

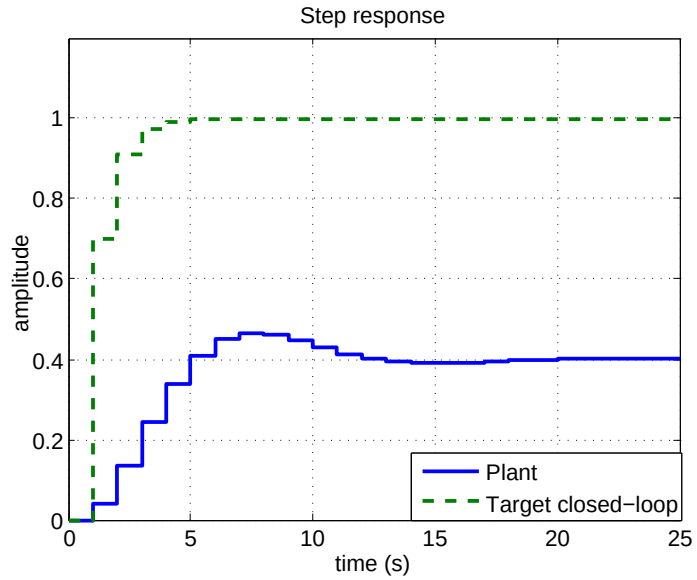

Figure 4.1: Step response of the plant and the target closed-loop

As it can be seen, the change in the original performance index is not drastic in the sense that λ only appears as a constant factor multiplying $\Psi^T\Psi$. The computation effort is the same as for the unweighted case. It also has to be noticed that these two objectives (the minimization of the error and the minimization of the control effort) are opposite one to the other. It is not possible to minimize the error without a more aggressive control signal. But, since it is unlikely to achieve the desired closed-loop, it is useful to limit in some sense the control effort and with it, give some robustness to the solution (robustness in the sense of caution).

Giving numeric values to the plant and the target transfer function of equations (4.1) and (4.2):

$$P(z) = \frac{0.04176z^{-1} + 0.03531z^{-2}}{1 - 1.414z^{-1} + 0.6065z^{-2}}$$
$$M(z) = \frac{0.7z^{-1}}{1 - 0.3z^{-1}}$$

The step response of the plant and the desired closed-loop are presented in Fig. 4.1 for reference. Considering the controller structure as:

$$C(z,\theta) = \frac{\theta_0 + \theta_1 z^{-1} + \theta_2 z^{-2} + \theta_3 z^{-3} + \theta_4 z^{-4}}{1 - z^{-1}}$$

The step response test for different values of λ are presented in Fig. 4.2. In Fig. 4.2a, the control effort is shown, while in Fig. 4.2b the corresponding output is presented. It has to be noticed that with this controller structure and only five parameters it is not possible to achieve the desired closed-loop transfer function. With the increment in the value of λ, the response is

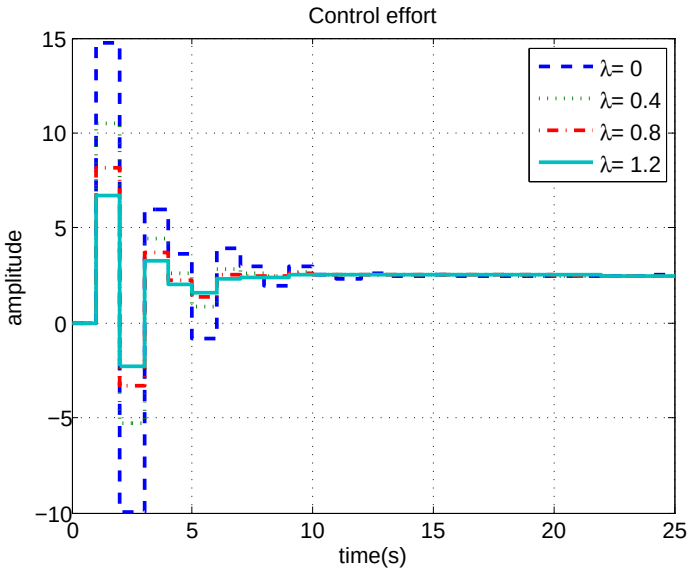

(a) Control effort

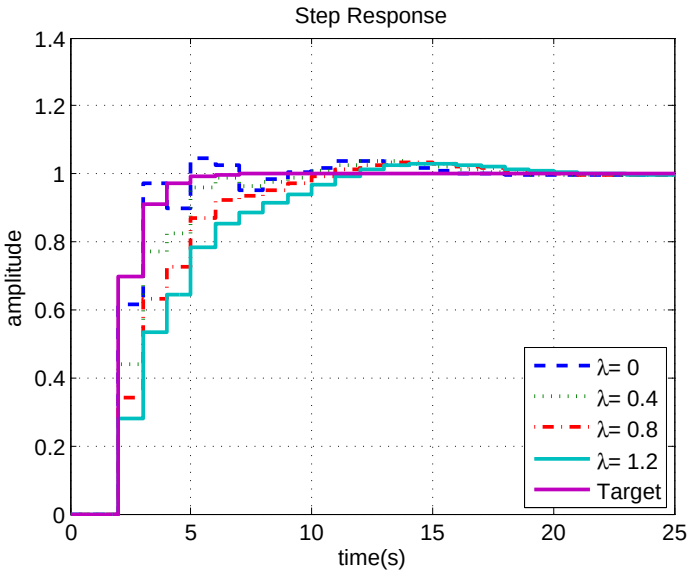

(b) Output

Figure 4.2: Test using the weighting factor for the input during the optimization step.

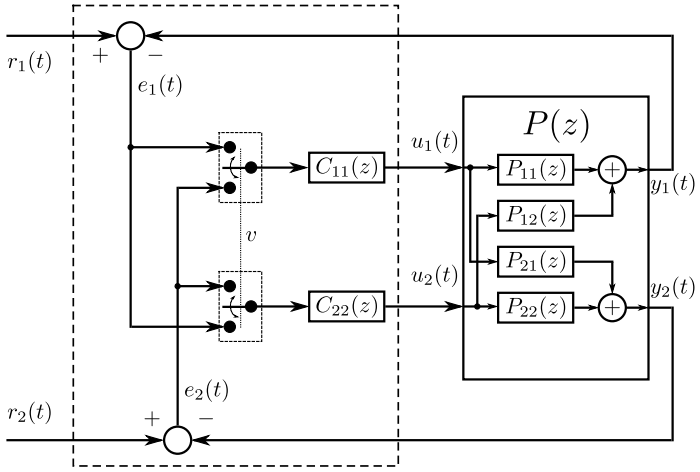

Figure 4.3: MIMO VRFT with pairing selection.

slower. The change in the control signal has the same form in all cases but different amplitude. This means that the optimization is finding the optimal compromise between the achievable closed-loop behavior and the minimization of the control effort.

Using this extra degree of freedom, the designer is able to use faster closed-loop transfer functions, but at the same time, try to keep the control effort somehow bounded. The great contribution of the original authors of the VRFT is the idea of the virtual reference signal. Once this signal has been computed, it is possible to apply it to several control strategies and take into account several things as the weighting that has been discussed here.

Since the control problem can be cast as quadratic optimization, it is also possible to include constraints, as for example, the 2DoF PI in section 3.2, or even to limit the range where the zeros or the poles of the controller can be.

4.2. MIMO VRFT with pairing selection

The VRFT methodology can be applied to the MIMO case. In Nakamoto (2004), a matrix approach was taken with the constraint of having the same desired closed-loop transfer functions for all the loops. In this work a less restrictive method is used and the problem of choosing the pairings of the input-outputs of the plant is accounted.

In Fig. 4.3 the control structure for the Two Inputs Two Outputs (TITO) case is presented with a decentralized approach. In this case, the pairing is decided with the variable v: if $v = 1$ the output y_1 is controlled using u_1 as the manipulated variable and then y_2 is controlled with the u_2 input. If $v = 0$ the manipulated variables are shifted.

The VRFT approach can be applied in such a way that the 2 controllers' parameters and the decision variable v can be determined using only a set of input-output data, without a

modeling step.

4.2.1. Application of the VRFT framework to the TITO case

Consider the TITO case. Assume that a batch of N open-loop samples taken from the plant $P(z)$ is available: $\{u_1(t),u_2(t),y_1(t),y_2(t)\}$. Using the ideas presented in Campi et al. (2002), it is possible to find a virtual reference signal for each loop. These signals will then be used to find the parameters of the controllers C_{11} and C_{22}. The desired target closed-loop transfer functions are $M_1(z)$ for $y_1(t)$ and $M_2(z)$ for the $y_2(t)$ loop. These signals are defined as:

$$\begin{aligned} \bar{r}_1(t) &= M_1^{-1}(z) \\ \bar{r}_2(t) &= M_2^{-1}(z) \end{aligned} \tag{4.8}$$

If the controllers are linear in the parameters:

$$\begin{aligned} C_{11}(z,\theta_{11}) &= \beta_{11}^T(z)\theta_{11} \\ C_{22}(z,\theta_{22}) &= \beta_{22}^T(z)\theta_{22} \end{aligned} \tag{4.9}$$

where θ_{11} and θ_{22} are vectors containing the parameters for each controller and $\beta_{11}(z)$ and $\beta_{22}(z)$ are the transfer functions vector defining the controllers. If the variable v is used to define the pairing of the input-output signals, (as presented in Fig. 4.3), then the following mixed-integer optimization can be set to find the optimal controller's parameters in a least square sense:

$$\begin{aligned} \underset{\theta_{11},\theta_{22},v}{\text{minimize}} \quad & J(\theta_{11},\theta_{22},v) \\ \text{subject to} \quad & v(1-v)=0 \end{aligned} \tag{4.10}$$

where

$$\begin{aligned} J(\theta_{11},\theta_{22},v) = v\cdot & \left\| \begin{bmatrix} u_1 \\ u_2 \end{bmatrix} - \Psi_1 \begin{bmatrix} \theta_{11} \\ \theta_{22} \end{bmatrix} \right\|^2 \\ + (1-v)\cdot & \left\| \begin{bmatrix} u_1 \\ u_2 \end{bmatrix} - \Psi_2 \begin{bmatrix} \theta_{11} \\ \theta_{22} \end{bmatrix} \right\|^2 \end{aligned} \tag{4.11a}$$

$$\Psi_1 = \begin{bmatrix} \Phi_{11} & 0 \\ 0 & \Phi_{22} \end{bmatrix} \tag{4.11b}$$

$$\Psi_2 = \begin{bmatrix} \Phi_{12} & 0 \\ 0 & \Phi_{21} \end{bmatrix} \tag{4.11c}$$

$$\Phi_{11} = \begin{bmatrix} \beta_{11}^T(z)e_1(1) \\ \vdots \\ \beta_{11}^T(z)e_1(N) \end{bmatrix} \tag{4.11d}$$

$$\Phi_{22} = \begin{bmatrix} \beta_{22}^T(z)e_2(1) \\ \vdots \\ \beta_{22}^T(z)e_2(N) \end{bmatrix} \tag{4.11e}$$

$$\Phi_{12} = \begin{bmatrix} \beta_{11}^T(z)e_2(1) \\ \vdots \\ \beta_{11}^T(z)e_2(N) \end{bmatrix} \tag{4.11f}$$

$$\Phi_{22} = \begin{bmatrix} \beta_{22}^T(z)e_1(1) \\ \vdots \\ \beta_{22}^T(z)e_1(N) \end{bmatrix} \tag{4.11g}$$

The matrices Ψ_1 and Ψ_2 can be seen as the direct and transverse control effects, given the computed virtual errors $\bar{e}_1$ and $\bar{e}_2$. The constraint $v(1-v) = 0$ is just a way to satisfy that v can only be 0 or 1. If $v = 1$ the direct matrix is used and the first pairing propose by the designer is used, while if $v = 0$, the other pairing is used. This optimization can be programed either using a **for** loop to check all the possibilities or by writing the corresponding problem using optimization tools like *Yalmip* (Löfberg (2004)) and *Sedumi* (Sturm (1999)).

4.2.2. MIMO control for the $n \times n$ case

Now, the complete MIMO case for n inputs and n outputs is presented. The optimization for the TITO case, can also contain 2 more "decoupling" controllers that theoretically can separate the effect of one of the loops over the other. For the case of section 4.2.1, the method will automatically chose the best pairing and parameters, but the interaction between loops is not directly considered. Fig. 4.4 represents the "complete" control structure with these two extra controllers. If all the decoupling controllers are used, the pairing selection can still be used, but if the structure of the controllers is the same for all the loops (which is generally the case) the only difference between one pairing and the other is a permutation of some of the controllers.

Even with this fact, for the $n \times n$ MIMO case the complete optimization problem is presented for the sake of completeness. Each controller is linearly parameterized. For example controller $C_{12}(z, \theta_{12})$ in Fig. 4.4, is defined as $C_{12}(z, \theta_{12}) = \beta_{12}^T \cdot \theta_{12}$.

Supposing that all the input output signals are available and that all the virtual signals has been computed according to their respective desired closed-loop transfer function, the optimization

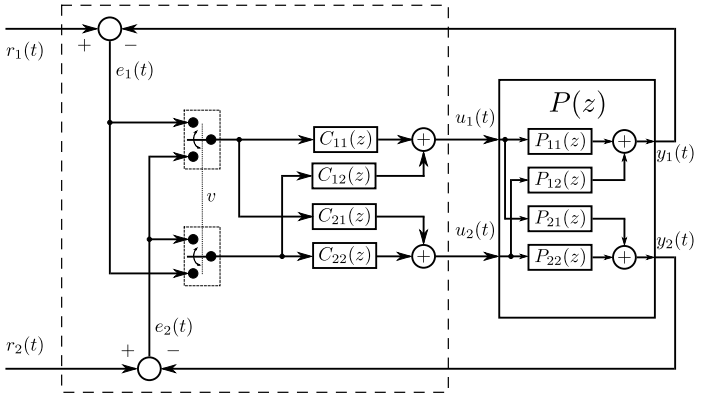

Figure 4.4: Control structure for the MIMO plant. Two inputs, two outputs case.

problem is defined as:

$$\begin{aligned} &\underset{\substack{\Theta_1,\Theta_2,\ldots,\Theta_n \\ v_1,v_2,\ldots,v_{n!}}}{\text{minimize}} && J(\Theta_1,\Theta_2,\ldots,\Theta_n,v_1,v_2,\ldots,v_{n!}) \\ &\text{subject to} && \begin{cases} v_i(1-v_i)=0, \forall i=1,\ldots,n! \\ \sum_{i=1}^{n!}(v_i)=1 \end{cases} \end{aligned} \tag{4.12}$$

with

$$J(\Theta_1,\Theta_2,\ldots,\Theta_n,v_1,v_2,\ldots,v_{n!}) = \sum_{i=1}^{n!}\left[v_i \cdot \left|\left|\begin{bmatrix} u_1 \\ u_2 \\ u_3 \\ \vdots \\ u_n \end{bmatrix} - \Psi_i \cdot \begin{bmatrix} \Theta_1 \\ \Theta_2 \\ \Theta_3 \\ \vdots \\ \Theta_n \end{bmatrix}\right|\right|^2\right] \tag{4.13a}$$

$$\Theta_1 = \left[\theta_{11}^T,\ldots,\theta_{1n}^T\right]^T \tag{4.13b}$$

$$\Theta_2 = \left[\theta_{21}^T,\ldots,\theta_{2n}^T\right]^T \tag{4.13c}$$

$$\vdots = \vdots$$

$$\Theta_n = \left[\theta_{n1}^T,\ldots,\theta_{nn}^T\right]^T \tag{4.13d}$$

$$\Psi_i = \begin{bmatrix} \Phi_{1i} & 0 & \cdots & \cdots & \cdots & 0 \\ 0 & \Phi_{2i} & 0 & \cdots & \cdots & 0 \\ 0 & 0 & \Phi_{3i} & 0 & \cdots & 0 \\ \vdots & \vdots & \vdots & \vdots & \vdots & 0 \\ 0 & 0 & 0 & 0 & 0 & \Phi_{ni} \end{bmatrix} \tag{4.13e}$$

$$\Phi_{11} = \left[\beta_{11}^T(z)e_1 \cdots \beta_{1n}^T(z)e_n\right] \tag{4.13f}$$
$$\vdots = \vdots$$
$$\Phi_{1n!} = \left[\beta_{11}^T(z)e_n \cdots \beta_{1n}^T(z)e_1\right] \tag{4.13g}$$
$$\Phi_{21} = \left[\beta_{21}^T(z)e_1 \cdots \beta_{2n}^T(z)e_n\right] \tag{4.13h}$$
$$\vdots = \vdots$$
$$\Phi_{2n!} = \left[\beta_{21}^T(z)e_n \cdots \beta_{2n}^T(z)e_1\right] \tag{4.13i}$$
$$\vdots = \vdots$$
$$\Phi_{n1} = \left[\beta_{n1}^T(z)e_1 \cdots \beta_{nn}^T(z)e_n\right] \tag{4.13j}$$
$$\vdots = \vdots$$
$$\Phi_{nn!} = \left[\beta_{n1}^T(z)e_n \cdots \beta_{nn}^T(z)e_1\right] \tag{4.13k}$$

For a $n \times n$ system, the number of controllers is $n \times n$ and the options for the pairing are $n!$. Φ_{11} to $\Phi_{1n!}$ represents all the permutations of the virtual error signals $\bar{e}_1$ to $\bar{e}_n$ filtered by the parameterized base functions β_{11}^T to β_{1n}^T. This means that, for all the possible pairings and all the input variables, it is needed to compute $n \cdot n!$ different matrices. The constraints of the optimization problem allow just one of all the possible pairings by letting the variables v_i either to be 1 or 0, but just one of the variables can be active.

It has to be noticed that for the TITO case, it is possible to use only one decision variable v, because one of the constraints can be easily written in terms of the other decision variable and introduced directly in the criterion.

4.2.3. Comparison of the VRFT with others methods

A practical example is presented to compare the MIMO VRFT with other data driven approaches. The methodology is applied to the LV100 gas turbine engine model used in Hjalmarsson (1999); Miskovic et al. (2005). In those papers, the IFT and the CbT are applied respectively using 4 different controllers (including the off-diagonal controllers). For the sake of comparison, the TITO case with pairing selection of Fig. 4.4 is applied.

The model in its continuous time form has five states (Hjalmarsson, 1999):

- Gas generator spool speed N_g.
- Power output N_p.
- Temperature T
- Fuel flow actuator level x_{W_f}.
- Variable area turbine nozzle actuator level $x_{V_{ATN}}$.

The inputs are the fuel flow W_f and the variable area turbine nozzle V_{ATN}. The output

signals are the gas generator spool speed and temperature. The model in state space form is given by

$$\begin{bmatrix} \dot{N}_g \\ \dot{N}_p \\ \dot{T} \\ \dot{x}_{W_f} \\ \dot{x}_{V_{ATN}} \end{bmatrix} = \begin{bmatrix} \text{-1.4122} & \text{-0.0552} & 0 & 42.9536 & 6.3087 \\ 0.0927 & \text{-0.1133} & 0 & 4.2204 & \text{-0.7581} \\ \text{-7.8467} & \text{-0.2555} & \text{-3.3333} & 300.4167 & \text{-4.4894} \\ 0 & 0 & 0 & \text{-25.0000} & 0 \\ 0 & 0 & 0 & 0 & \text{-33.3333} \end{bmatrix} \begin{bmatrix} N_g \\ N_p \\ T \\ x_{W_f} \\ x_{V_{ATN}} \end{bmatrix}$$
$$+ \begin{bmatrix} 0 & 0 \\ 0 & 0 \\ 0 & 0 \\ 1 & 0 \\ 0 & 1 \end{bmatrix} \begin{bmatrix} W_f \\ V_{ATN} \end{bmatrix}$$
$$\begin{bmatrix} N_g \\ \text{T} \end{bmatrix} = \begin{bmatrix} 1 & 0 & 0 & 0 & 0 \\ 0 & 0 & 1 & 0 & 0 \end{bmatrix} \begin{bmatrix} N_g \\ N_p \\ T \\ x_{W_f} \\ x_{V_{ATN}} \end{bmatrix} \tag{4.14}$$

The data used to find the VRFT controllers is depicted in Fig. 4.5. The controllers are PI-like discrete time controllers with sampling time $T_s = 0.1s$. The desired closed-loop transfer function for both loops is given by:

$$M(z) = \frac{0.4z^{-1}}{1 - 0.6z^{-1}} \tag{4.15}$$

The resulting controllers are presented in Table 4.1. For the VRFT case, the controllers are shifted. The difference in the value of J between both pairings is just 2.3674x10^{-9}, for this reason, this shift in the pairing has not to be considered as an important design change, but product of the sensibility of the numerical computation. But since all the four controllers are being used, there is no real difference in the pairing. If, for example, the controller parameterization is different, the selection of the pairing would become important and the final value of J will be considerably different between both cases.

In Fig. 4.6 and Fig. 4.7, the response of the controllers to a step changes in the references are presented with the value of the Integral of the Absolute Error (IAE), which is also presented in Table 4.1.

The VRFT is able to control the plant with a lower IAE than the other methods, using only one set of data and just one iteration. With respect to the IFT, the IAE is 62.19% and it has a very similar response to the CbT but with only one single experiment. Only for the interaction rejection in loop 2, the CbT has a better performance than the VRTFT, in all other cases, the VRFT gives better results.

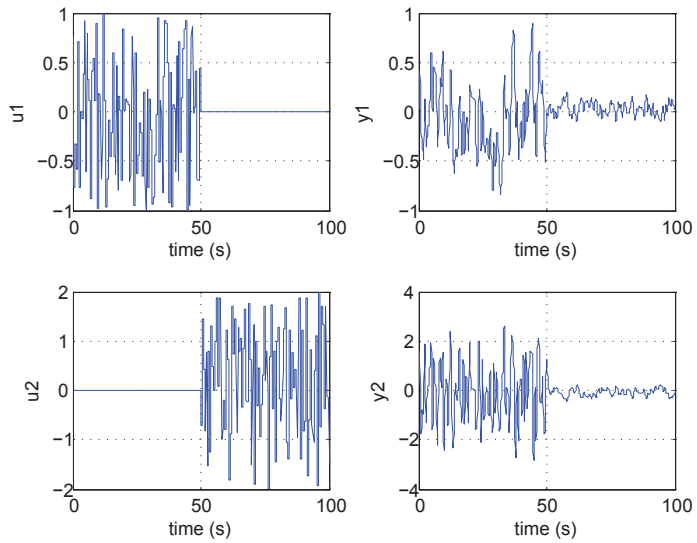

Figure 4.5: Data used to obtain the VRFT controllers.

	IFT	CbT	VRFT
C_{11}	$\frac{0.248-0.03z^{-1}}{1-z^{-1}}$	$\frac{0.3636-0.9866z^{-1}}{1-z^{-1}}$	$\frac{0.355-0.2507z^{-1}}{1-z^{-1}}$
C_{12}	$\frac{0.38-0.199z^{-1}}{1-z^{-1}}$	$\frac{0.3653-0.2691z^{-1}}{1-z^{-1}}$	$\frac{0.3393-0.06546z^{-1}}{1-z^{-1}}$
C_{21}	$\frac{16.47-15.91z^{-1}}{1-z^{-1}}$	$\frac{18.69-18.16z^{-1}}{1-z^{-1}}$	$\frac{-3.222+2.293z^{-1}}{1-z^{-1}}$
C_{22}	$\frac{0.063-0.054z^{-1}}{1-z^{-1}}$	$\frac{-3.453+2.652z^{-1}}{1-z^{-1}}$	$\frac{19.64-19.06z^{-1}}{1-z^{-1}}$
IAE	2.10399	0.8424 (-59.96%)	0.7954 (-62.19%)
IAE Reference change loop 1	0.3120	0.2591(-16.98%)	0.2486 (-20.32%)
IAE interaction effect loop 1	0.8647	0.2659(-69.24%)	0.2516 (-70.90%)
IAE interaction effect loop 2	0.1160	0.0348(-70%)	0.0478 (-58.79%)
IAE Reference change loop 2	0.8113	0.2826(-65.17%)	0.2486 (-69.36%)
Iterations	6	8	1
Experiments	30	8	1

Table 4.1: Controller for the LV100 plant.

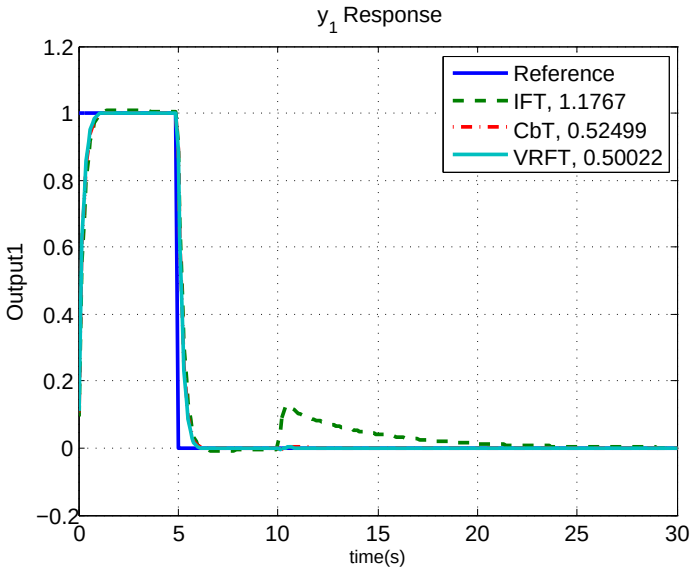

Figure 4.6: Response of the y_1 output of the three data driven methods.

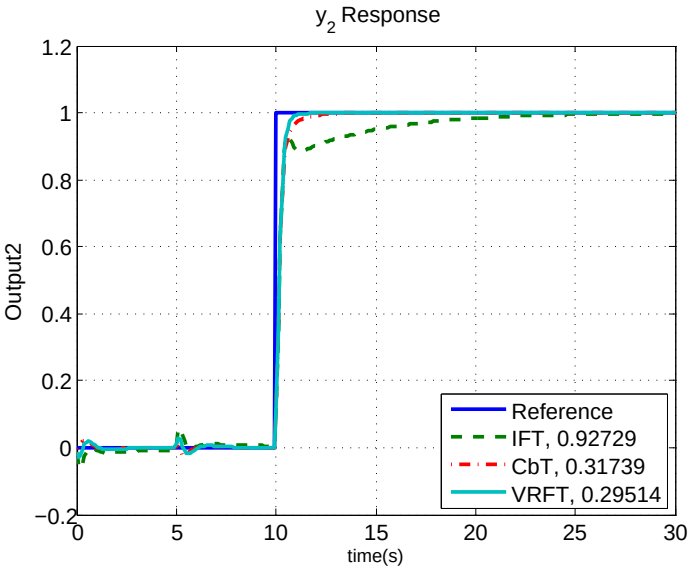

Figure 4.7: Response of the y_2 output of the three data driven methods.

4.3. Using Data for the Internal Model Control methodology

4.3.1. Overview of the Internal Model Control

Internal Model Control (IMC) is a popular and well known control method that incorporates the model of the process directly into the controller Morari and Zafirou (1989). The standard structure is depicted in Fig. 4.8. $P(z)$ represents the Plant, while $\bar{P}(z)$ is its model. $Q(z)$ is the IMC controller. In the absence of uncertainty, the control acts as if it was in open-loop control for the reference tracking but when a disturbance enters into the system, the same controller acts as closed-loop for the disturbance rejection. If $Q(z)$ is designed as $Q(z) = P(z)^{-1}f(z)$ and $\bar{P}(z) = P(z)$, the output ideally becomes

$$y = f(z)r + (1 - f(z))d \tag{4.16}$$

It is clear that, to have perfect model matching control (in closed-loop, the desired dynamics are given by $f(z)$), $Q(z)$ must try to cancel the dynamics of the plant. This characteristic leads to the well know property that an IMC system would be nominally internally stable if $Q(z)$ is stable, in case the model is equal to the plant. Finding a perfect model is rarely achievable and if it were, $Q(z)$ may not be possible to contain the inverse of this model due to physical limitations or because the inverse of the plant may lead to an unstable controller. In Morari and Zafirou (1989) a two-step design is proposed for this kind of controller:

1. Solve the nominal performance criterion given, for example, by

$$\min_{\bar{Q}(z)} \left\| \left(1 - \bar{P}(z)\bar{Q}(z)\right) W(z) \right\|_p \tag{4.17}$$

   Where $W(z)$ is a filter chosen to give more importance in certain frequencies and $\|\cdot\|_p$ is a given norm that defines the performance criterion. The optimal solution of this problem yields to a sensitivity function given by $S^*(z) = 1 - \bar{P}(z)\bar{Q}(z)$ and the complementary sensitivity function given by $M^*(z) = \bar{P}(z)\bar{Q}(z)$, that is, the response to a change in the reference is as if it were in open loop, while the response to a disturbance is in closed-loop.

2. To introduce robustness considerations, the complementary sensitivity has to be rolled off at high frequencies, therefore, it is necessary to add a low pass filter $f(z)$ to the controller $\bar{Q}(z)$, to obtain the final controller $Q(z) = \bar{Q}(z)f(z)$. Suppose that the multiplicative uncertainty is bounded by a frequency dependent function $\bar{l}_m(\omega)$,

$$\left| \frac{P(e^{\jmath\omega}) - \bar{P}(e^{\jmath\omega})}{\bar{P}(e^{\jmath\omega})} \right| \leq \bar{l}_m(\omega)$$

   The closed-loop system is robustly stable if and only if

$$|f(e^{\jmath\omega})| < \frac{1}{\left|\bar{P}(e^{\jmath\omega})\bar{Q}(e^{\jmath\omega})\bar{l}_m(\omega)\right|} \qquad \forall\omega \tag{4.18}$$

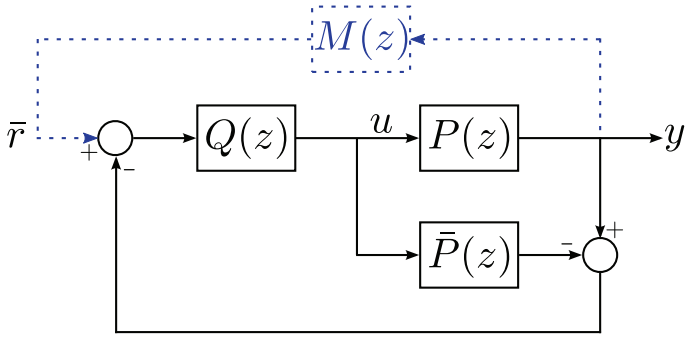

Figure 4.8: Standard Structure of the IMC. $\bar{P(z)}$ represents the plant model and $Q(z)$ is the IMC controller. The dashed line represents the virtual signal for the VRFT procedure.

IMC control has become very popular because, finding the controller and the conditions for robust stability can be cast in a very simple form. As seen in (4.16), the $Q(z)$ controller just need to be set as the best approximation of the inverse of the model multiplied by a filter that defines the desired behavior in closed-loop. In addition to this, under certain conditions on the model of the plant, the final controller (the combination of $Q(z)$ and $\bar{P}(z)$) can be rewritten as a PID controller, allowing to use the IMC method directly to tune this kind of controllers, which are widely used in industry (Aström and Hägglund, 2001).

Having a good model and an approximation of the uncertainty is vital for IMC. Since the model is an integral part of the controller, the use of data-driven control is proposed to jump from the data to the controller directly and to used the same information to find an approximation of the plant. The VRFT is the selected framework for this task, given its flexibility to apply the "virtual signal" concept into different structures.

4.3.2. The IMC-VRFT

For the case of IMC, in Fig. 4.8, the experimental setup for VRFT is depicted. If the target complementary sensitivity function is given by $M(z)$, then the virtual reference $\bar{r}(t)$ is computed as

$$\bar{r}(t) = M^{-1}(z)y(t) \tag{4.19}$$

From Fig 4.8, it can be found that the ideal controller would be given by

$$\begin{aligned} Q_0(z) &= M(z)P(z)^{-1} \\ \bar{P}_0(z) &= M(z)Q_0(z)^{-1} \end{aligned} \tag{4.20}$$

where $P_0(z)$ is the ideal plant model that is derived from the ideal controller. Note here the model is purely instrumental and defined from the controller. This is opposite as in IMC where the controller is directly derived from the model. This basic idea leads to the following

optimization problem which gives the set of optimal parameters θ^* (in a least squares sense):

$$\min_{\theta} J(\theta) = \min_{\theta} \sum_{i=1}^{N} \left(u(i) - Q(z;\theta)\bar{r}(i)\right)^2 \tag{4.21}$$

Once $Q(z;\theta^*)$ has been determined, it is easy to compute the approximation of the process model of the plant from (4.20):

$$\bar{P}(z;\theta^*) = M(z)Q(z;\theta^*)^{-1} \tag{4.22}$$

It is important to note that $\bar{P}(z,\theta)$ is seen just as an "instrumental model", that results from the determination of the optimal controller. This instrumental model is used as part of the control loop and, as presented in the next section, as the manner to describe a "nominal plant". In Data-Driven control, there is no nominal model of the plant, therefore, to define a test to check if the controller is robustly stable, it is necessary to approximate the plant by this "instrumental model". The filter for robust operation presented in (4.18), is already included in $Q(z,\theta^*)$ since the closed-loop behavior is expected to be $M(z)$, but it is not possible to know if condition (4.18) is fulfilled just by solving this optimization problem. It is therefore, desirable to count with a data-based test to check if this condition holds.

4.3.3. Robust Stability for the IMC-VRFT

When the closed-loop system is stable for all perturbed plants around the nominal model up to the worst-case model uncertainty, it is said to be robustly stable (Skogestad and Postlethwaite, 2007). In Data Driven Control it is difficult to find a controller that assures robust stability of the plant since not even a nominal model is available (in van Heusden et al. (2011) the stability problem is addressed by adding some constraints in the frequency domain directly into the optimization problem). However, it is possible to use (4.18) and the batch of input-output data, to test if the controller is robustly stabilizing the plant, before the actual controller is implemented, by approximating the uncertainty function $\bar{l}_m(\omega)$ from the instrumental model $\bar{P}(z;\theta^*)$.

Using the results on *Empirical Transfer Function Estimate* (ETFE) from Ljung (1999), given an input-output set of N points of data $\{u(t), y(t)\}_N$ from a plant $G(z)$ which transfer function is assumed to be unknown, the estimate of the frequency response is given by

$$\hat{G}_N\left(e^{\jmath\omega}\right) = \frac{Y_N(\omega)}{U_N(\omega} \tag{4.23}$$

where $U_N(\omega)$ and $Y_N(\omega)$ are given by

$$\begin{aligned} U_N(\omega) &= \frac{1}{\sqrt{N}} \sum_{t=1}^{N} \left(u(t)e^{-\jmath\omega t}\right) \\ Y_N(\omega) &= \frac{1}{\sqrt{N}} \sum_{t=1}^{N} \left(y(t)e^{-\jmath\omega t}\right) \end{aligned} \tag{4.24}$$

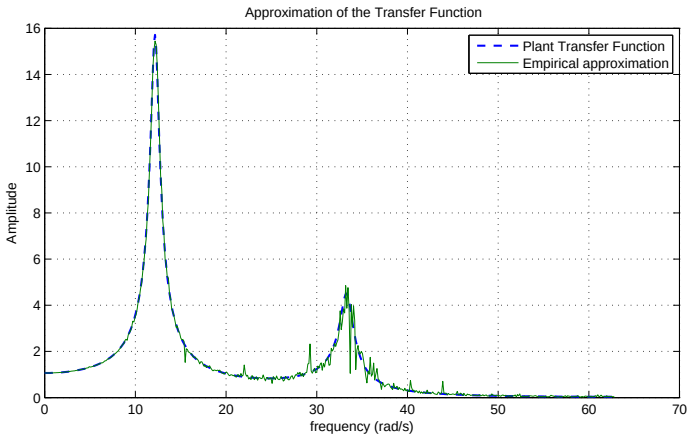

Figure 4.9: Approximation of the transfer function using open-loop data.

The essential frequency points are given in $\omega = 2\pi k/N,\ k = 0, 1, \ldots, N-1$. Other points are obtained by interpolation. For example, in Fig. 4.9 the comparison between the real frequency response and the empirical approximation is presented using a set of 1024 point of a PRBS signal on the plant given in Campi et al. (2002),

$$\begin{aligned} P(z) =& \frac{A(z)}{B(z)} \\ A(z) =& 0.2826z^{-3} + 0.5067z^{-4} \\ B(z) =& 1 - 1.418z^{-1} + 1.589z^{-2} \\ & - 1.316z^{-3} + 0.8864z^{-4} \end{aligned} \tag{4.25}$$

with sampling time $t_s = 0.05s$. As it can be seen the approximation is fairly good even for the resonant peaks.

According to Ljung (1999), the ETFE is an asymptotically unbiased estimate of the transfer function at increasingly (with N) many frequencies, but the variance of the ETFE do not decrease as N increases. That is why, in Fig. 4.9, the ETFE seems to be "noisy". To tackled this problem, the use of filtering windows is recommended to smooth the ETFE.

Approximation of $\bar{l}_m(\omega)$ and the robust stability test

If the uncertainty bound $\bar{l}_m(\omega)$ can be approximated using the ETFE, it will be possible to perform a data-based test to check Robust Stability using (4.18). In the case of the IMC-VRFT, the assumption on the instrumental model $\bar{P}(z)$ is that it is close enough to the real plant transfer function, in order to left the "nominal" stability depending on $Q(z)$: if $Q(z)$ is stable, the "nominal" closed-loop system is stable given that the plant is stable. If the controller has been found using the proposed approach, the filter $f(z)$, is assumed to be

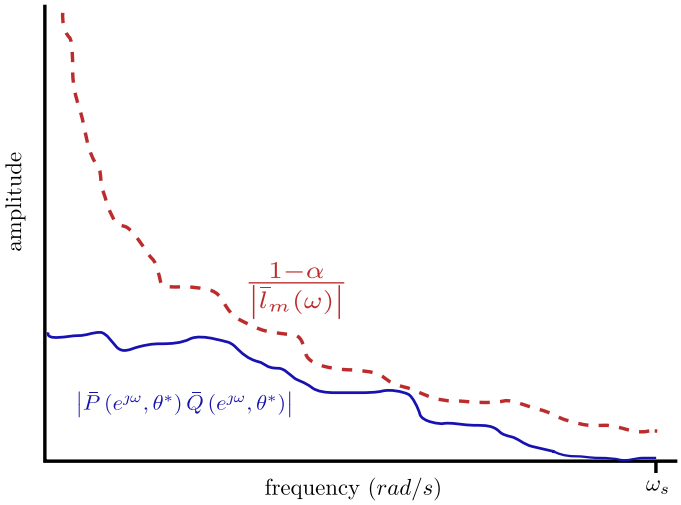

Figure 4.10: Graphical interpretation of the robust stability test.

already included in $Q(z)$ and (4.18) can be rewritten as

$$\left|\hat{\bar{P}}\left(e^{\jmath\omega},\theta^*\right)\hat{Q}\left(e^{\jmath\omega},\theta^*\right)\bar{l}_m(\omega)\right| \leq 1 \tag{4.26}$$

or, if a "security" constant $\alpha \geq 0$ is added to cope with possible errors when approximating $\bar{l}_m$

$$\left|\hat{\bar{P}}\left(e^{\jmath\omega},\theta^*\right)\hat{Q}\left(e^{\jmath\omega},\theta^*\right)\bar{l}_m(\omega)\right| \leq 1-\alpha \tag{4.27}$$

A graphical interpretation of (4.27) can be seen in Fig. 4.10: if at some point the dashed line falls below the solid line (which represents the complementary sensitivity function if the instrumental model is close enough to the transfer function of the plant) it means one is trying to extend the system beyond the limits uncertainty allows. At this point (4.27) fails, and it is not possible to assure robust stability with controller $Q(z,\theta^*)$ and given value of α.

To approximate (4.27), the frequency response of $Q(z,\theta^*)$ and $\bar{P}(z,\theta^*)$ can be calculated using the results of the optimization. $\bar{l}_m(\omega)$ is approximated using the definition of the multiplicative uncertainty and the ETFE approximation. The test can be stated as in Algorithm 1. If the test fails, the designer has two options: it is possible to increase the number of parameters of the controller or to relax the closed-loop specification $M(z)$. Once the new controller is found, the test can be performed again to check if the robust condition holds for the new setting.

4.3.4. Application example: continuous polymerization reaction

The plant for this example is a polymerization reaction that takes place in a jacketed CSTR. This plant is a 4 states non-linear plant used in Kansha et al. (2008) for a PID-like Adaptive VRFT control. The model for simulation is given by

Algorithm 1: Robust Stability Test

Find N points of input-output open-loop data from the plant: $\{u(t), y(t)\}_N$;
Define a value for α such as $\alpha \geq 0$;
Find $Q(z, \theta^*)$ and $\bar{P}(z, \theta^*)$, $Q(z, \theta^*)$ and $\bar{P}(z, \theta^*)$ have to be stable;
Define a set of frequencies ω;
Compute $y_{diff}(t)$ as $y_{diff}(t) = y(t) - \bar{P}u(t)$;
Compute $ymodel(t)$ as $y_{model}(t) = \bar{P}u(t)$;
Compute $\hat{G}_{diffN}\left(e^{\jmath\omega}\right)$ using $y_{diff}(t)$ as the output and $u(t)$ as the input with (4.23);
Compute $\hat{\bar{P}}_N\left(e^{\jmath\omega}\right)$ using $y_{model}(t)$ as the output and $u(t)$ as the input with (4.23);
Compute $\bar{l}_m(\omega) = \frac{\mathrm{abs}(\hat{G}_{diffN}(e^{\jmath\omega}))}{\mathrm{abs}(\hat{\bar{P}}_N(e^{\jmath\omega}))}$;
for *each* ω **do**
  if $\left|\hat{\bar{P}}\left(e^{\jmath\omega}, \theta^*\right)\hat{Q}\left(e^{\jmath\omega}, \theta^*\right)\bar{l}_m(\omega)\right| \leq 1 - \alpha$ **then**
    $failRobust(\omega) = 0$ (The system has Robust Stability for the given ω);
  else
    $failRobust(\omega) = 1$ (It is not possible to assure robust stability);
  end
end

Steady State operating condition	
C_m=5.506774 kmol/m^3	D_1=49.38182 kmol/m^3
C_I=0.132906 kmol/m^3	u=0.016783 m^3/h
D_0=0.0019752 kmol/m^3	y=25000.5 kg/kmol

Table 4.2: Steady state condition of the polymerization reactor.

$$\begin{aligned}
\frac{dC_m}{dt} &= -(k_P + k_{fm})C_m P_0 + \frac{F(C_{m_{in}} - C_m)}{V} \\
\frac{dC_I}{dt} &= -k_I C_I + \frac{F_I C_{I_{in}} - FC_I}{V} \\
\frac{dD_0}{dt} &= (0.5k_{T_C} + k_{T_d})P_0^2 + k_{fm}C_m P_0 - FD_0 \\
\frac{dD_1}{dt} &= M_m(k_P + k_{fm})C_m P_0 - \frac{FD_1}{V}
\end{aligned} \tag{4.28}$$

where $P_0 = \left(\frac{2fk_I C_I}{k_{T_d}+k_{T_c}}\right)^{0.5}$ and $y = \frac{D_1}{D_0}$. The parameters for the plant model are presented in Table 4.2 and Table 4.3 for completeness. The control objective is to regulate the product number average molecular weight(y) by manipulating the flow rate of the initiator(FI).

The procedure followed is the same as in the previous example. However, here an additional filter ($F_{rip}(z)$) was added to $Q(z)$ in order to eliminate the intersample rippling,

Model Parameters	
k_{Tc}=1.3281x10^{10} m^3/(kmol h)	F=1.00 m^3/h
k_{Td}=1.0930x10^{11} m^3/(kmol h)	V=0.1 m^3
k_I=1.0225x10^{-1} L/h	$C_{I_{in}}$=8.0 kmol/m^3
k_p=2.4952x10^6 m^3/(kmol h)	M_m=100.12 kg/kmol
k_{fm}=2.4522x10^3 m^3/(kmol h)	$C_{m_{in}}$=6.0 kmol/m^3
f^*=0.58	

Table 4.3: Model parameters of the polymerization reactor.

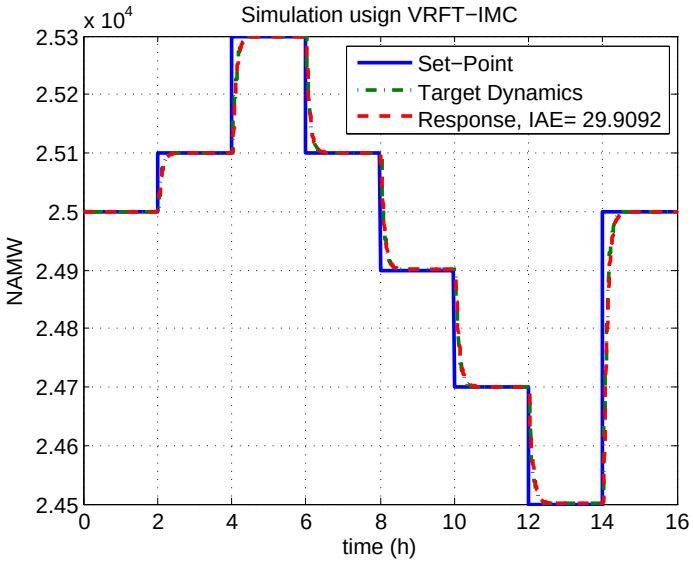

Figure 4.11: Response of the polymerization reaction using the IMC-VRFT. The negative real part of the poles were eliminated from controller Q.

i.e. eliminating the poles with negative real part of the controller (see Morari and Zafirou (1989)). The result of the application of the IMC-VRFT control in the operation point $u = 0.016783m^3/h, y = 25000.5kg/kmol$ is presented in Fig. 4.11. The batch of open loop data was collected using a random Gaussian signal as the input to the plant. The resulting controller and instrumental model became

$$\begin{aligned} Q(z) &= \frac{-1.238\text{x}10^{-5} + 9.593\text{x}10^{-6}z^{-1}}{1 + 0.7578z^{-1}} \\ \bar{P}(z) &= \frac{-0.28z^{-1} - 0.2122z^{-2}}{\left(\begin{array}{c} 1.238\text{x}10^{-5} - 1.851\text{x}10^{-5}z^{-1} \\ +6.907\text{x}10^{-6}z^{-2} \end{array}\right)} \\ F_{rip}(z) &= 0.5689 + 0.4311z^{-1} \end{aligned} \tag{4.29}$$

with a sampling time $T_s = 0.03$. In the neighborhood of $y = 25000.5kg/kmol$ the response

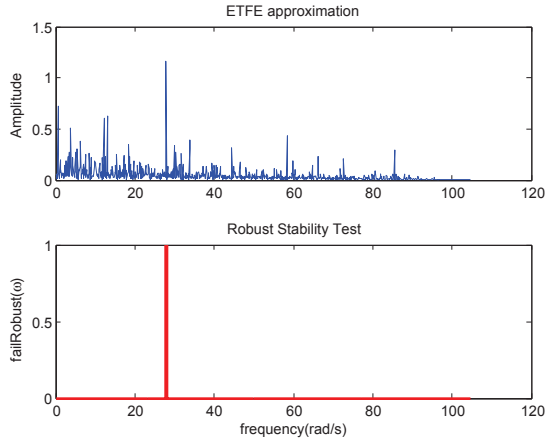

Figure 4.12: Robust stability test done over the polymerization plant.

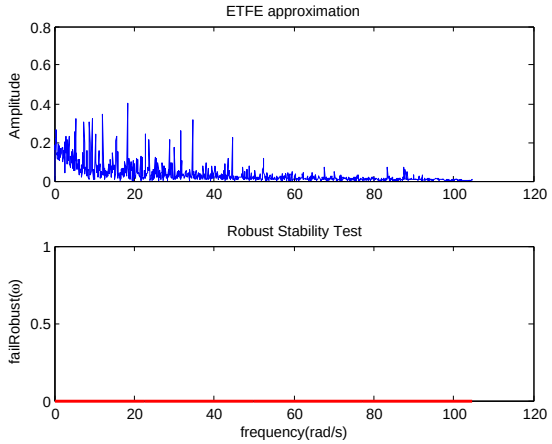

Figure 4.13: Robust stability test done over the polymerization plant with a slower desired response.

of the closed-loop system is almost equal to the specified desired response which is given by

$$M(z) = \frac{0.28z^{-1}}{1 - 0.72z^{-1}} \tag{4.30}$$

The stability test is presented in Fig. 4.12 for $\alpha = 0$. As it can be seen, only a point is over 1, representing that one may not be able to guarantee the robust stability. If the desired response is made slower $M(z) = \frac{0.15z^{-1}}{1-0.85z^{-1}}$, the test results as presented in Fig. 4.13, meaning that robustness is achieved. But it is important to note that since this test is dependent on the input-output data, a single point may be misleading to say that the result is not robustly stabilizing since it could be higher than one because certain approximation error.

Part II.

Applications of the Virtual Reference Feedback Tuning

5. Application to wastewater treatment plants

The Benchmark Simulation Model 1 (BSM1) is an effort made under COST Action 682 (Integrated Wastewater Management) and 624 [1]. According to Copp (2002) This action "is dedicated to the optimization of performance and cost-effectiveness of water management systems. (...) The "simulation benchmark" is a fully defined protocol and was developed as a tool for evaluating activated sludge wastewater treatment control strategies."

In this chapter, the basics on Wastewater Treatment Plant (WWTP) are covered by a literature review. Firstly on a general overview on WWTP is presented as an introduction to the topic and to the BSM1. In section 5.1.1 the Activated Sludge Model 1 (ASM1) is presented as the principal component of a the BSM1. The ASM1 is a dynamical model that attempts to model the processes in the bioreactors of a WWTP, focusing on carbon and nitrogen removal. The other main component of the BSM1 is the settler model, that was chosen to be the double-exponential model from Takács et al. (1991) and is treated in section 5.1.2. On section 5.2, the different applications of the VRFT to the WWTP's are presented and discussed.

5.1. Introduction to wastewater treatment plants

Today, environmental awareness is an important issue in politics, economy and daily life. It is not strange to find news about how the human activities have affected nature (for example global warming, energy resources, extinction of animal and plant species, and a long etcetera). This rise in concern about the effects of urban life in the ecological cycle has in turn, activated several research areas that has attempted to tackle part of this problem in one or another way. Today, much of the civil research concentrates on new sources of clean energy, transportation and of course, wastewater treatment.

Wastewater is defined as the residual water after it has been used in residential zones, industrial or rain water, that is collected through sewers and is intended to be deposited in a receiving waters (for example rivers or the sea), after it has been adequately threated. According to Olsson and Newell (1999) "while the primary goal of a treatment plant is to achieve an average reduction in nutrient levels, the secondary goal is disturbance rejection, to achieve good effluent quality in spite of the many disturbances". These disturbance mainly refers to the large variability of the influent, with respect to its components' concentrations, the flow volume, etc. For example in Henze et al. (1997), it is shown an example were the influent

[1] COST stands for the European Cooperation in the field of Scientific and Technical Research

flow at midday can reach up to 244% of the average flow in one day, while minimun could reach 32% of the average flow. Temperature is also a source of disturbances, but as it will be seen in the section about modeling, this is a factor that is not taken into account in current models.

Biological processes are normally used in WWTP, being the Activated Sludge Process (ASP) one of the most important methods (Henze et al., 1997). Bacteria, is the most important component of the sludge since, they help to the removal of carbon components as well as nitrogenous components from the influent. The basic idea of the ASP, is clearly presented in Jeppsson (1996):

> The basic idea of the activated sludge process is to maintain "active sludge" suspended in wastewater by means of stirring or aeration. The suspended material contains not only living biomass, that is, bacteria and other microorganisms, but also organic and inorganic particles. Some of the organic particles may be broken down into simpler components by a process known as hydrolysis, while other organic particles are not affected (inert material). The biomass in the process will use the organic material as its energy source (usually in combination with oxygen or another oxidation agent), that is, the organic material will be removed from the wastewater while more biomass is produced. The amount of suspended material in the process is normally controlled by means of adding a sedimentation tank at the end of the process, where the biomass is transported towards the bottom by gravity settling and is either recirculated back to the biological process or removed from the system as excess sludge, whereas the now purified wastewater is withdrawn from the top of the sedimentation tank and released either for further treatment or directly into a receiving water.

But, as point out by Olsson and Newell (1999), not only the ASP plays a part in the WWTP's, but a primary physical treatment takes place before the bioreactors where the large particles are screened and floating greases and oils are skims off. An also, a final settling is performed after the biological process. The objective of this settling is to separate the effluent ("clean" water) to the recirculating flow, that is used to keep certain degree of control of the bacteria population. In sections 5.1.1 and 5.1.2 a more detailed overview on the ASP and the settler modeling are presented.

5.1.1. Activated sludge model

The Activated Sludge Treatment plant is one of the most used process in Wasted Water Treatment Plants. As stated by Henze et al. (1997):

> The principle in activated sludge plants is that a mass of activated sludge is kept moving in water by stirring or aeration. Apart from the living biomass, the suspended solids contain inorganic as well as organic particles. Some of the organic particles can be degraded by subjecting them to hydrolysis whereas other are non-degradable (inert).
>
> The amount of suspended solids in the treatment plant is regulated through recy-

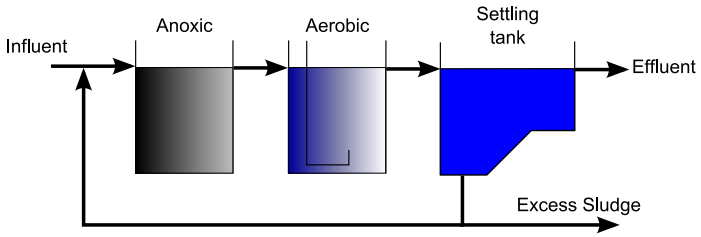

Figure 5.1: Simple layout of an activated sludge process.

cle of the suspended solids and by removing the so-called excess sludge.

At least, "Activated Sludge" Plants, must have an aeration thank and a settling thank where the treated wastewater is deposited in the receiving water while a concentrated sludge is withdrawn from the bottom (Henze et al., 1997). This concentrated sludge can be recycled in order to maintain a high density of biomass in the thanks. If the plant is also used for nitrogen removal, anoxic thanks (without aeration and ideally, without oxygen) are also set in the plant. A very basic layout is presented in fig. 5.1. In the Activated Sludge Process (ASP), the carbon and nitrogen removal are the most important subprocess that are modeled. This two subprocess are considered in the Activated Sludge Model No 1 (ASM1) which is one of the most used and important models in the WWT research field (Gernaey et al., 2004). It is promoted by the IAWPRC Task group on mathematical modeling for design and operation of biological wastewater treatment. Some other models have appear after the ASM1, the ASM2 and ASM2d includes the modeling of phosphorus removal while the ASM3 is aimed to improve ASM1 while taking into account the importance of storage polymers in the heterotrophic activated sludge conversions (Gernaey et al., 2004).

In the following, the carbon and the nitrogen removal are studied and at the end of the section, the ASM1 is detailed.

Carbon Removal in the Activated Sludge Process

In fig. 5.2 the interactions between several components are presented. As it can be seen, the growth of heterotrophs is the principal process that promotes the removal of carbon. In fig. 5.2 the aerobic grown is the important factor while also anoxic growth of heterotrophs also helps in the removal of carbon. The difference is that, the bacteria in the first case, take the oxygen from the air in the aerated tank while in the second case the oxygen is taken from nitrites and nitrate compound.

If only the carbon removal is taken into account, in an aerated tank, three different mass balance have to be wrote, for the heterotrophic biomass concentration ($X_{B,H}$, mg/l), the

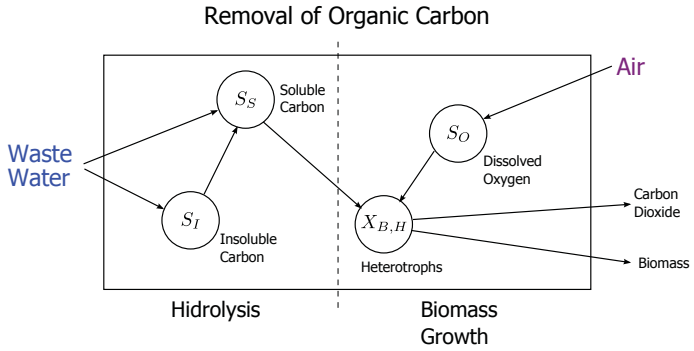

Figure 5.2: Carbon removal in the ASP.

soluble carbon nutrient concentration (S_S, mg/l), and the oxygen concentration (S_O, mg/l):

$$\frac{d}{dt}\left(VX_{B,H}\right) = q_{in}X_{B,H,in} - q_{out}X_{B,H,out} + r_H V \tag{5.1}$$

$$\frac{d}{dt}\left(VS_S\right) = q_{in}S_{S,in} - q_{out}S_{S,out} + r_S V \tag{5.2}$$

$$\frac{d}{dt}\left(VS_O\right) = q_{in}S_{O,in} - q_{out}S_{O,out} + r_O V + K_L a\left(S_{O,sat} - S_O\right)V \tag{5.3}$$

V is the volume of the tank (is considered to be constant), q_{in} is the input flow, $q_o ut$ is the output flow, r_H is the reaction rate for biomass growth (mg/l/day), r_S is the nutrient reaction rate (mg/l/day), r_O is the oxygen consumption rate (mg/l/day) and the $K_L a$ is the mass transfer from the aeration. Moreover if the tank is supposed to be well-mixed $X_{B,H} = X_{B,H,out}$, $S_S = S_{S,out}$ and $S_O = S_{O,out}$. The values of the reaction rates depends on the stoichiometry (the relationship between components in a reaction) and the kinetics of the reaction. This values often are based on empirical experiments. For example, the kinetics usually are modeled with a Monod rate expression (Monod, 1949). In general, the biological growth can be expressed as (Henze et al., 1997):

$$r_{V,X_{B,H}} = \mu_{max} \cdot f(S) \cdot X_{B,H} \tag{5.4}$$

where $r_{V,X_{H,B}}$ is the volumetric biological growth (dimension M $\cdot$L^{-3} $\cdot$T^{-1}), μ_{max} is the maximum specific growth rate (dimension T^{-1}), $f(S)$ describes the growth kinetics depending on the substrate concentration, and $X_{H,B}$ is the concentration of biomass (dimension M$_X$ $\cdot$L^{-3}). In the other hand, the substrate consumption can be written as:

$$r_{V,S} = \frac{\left(r_{V,X_{B,H}}\right)}{Y_{max}} \tag{5.5}$$

Y_{max} is the maximum yield constant (dimension M$_{XB}$ $\cdot$M$_S^{-1}$). In the case of decay of biomass, it is supposed that the rate of date is proportional to the concentration of biomass, that is $r_{V,X_{B,H}} = b \cdot X_B$. The common way to express this rates is in table manner. For example in Olsson and Newell (1999) and for this simple process, the rates are express as: In

Process	Components			Kinetics
	Nutrient	Oxygen	Biomass	
Aerobic heterotrophic growth	$-\frac{1}{Y_H}$	$\frac{Y_H-1}{Y_H}$	1	$\hat{\mu}_H \left(\frac{S_S}{K_S+S_S}\right)\left(\frac{S_O}{K_{OH}+S_O}\right) X_{B,H}$
Decay of heterotroph	$1-f_p$		-1	$b_H X_{B,H}$

Table 5.1: Reaction rates for the carbon removal process.

each row, the stoichiometry of each process is presented with the respective kinetics. In each column, the state variables are presented. With this format, each reaction rate can be found by summing the product of each stoichiometry component with the kinetic of the process for each row. For example, for the nutrient reaction rate we found that:

$$r_S = -\frac{1}{Y_H} \cdot \hat{\mu}_H \left(\frac{S_S}{K_S + S_S}\right)\left(\frac{S_O}{K_{OH} + S_O}\right) X_{B,H} + (1 - f_p) \cdot b_H X_{B,H}$$

Then this rate is introduced in (5.2). As it can be seen, the model becomes highly non-linear even due the mass balance is simple.

$$\begin{aligned}\frac{d}{dt}(VS_S) = {} & q_{in}S_{S,in} - q_{out}S_{S,out} \\ & + \left(-\frac{1}{Y_H} \cdot \hat{\mu}_H \left(\frac{S_S}{K_S + S_S}\right)\left(\frac{S_O}{K_{OH} + S_O}\right) X_{B,H}\right. \\ & \left. + (1 - f_p) \cdot b_H X_{B,H}\right) V\end{aligned}$$

In the ASM1, 13 state variables are considered (with corresponding conversion rates), with 8 different biological processes. This represents 5 stoichiometric parameters and 14 kinetic parameters. As it can be seen, even for this simple and structured modeling procedure, the final model becomes very complex and difficult to calibrate.

Nitrogen Removal in the ASP

It is considered that the nitrogen enters the plant as ammonium compounds and is removed from the system by a two step mechanism: nitrification and denitrification (Olsson and Newell, 1999). In the nitrification step, the autotroph bacteria in the aerated tank use the ammonium compounds, the carbon compounds and the dissolved oxygen to synthesize nitrites and nitrates. Then in the anoxic tank, the growth of heterotroph biomass is carried out using the nitrites and nitrates as the oxygen source and liberate the nitrogen as gas, removing it from the wastewater. This process is depicted in fig. 5.3.

The modeling of this process kinetics is made in a similar way that carbon removal process.

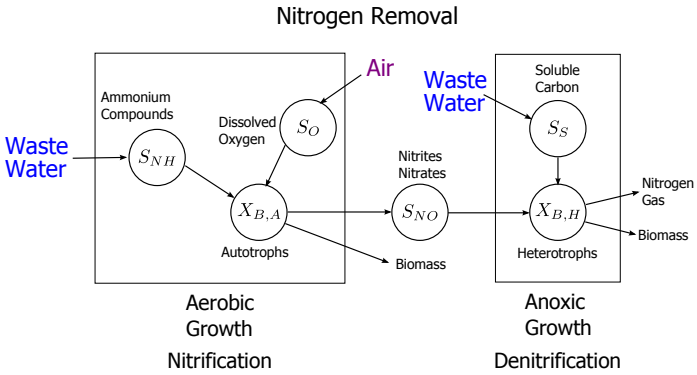

Figure 5.3: Nitrogen Removal in the ASP.

Variable	Definition
S_I	Soluble inert organic matter
S_S	Readily biodegradable substrate
X_I	Particulate inert organic matter
X_S	Slowly biodegradable substrate
$X_{B,H}$	Active heterotrophic biomass
$X_{B,A}$	Active autotrophic biomass
X_P	Particulate products arising from biomass decay
S_O	Oxygen
S_{NO}	Nitrate and nitrite nitrogen
S_{NH}	$NH_4^+ + NH_3$ nitrogen
S_{ND}	Soluble biodegradable organic nitrogen
X_{ND}	Particulate biodegradable organic nitrogen
S_{ALK}	Alkalinity

Table 5.2: State variables in the ASM1.

As it can bee seen, basically, the important factor are the organic matter (in its form of biodegradable, inert, soluble and particulate), nitrogen matter and oxygen.

The Activated Sludge Model 1

The ASM1 is promoted by the Task Group on Mathematical Modeling for Design and Operation of Activated Sludge Processes of the International Association on Water Pollution Research and Control (IAWPRC). It was first published in 1987 and was aimed to be use as a common platform for researchers in the field and to include the nitrogen removal in the model. A detailed presentation of the model can be found in Henze et al. (2002) while the basics are covered in Henze et al. (1997) and Olsson and Newell (1999).

In table 5.3 the kinetics and the stoichiometric parameters are reproduced as presented in Henze et al. (2002) where all the organic constituents are expressed as equivalent chemical

Process (j)/ Component (i)	1 S_I	2 S_S	3 X_I	4 X_S	5 $X_{B,H}$	6 $X_{B,A}$	7 X_P	8 S_O	9 S_{NO}	10 S_{NH}	11 S_{ND}	12 X_{ND}	13 S_{ALK}	Process Rate, $\rho_j\,[ML^{-3}T^{-1}]$
1 Aerobic growth of heterotrophs		$-\frac{1}{Y_H}$			1			$-\frac{1-Y_H}{Y_H}$		$-i_{XB}$			$-\frac{i_{XB}}{14}$	$\hat{\mu}_H\left(\frac{S_S}{K_S+S_S}\right)\left(\frac{S_O}{K_{O,H}+S_O}\right)X_{B,H}$
2 Anoxic growth of heterotrophs		$-\frac{1}{Y_H}$			1				$-\frac{1-Y_H}{2.86Y_H}$	$-i_{XB}$			$\frac{1-Y_H}{14\cdot 2.86Y_H}-\frac{i_{XB}}{14}$	$\hat{\mu}_H\left(\frac{S_S}{K_S+S_S}\right)\left(\frac{K_{O,H}}{K_{O,H}+S_O}\right)$ $\times\left(\frac{S_{NO}}{K_{NO}+S_{NO}}\right)\eta_g X_{B,H}$
3 Aerobic growth of autotrophs						1		$-\frac{4.57-Y_A}{Y_A}$	$\frac{1}{Y_A}$	$-i_{XB}-\frac{1}{Y_A}$			$-\frac{i_{XB}}{14}-\frac{1}{7Y_A}$	$\hat{\mu}_A\left(\frac{S_{NH}}{K_{NH}+S_{NH}}\right)\left(\frac{S_O}{K_{O,A}+S_O}\right)X_{B,A}$
4 Decay of heterotrophs				$1-f_P$	-1		f_P					$i_{XB}-fri_{XP}$		$b_H X_{B,H}$
5 Decay of autotrophs				$1-f_P$		-1	f_P					$i_{XB}-fri_{XP}$		$b_A X_{B,A}$
6 Ammonification of soluble organic nitrogen										1	-1		$\frac{1}{14}$	$k_a S_{ND} X_{B,H}$
7 Hydrolysis of entrapped organics		1		-1										$k_h\frac{X_S/X_{B,H}}{K_X+(X_S/X_{B,H})}\left[\left(\frac{S_O}{K_{O,H}+S_O}\right)+\eta_h\left(\frac{K_{O,H}}{K_{O,H}+S_O}\right)\left(\frac{S_{NO}}{K_{NO}+S_{NO}}\right)\right]X_{B,H}$
8 Hydrolysis of entrapped organics nitrogen											1	-1		$\rho_7\left(\frac{X_{ND}}{X_S}\right)$
Observed Conversion Rates $[ML^{-3}T^{-1}]$									$r_i=\sum_j v_{ij}\rho_j$					
Stoichiometric Parameters: Heterotrophic yield Y_H Autotrophic yield: Y_A Fraction of biomass yielding particulate products: f_p Mass N/Mass COD in biomass: i_{XB} Mass N/Mass COD in products from biomass: i_{XP}	Soluble Inert organic matter $[M(COD)L^{-3}]$	Readily biodegradable matter $[M(COD)L^{-3}]$	Particulate Inert organic matter $[M(COD)L^{-3}]$	Slowly biodegradable substrate $[M(COD)L^{-3}]$	Active heterotrophic biomass $[M(COD)L^{-3}]$	Active autotrophic biomass $[M(COD)L^{-3}]$	Particulate products arising from biomass decay $[M(COD)L^{-3}]$	Oxygen (negative COD) $[M(-COD)L^{-3}]$	Nitrate and nitrite nitrogen $[M(N)L^{-3}]$	$NH_4^+ + NH_3$ nitrogen $[M(N)L^{-3}]$	Soluble biodegradable organic nitrogen $[M(N)L^{-3}]$	Particulate biodegradable organic nitrogen $[M(N)L^{-3}]$	Alkalinity- Molar Units	Kinetic Parameters: Heterotrophic growth and decay $\hat{\mu}_H, K_S, K_{O,H}, K_{NO}, b_H$ Autotrophic growth and decay: $\hat{\mu}_A, K_{NH}, K_{O,A}, b_A$ Correction factor for anoxic growth of heterotrophs: η_g Ammonification: k_a Hydrolysis: k_h, K_X Correction Factor for anoxic hydrolysis: η_h

Table 5.3: ASP model for carbon oxidation, nitrification and denitrification.

oxygen demand (COD). According to Olsson and Newell (1999), COD is a "test (that) measures the amount of oxygen required for chemical oxidation of organic matter in the sample to carbon dioxide and water. The laboratory test procedure is to add a known quantity of standard potassium dichromate solution, sulfuric acid reagent containing silver sulfate, and a measured volume of sample to a flask. This mixture is vaporised and condensed for 2 hours. After the mixture is cooled and diluted with distilled water and the condenser has been washed down the dicromated remaining, in the specimen, it is titrated with standard ferrous ammonium sulfate using ferroin indicator" Using the volumes of titrate and sample, it is possible to compute the COD.

The processes involved in the model are the g*growth of biomass, decay of biomass, ammonification of organic nitrogen, and hydrolysis of particulate organics which are entrapped in the biofloc*. The model comprises the state variables presented in table 5.2.

5.1.2. Settler modeling

For the BSM1, a secondary settler for the clarification and settling of the wastewater after the biological treatment is included. The modeling of the settling of the sludge is based on the one presented in Takács et al. (1991). It is supposed that there is no biological process in the settler, that the incoming solids are distributed instantaneously and uniformly across the entire cross-sectional area and only vertical flow is considered. It is considered that the settler can be divided in several layers and based on empirical observation, the solid flux due to gravity in each layer (J_s) is considered to be dependent on the sludge concentration of each layer as:

$$J_s = v_s(X)X \tag{5.6}$$

where v_s is the velocity function, which is a modified version of the Vesilind velocity (Takács et al., 1991) aimed to take into account the clarifying function in the upper layers where the concentration of the sludge is lower:

$$\begin{aligned} v_s &= v_0 \left(e^{-r_h(X-X_{min})} - e^{-r_p(X-X_{min})} \right) \\ & 0 < v_s < v_{max} \\ & X_{min} = f_{ns} X_f \end{aligned} \tag{5.7}$$

where r_h is the hindered zone settling parameter, r_p is the flocculant zone settling parameter, v_0 is the Vesilind settling velocity, v_{max} is the maximum settling velocity, f_{ns} is the fraction of the flow that will not settle and X_f is the input concentration of the sludge.

When the differential equation of the model has to be written down, the figure found in Takács et al. (1991) (and reproduced in Fig. 5.4) becomes useful.

The concentration in each layers are considered as the state variables. Two velocities are taken into account: the velocity produced by the bulk movement of the water and other due to gravity. For each layer, the bulk velocity is dependent of the output flows (the effluent flow rate Q_i determines the upward velocity of each layer $J_{up,i}$, while the recycle and wastage flow rate Q_r determines the downward velocity of each layer $J_{dn,i}$). The velocity due to gravity

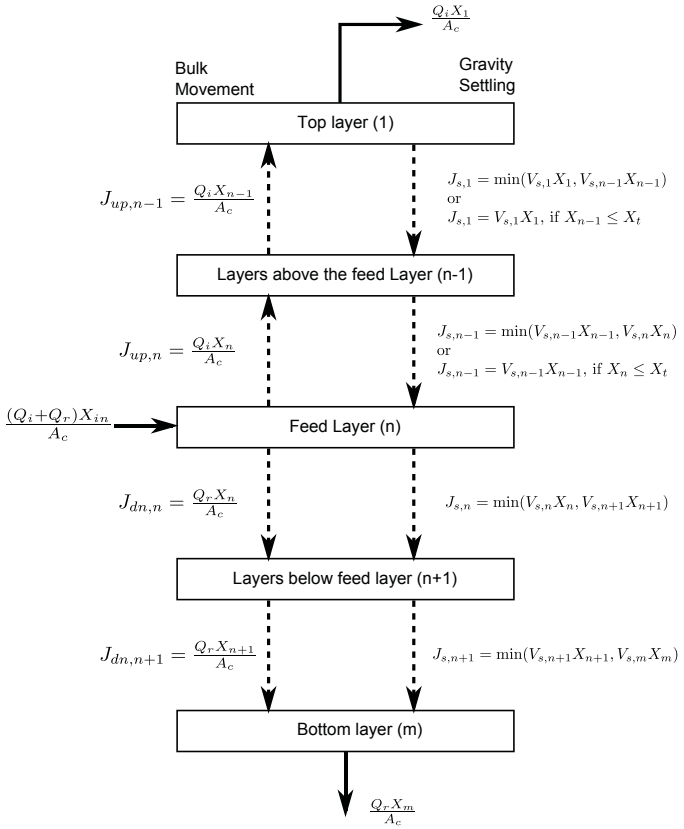

Figure 5.4: Mass balance for the solids in the settler.

is computed using 5.7 depending on the concentration between each layer and a threshold concentration. For example, the solid balance for the feed layer in fig 5.4 would be:

$$\frac{dX_n}{dt} \cdot h = \frac{(Q_i + Q_r)\, X_{in}}{A_c} - \frac{Q_i X_n}{A_c} - \frac{Q_r X_n}{A_c} + J_{s,n-1} - J_{s,n} \tag{5.8}$$

where h is the height of the layers and A_c is the surface area of the layers, X_n is the concentration on layer n, Q_i is the effluent flowrate, Q_r is the wastage and recycle flowrate and $J_{s,n}$ is the settling velocity leaving layer n. For other soluble components, it is supposed that they are completely mixed and the change in its concentration only depends on the bulk velocity and the concentration in each layer.

5.1.3. The BSM1

The BSM1 is a benchmark model to test different control strategies on WWTP's. It is detailed in Copp (2002) and in Alex et al. (2008). The layout of the plant is presented in Fig. 5.5. The

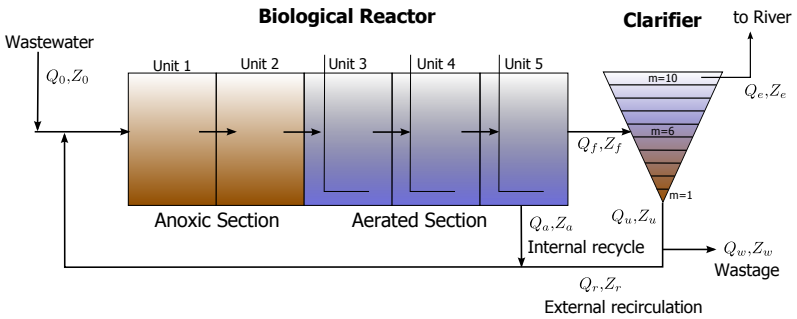

Figure 5.5: Layout of the BSM1. The first 2 bioreactor are anoxic (have nitrogen compounds but not are not aerated) and the last 3 are aerated.

WWTP has five bioreactors: the first two are anoxic (theoretically, they do not have oxygen) and the last two are aerated. A portion of the flow is recycled to the first bioreactor while the rest is introduced in the clarifier, where the biomass is separated from the effluent. The rest is separated in two: a portion is recycled and the rest is disposed (wastage).

Each one of the reactor are modeled as with the Activated Sludge Model 1 (Henze et al., 2002) that is detailed in section 5.1.1. In the aerated section, carbon removal is achieved by aerobic grown of heterotroph. For ammonia removal, a two steps process takes place: in the aerated section the ammonia is nitrificated by the growth of autotroph that use oxygen to convert ammonia into nitrite and nitrate. In the anoxic section, the nitrite and nitrate oxygen is used by the growth of heterotroph. The Clarifier is modeled according to the double exponential model from Takács et al. (1991).

The basic control strategy for this plant is a two-loops approach. The first loop would be to control the Dissolved Oxygen (DO) in the 5th thank by actuating on the oxygen transfer coefficient ($K_L a$) and the second would be to control the nitrate level in the last anoxic bioreactor by manipulating the internal recycle flow Q_a. The DO loop has very fast dynamics while the second is slower, so a perturbation or an action on the nitrate loop, would no affect the DO loop as much as a change in the DO loop over the nitrate control loop.

Quoting from Alex et al. (2008)

> The plant is designed for an average influent dry-weather flow rate of 18446 $m^3.d^{-1}$ and an average biodegradable COD in the influent of 300 $g.m^{-3}$. Its hydraulic retention time (based on average dry weather flow rate and total tank volume - i.e. biological reactor + settler- of 12000 m^3) is 14.4hours. The biological reactor volume and the settler volume are both equal to 6000 m^3. The wastage flow rate equals 385 $m^3.d^{-1}$.

The aim of the benchmark is to provide a standard model to compare different control strategies. For this reason, along with the definition of the plant, the mathematical model and some tips for the implementation, three different influent data are provided. This data represents the influent to the plant over two weeks, taking into account daily variations and storm events. The “Dry Influent” is presented in fig. 5.6 for the flow and the soluble components.

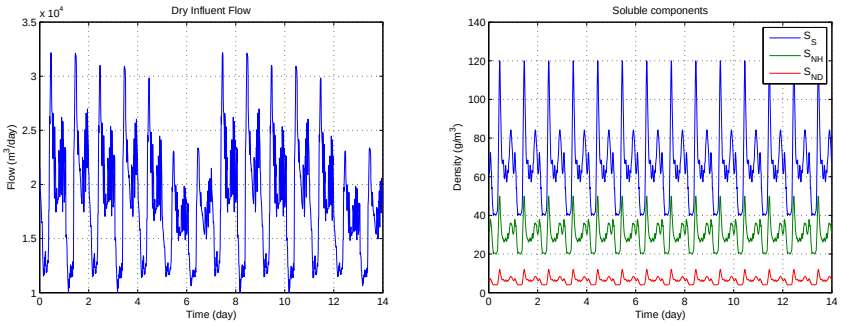

(a) Influent Flow **(b)** Influent Soluble components

Figure 5.6: "Dry Influent" flow and soluble components. Also the particulate components, alkalinity and the computation of the total suspended solids is part of the data.

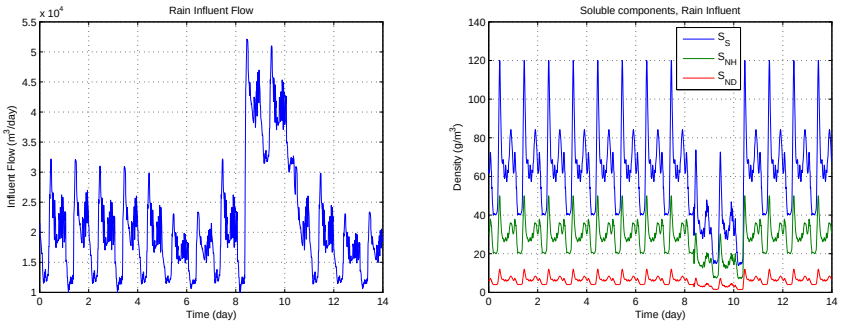

(a) Rain Influent Flow **(b)** Rain Influent Soluble components

Figure 5.7: Flow and soluble components for the rain influent data.

The other two influent data are based on the Dry Influent but the "Rain Influent" contains two storm event in the second week while the "Storm Influent" has a long rain event in the second week; these two influents are presented in fig. 5.7 and 5.8.

Performance Assessment

The benchmark also presents a series of performance index to measure the effectiveness of the control strategy. The average values of Nitrogen, Chemical Oxygen Demand (COD), Nitrate, Total suspended Solids and the Biochemical Oxygen Demand has to be under certain value, as presented in table 5.4.

The authors of the benchmark proposed two levels of performance:

- Control Level: in this case, the controller are tested using the Integral of the Absolute Error (IAE), the Integral of the Squared Error (ISE), the maximal deviation from the

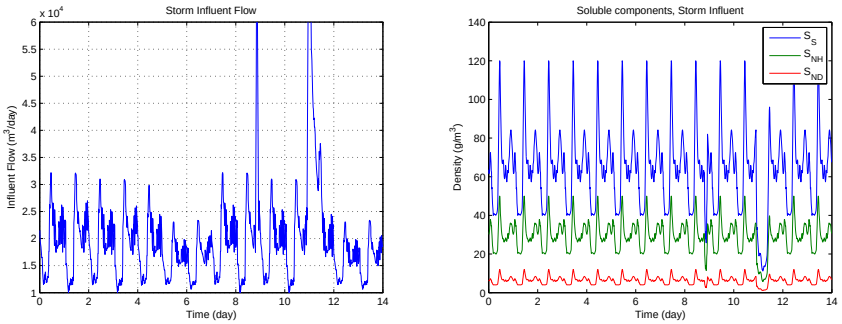

(a) Storm Influent Flow **(b)** Storm Influent Soluble components

Figure 5.8: Flow and soluble components for the storm influent data.

Variable	Value
N_{tot}	<18 gN.m^{-3}
$\mathrm{COD_t}$	<100 gCOD.m^{-3}
$\mathrm{S_{NH}}$	<4 gN.m^{-3}
TSS	<30 gSS.m^{-3}
$\mathrm{BOD_5}$	<10 gBOD.m^{-3}

Table 5.4: Maximum effluent limits in the BSM1.

setpoint and by error variance.

- Quality Indexes: In this level of assessment, the performance of the plant is considered by direct measuring from its state. Four measures are made:
  - Effluent Quality Index (EQI): Which measures the quantity of pollution of the effluent that is discharged in the receiving waters. It is calculated as:

$$EQI = \frac{1}{1000T}\int_{t=7days}^{t=14days} (EQI_{comp})\, Q_e(t)\mathrm{dt} \tag{5.9}$$

where

$$\begin{aligned} EQI_{comp} &= B_{SS}\cdot SS_e(t) + B_{COD}\cdot COD_e(t) \\ &\quad + B_{Nkj}\cdot S_{Nkj,e}(t) + B_{NO}\cdot S_{NO,e}(t) \\ &\quad + B_{BOD5}\cdot BOD_e(t) \\ S_{Nkj,e} &= S_{NH,e} + S_{ND,e} + X_{ND,e} + i_{XB}\,(X_{B,H,e} + X_{X,A,e}) \\ &\quad + i_{XP}\,(X_{P,e} + X_{i,e}) \\ SS_e &= 0.75\,(X_{s,e} + X_{l,e} + X_{B,H,e} + X_{p,e}) \end{aligned}$$

Factor	B_{SS}	B_{COD}	B_{NKj}	B_{NO}	B_{BOD5}
Value (g pollution units.g^{-1}	2	1	30	10	2

Table 5.5: Conversion factor for effluent quality measures.

$$BOD_{5,e} = 0.25\,(S_{S,e} + X_{S,e} + (1 - f_p)\,(X_{B,H,e} + X_{B,A,e}))$$
$$COD_e = S_{S,e} + S_{l,e} + X_{S,e} + X_{I,e} + X_{B,H,e} + X_{B,A,e} + X_{P,e}$$

and the weighting factors B_i convert the different types of pollution into pollution units. This factors were deduced from Vanrolleghem et al. (1996) and presented in Alex et al. (2008) as well. They are shown in table 5.5 for reference.

– Cost Factors for Operation: This measure indicates the cost of the controlled operation of the plant. It includes the sludge to be disposed, the aeration energy, the pumping energy, the consumption of external carbon sources and the mixing energy. For the sludge production to be disposed, the total solids flow from wastage and the solids accumulated in the system are considered. Since only the last 7 days of operation are considered for the computation of the indexes, the equations take into account only the values from day 7 to day 14: The Total Solids at time t is given by $TSS(t)$:

$$TSS(t) = TSS_a(t) + TSS_s(t)$$

where

$$TSS_a(t) = 0.75 \sum_{i=1}^{n} \left[(X_{s,i} + X_{I,i} + X_{B,A,i} + X_{P,i})\,V_i\right]$$
$$TSS_s(t) = 0.75 \sum_{j=1}^{m} \left[(X_{s,j} + X_{I,j} + X_{B,A,j} + X_{P,j})\,z_j A\right]$$

with $n = 5$ the number of bioreactor and $m = 10$ the numbers of layers of the settler. The Sludge Production (SP, kg.d $^{-1}$) is then given by

$$SP = \frac{1}{T}\Bigg(TSS(14day) - TSS(7day) + 0.75 \int_{7\text{day}}^{14\text{day}} (X_{s,w} + X_{I,w} + X_{B,H,w} + X_{B,A,w})\,Q_w(t)\;\mathrm{d}t\Bigg) \quad (5.10)$$

In the BSM1, the Pumping Energy (PE, kWh.d^{-1}) is calculated as:

$$PE = \frac{1}{T} \int_{7\text{day}}^{14\text{day}} 0.004 \cdot Q_a(t) + 0.008 \cdot Q_r(t) + 0.05 \cdot Q_w(t)\;\mathrm{d}t \quad (5.11)$$

And the Aeration Energy (AE, kWh.d^{-1}) is calculated as:

$$AE = \frac{S_O^{sat}}{T \cdot 1.8 \cdot 1000} \int_{7\text{day}}^{14\text{day}} \sum_{i=1}^{5} V_i K_L a_i(t) \, \mathrm{d}t \tag{5.12}$$

The Mixing Energy (ME, kWh.d^{-1}) used in the anoxic compartments is given by:

$$ME = \frac{24}{T} \int_{7\text{day}}^{14\text{day}} \sum_{i=1}^{5} \left[\begin{array}{c} 0.005 \cdot V_i \text{ if } K_L a_i(t) < 20 \text{ d}^{-1} \\ 0 \text{ otherwise} \end{array} \right] \mathrm{d}t \tag{5.13}$$

And the Overall Cost Index (OCI) is given by

$$OCI = AE + PE + 5 \cdot SP + 3 \cdot EC + ME \tag{5.14}$$

where EC is the external carbon consumption.

5.2. Different applications to WWTPs

In this section, the different application of the VRFT to WWTP are presented. First in section 5.2.1, an exploratory application is done using the BSM1 and the basic two degrees of freedom controllers. Then, in section 5.2.2 one step further is taken when feedforward control is added to try to cope with the disturbances produce by the variation in the influent characteristics. Finally in section 5.2.3

5.2.1. First Application of the VRFT to the BSM1

In order to test the VRFT approach on the BSM1, two basic loops were implemented:

- Dissolved Oxygen Loop: The DO is controlled in the output of the fifth tank by manipulating the oxygen transfer coefficient ($K_L a$). In the benchmark, the DO setpoint is 2mg/l. The output of the controller is limited between 0 and 360d^{-1}.
- Nitrate Nitrogen Loop: In this case, the Nitrate Nitrogen (SNO) in the second anoxic tank is controlled by manipulating the internal recycle flow (Q_a). The setpoint is 1mg/l and the output of the controller has to be between 0 and 92230 m^{3}d^{-1}.

The data was obtained by performing a test on the plant in steady state (constant disturbances). As stated in chapter 2, the Data-Driven methods do not need a model to compute the controller. The model presented in section 5.1.3 is very complex to be readily used to directly find the necessary controllers. The advantage of this data-driven approach is that, one is able to use the already well tuned model to directly compute a restricted order controller using the data from simulation. The idea is that, if one is able to have a model that is close to the real process, once the controller has been found using simulated data from this model, the

Control	S_{NH} $< 4mgN/l$	TSS $< 30mgN/l$	N_{tot} $< 18mgN/l$	COD $< 100mgCOD/l$	BOD_5 $< 10mgBOD/l$
Default Controllers	2.5392	13.0038	16.9245	48.2201	2.7568
VRFT Controllers	2.548	12.9912	17.2755	48.2095	2.7567
Difference	0.346%	-0.096%	2.07%	-0.021%	0.003%

Table 5.6: Important mean factor for dry weather Influent.

same controller could be use in the plant. A decentralized control of these two control loops is tackled in this case (Vilanova et al., 2009). The data used to find the Oxygen Controller is presented in Fig. 5.9. While the system is in steady state, the coefficient of oxygen transfer is changed and the effect on the dissolved oxygen is recorded. The target transfer functions for this loop are given by:

$$M(z) = \frac{0.3408z^{-1}}{1 - 0.6592z^{-1}} \tag{5.15}$$

$$S(z) = \frac{1 - z^{-1}}{1 - 0.4346z^{-1}} \tag{5.16}$$

This transfer functions were selected based in the settling time which are approximately 15min and 7min respectively. The sampling period is 1min. When the controller computed using VRFT is introduced in the loop, the response to a step change in the reference and a step disturbance on the oxygen concentration at the fifth tank is given in Fig. 5.10. As it can bee seen, in this case, the closed-loop response is close to the target one, but for the disturbance change it takes more time to settle than the desired time, but the output of the process is very close to the setpoint. Since the dynamics of the nitrate-nitrogen loop are slower, the changes in the oxygen loop take approximately one day to disappear, as shown in Fig. 5.11, but for this case, the overshoot of the nitrate-nitrogen remains under the 35% of the setpoint. A similar experiment was carried out for the nitrate-nitrogen closed loop, but in this case, the settling of the closed-loop transfer functions were chosen to be of 12 hours for the step change in reference and 6 hours for a disturbance in the nitrate-nitrogen at the output of the second anoxic tank. In this case the sampling period is 10 minutes. Using the topology in equation (3.24) and Fig. 2.4, the parameters for the oxygen loop are given by: $[\alpha_1, \alpha_2, \alpha_3, \alpha_4]^T = [97.99, -75.76, 131.2, -108.9]^T$; and for the nitrate-nitrogen loop by: $[\alpha_1, \alpha_2, \alpha_3, \alpha_4]^T = [2821, -1769, 7134, -6082]^T$.

The controllers were tested for a dry weather influent that covers 14 days. To compute the performance indexes, the initial states has to be found with a preliminary simulation of 100 day with constant influent, followed by a dry weather influent simulation. The concentration of ammonia for this influent is presented in Fig. 5.12 to show the range of variability of the disturbance and the repetitive behavior across the week. The values presented here are computed from the last seven days of simulation, taken the data every 15 minutes.

In table 5.6, the mean values of the important components are presented for both the VRFT controllers and the Default controllers of the BSM1. For all values, the mean is under the maximum mean value. When compared with the default controllers, it can be seen that the performance is as good as for the default controllers, except for the total nitrogen component,

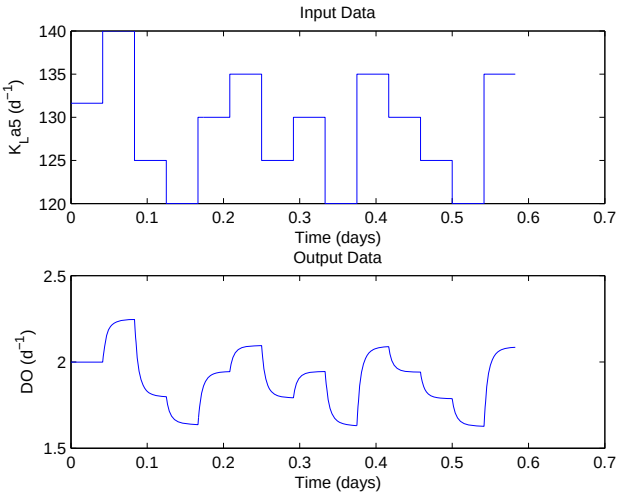

Figure 5.9: Data for the computation of the oxygen controller.

Control	Effluent Quality $kgpoll.units/d$	Operational Cost Index	Violation of S_{NO} (% of total time)	Violation of S_{NH} (% of total time)
Default Controllers	6123.0182	16382.4027	18.3036%	17.1131%
VRFT Controllers	6186.1812	16380.0646	21.4286%	17.7083%
Difference	1.031%	-0.001%	3.125%	0.5952%

Table 5.7: Performance Indexes for dry influent data.

which is 2.07% higher. But this results were found without any simplification of the model, using only data from the simulation and implementing the controller directly. The same conclusion is taken when observing the table 5.7: the performance index are very similar, except for the total nitrogen, for which the limit was violated 3.125% more of the total time. The results may be similar, but the VRFT provides an easy and methodological way of implementing simple controllers in a fast way, using the resources available at hand (in this case, the BSM1 model).

In Fig. 5.13 and Fig. 5.14, the plot of the violation in the limits are presented for the Total Nitrogen and the Ammonia in the effluent. It may be possible to keep all the peeks of the ammonia under the limit, if other layout is used, as in Vrecko et al. (2003), were only one of the tanks is anoxic and an oxygen controller is used in all the aerated tanks. It has to be remark that the controlled variables are not the ones that are taken into account in the performance of the plant. In Fig. 5.15, the closed-loop behavior of the controlled variables are plotted. As it can be seen, the oxygen loop has a good response to the disturbances, with a maximum deviation from the setpoint of approximately 5% of the setpoint.

In the other hand, the effect of the disturbances and the effect of the oxygen closed-loop make the nitrate loop to perform badly. It is possible to improve the performance using the

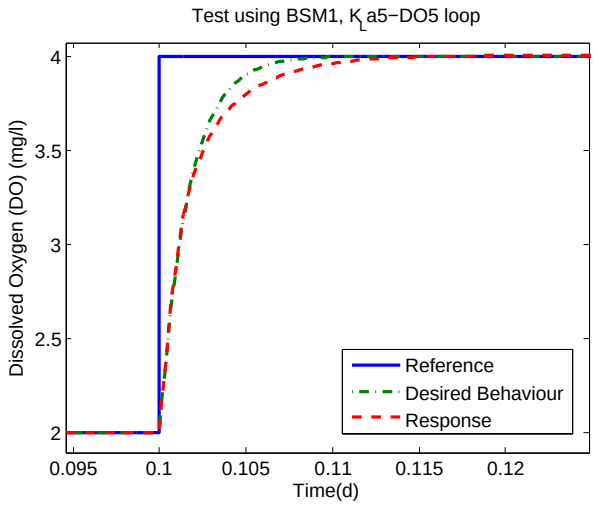

(a) Reference

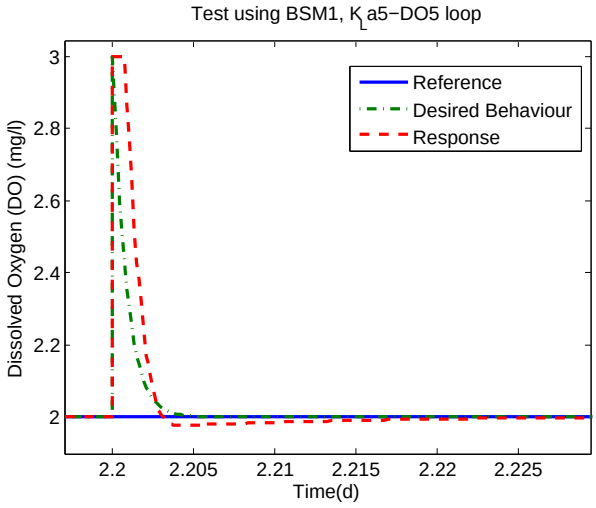

(b) Disturbance

Figure 5.10: Response of the oxygen loop to a step change in (a) the reference (b) a disturbance of the oxygen concentration at the output of the fifth tank.

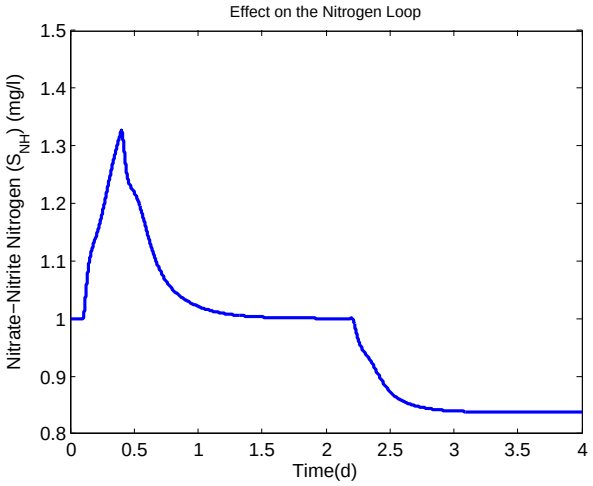

Figure 5.11: Effect of the change in reference and disturbance in the oxygen loop on the nitrate-nitrogen loop.

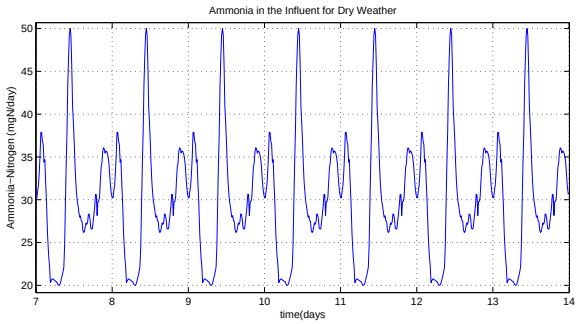

Figure 5.12: Influent ammonia for dry weather data.

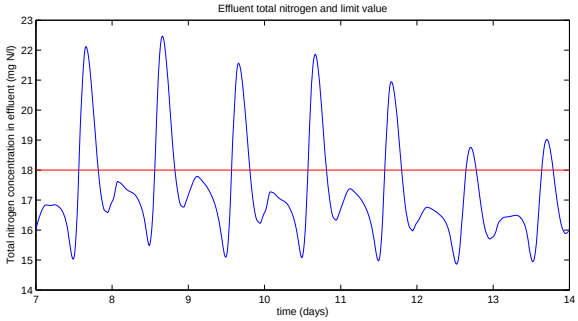

Figure 5.13: Effluent total nitrogen using the VRFT controllers.

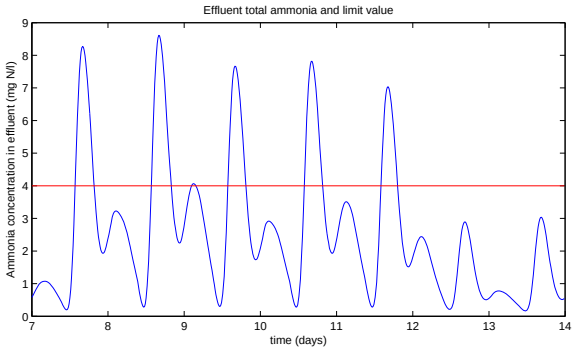

Figure 5.14: Effluent total ammonia using the VRFT controllers.

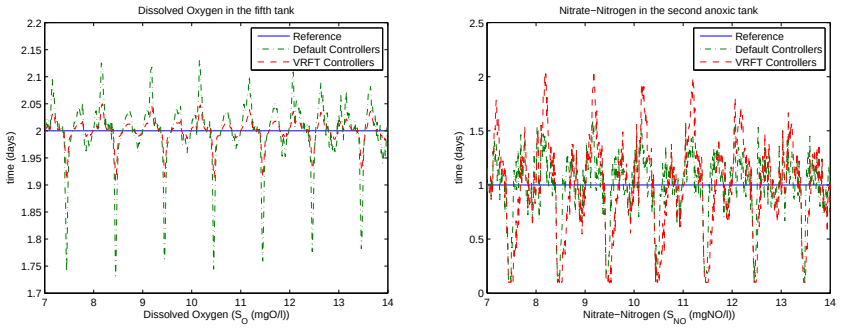

(a) Oxygen **(b)** Nitrate

Figure 5.15: Response of the controllers for the (a) oxygen and (b) nitrate-nitrogen loops.

same controllers only by changing the setpoint of the nitrate-nitrogen. If the reference is changed to 2mgSNO/l, the mean value of the Total Nitrogen is reduced to 16.5315mgN/l (for this reference, the difference between the VRFT controller and the Default controller reduce from 2.07% to 0.84%). The price to pay is an increment on the value of the ammonia which is rised 2.98% for the VRFT controller and 2.33% for the default controller. The percentage of the time in which the value of Total Nitrogen is above the limit is reduced 7.8869%. The total Nitrogen is ploted for this change in the reference of the nitrate-nitrogen in Fig. 5.16. It is interesting to note that, this change in the reference produces a big change in the nitrate-nitrogen, while the ammonia in the effluent, remains with the same percentage of time over the maximun value and just a little raise in the mean value.

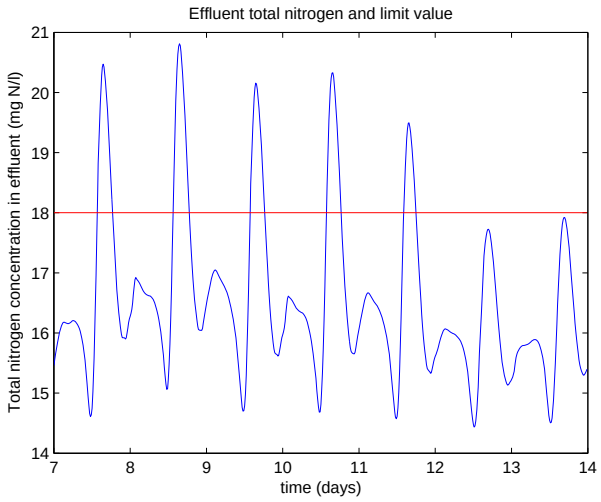

Figure 5.16: Violation of the total nitrogen, after changing the reference value of the S_{NO2}.

5.2.2. Application of feedforward control to the BSM1

The control strategy employing a feedforward control is depicted in Fig. 5.17. It has two control loops, the first one is the nitrate (S_{NO}) loop, that tries to keep nitrate concentration at a low setpoint value by actuating on the internal recycle flow rate to keep total effluent nitrogen below its limit. The second control loop is a cascade-feedforward controller: it manipulates the oxygen transfer rate (K_La) to maintain the Dissolved Oxygen set point. This Dissolved Oxygen setpoint is manipulated by a controller that measures the ammonia concentration at the fifth tank and at the influent. This strategy has also been tested in Ingildsen et al. (2002); Vrecko et al. (2003); Yong et al. (2005).

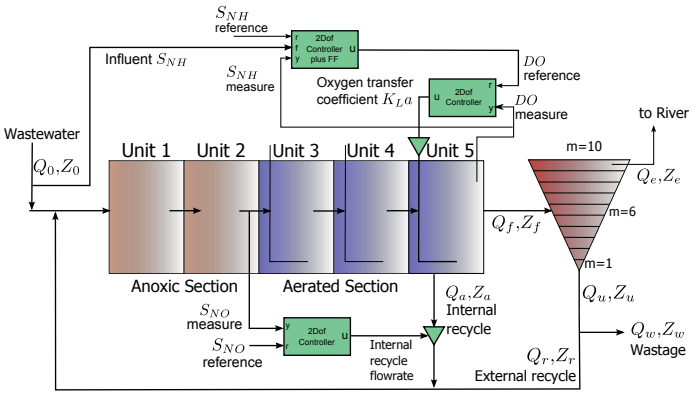

Figure 5.17: Layout of the BSM1.

All the controllers were set as two degrees of freedom discrete-time PI controllers (except for the Feedforward controller), with parameters found using the VRFT approach. The data used to obtain the PI controller is presented in Fig. 5.18. This data was recorded with a sampling time of 1 min for the Dissolved Oxygen loop and 10 min for the S_{NH} and S_{NO} loops.

Using this data, and a first order closed-loop dynamic as the target closed-loop with a settling time of approximately half day for the S_{NO} and S_{NH} loops and 15 min for the DO loop. These values were decided based on prior knowledge of the dynamics of the system. The controllers were found to be:

- For the S_{NO} loop

$$C_{rS_{\text{NO}}}(z) = \frac{2821 - 1769z^{-1}}{1 - z^{-1}}$$
$$C_{yS_{\text{NO}}}(z) = \frac{7134 - 6082z^{-1}}{1 - z^{-1}}$$

- For the DO loop

$$C_{rDO}(z) = \frac{97.99 - 75.76z^{-1}}{1 - z^{-1}}$$
$$C_{yDO}(z) = \frac{131.2 - 108.9z^{-1}}{1 - z^{-1}}$$

- For the S_{NH} loop

$$C_{rS_{\text{NH}}}(z) = \frac{-0.3612 + 0.2511z^{-1}}{1 - z^{-1}}$$
$$C_{yS_{\text{NH}}}(z) = \frac{-0.6713 + 0.5612z^{-1}}{1 - z^{-1}}$$
$$C_{fS_{\text{NH}}}(z) = \frac{\begin{pmatrix} -0.01265 - 0.03796z^{-1} \\ +0.05244z^{-2} + 0.1473z^{-3} \\ -0.146z^{-4} \end{pmatrix}}{1 - 0.5409z^{-1} - 0.4315z^{-2}}$$

The controlled system was first simulated for 14 days of dry weather data and then simulated for each one of influent data (dry, rainy and storm weather) that the benchmark provides. For the $C_{fS_{\text{NH}}}$ controller, a low order approximation of the dynamic of the plant was obtained with an ARX structure. The selected setpoints were 1 mgN/l for the S_{NO} loop and 2 mgN/l for S_{NH}. Then the performance was evaluated for the last 7 days and the mean values of the most important variables are presented in Table 5.8.

VRFT successfully maintains the mean values under the maximum limits. In Fig. 5.19, the data for the last 7 days for the Dry Weather is plotted for the Ammonia Nitrogen S_{NH} and Total Nitrogen TN (which are the variables that most likely could have a higher value than the limit). In Yong et al. (2005), a feedforward-feedback control is implemented, but with control over all the aerated tanks and assuming knowledge of kinetic parameters that are

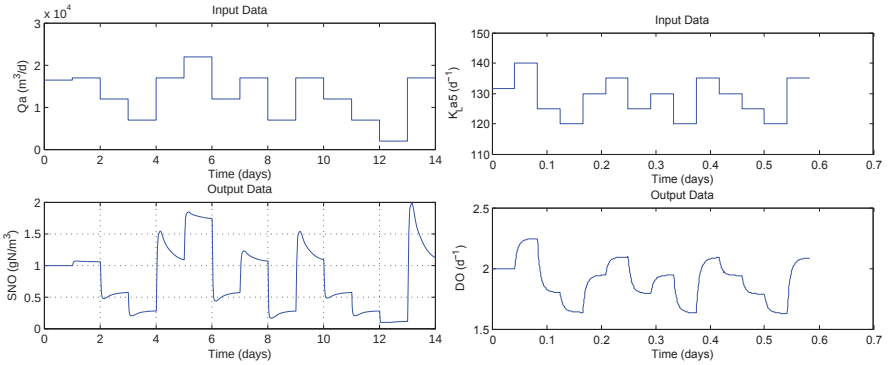

(a) Data for the S_{NO} control loop **(b)** Data for the DO control loop

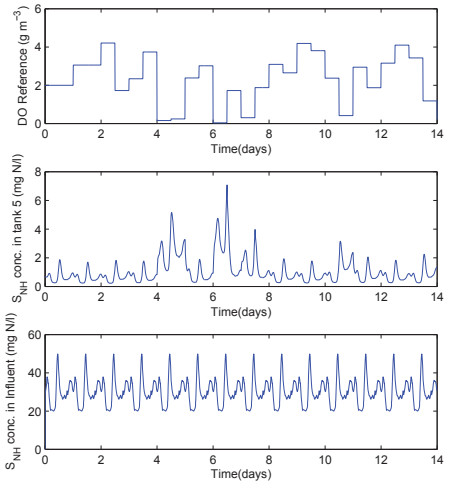

(c) Data for the S_{NH} control loop

Figure 5.18: Open loop simulated experiments for the VRFT method. The data for the S_{NH} control was obtained with the other two controllers in the loop.

Weather	S_{NH} $< 4\ mgN/l$	TSS $< 30\ mgN/l$	TN $< 18\ mgN/l$	COD $< 100\ mgCOD/l$	BOD $< 10\ mgBOD/l$
Dry	2.74	12.99	16.25	48.24	2.76
Rain	3.25	16.16	14.55	45.43	3.45
Storm	3.15	15.25	15.53	47.66	3.20

Table 5.8: Important mean values of the BSM1 after simulated 14 days. Results computed based on the last 7 days.

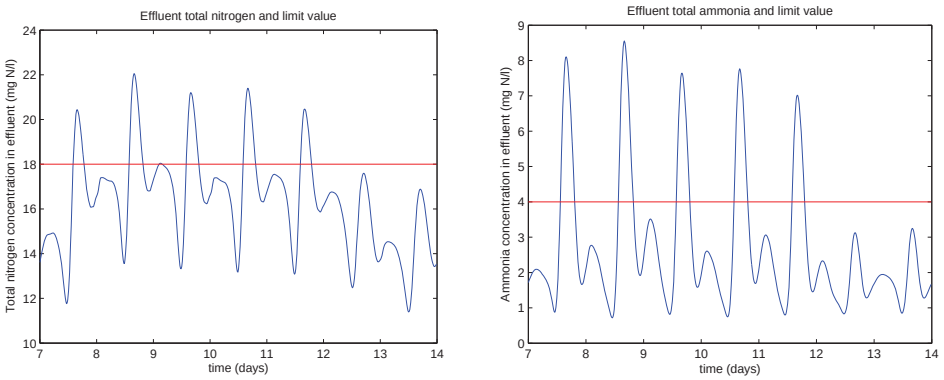

(a) Total N concentration **(b)** Ammonia concentration

Figure 5.19: Instantaneous values for the dry weather. The mean value is below the maximum values but still, some peaks cannot be maintained under the limit.

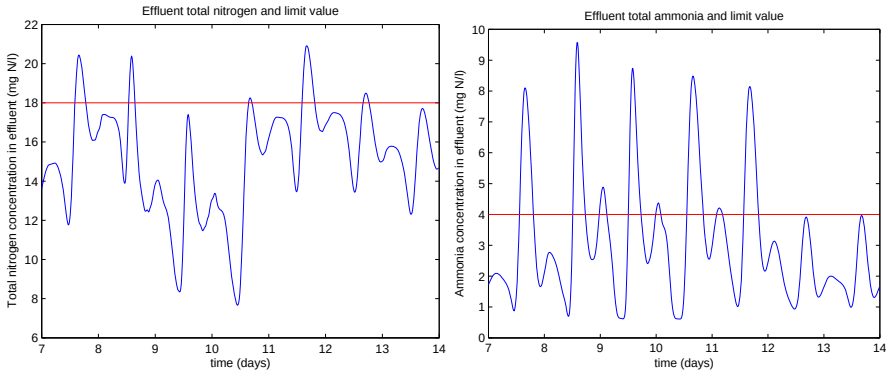

(a) Total N concentration **(b)** Ammonia concentration

Figure 5.20: Instantaneous values for the rain weather.

difficult to obtain in practice. In this case, the mean value of ammonia at the effluent for the dry weather was 2.11 mg/l (23% less than the result with the VRFT) and the mean value of the Total Nitrogen was 17.26 mg/l (5.82% more than VRFT) with the advantage that with the VRFT approach one does not need to know any parameter that cannot be measured online. A similar approach was followed by Zhang and Hoo (2007), in this case for the S_{NH} parameter, the VRFT approach gave 12.91% less for the dry weather, 0.63% less for the rain weather and 2.88% more for the storm weather.

One of the disadvantages of this methodology is that it produces a very aggressive controller, which in turn affects the energy consumption, as shown in Fig. 5.22 . This behavior was expected since the controller is delivered from an optimization that does not take into account the control effort.

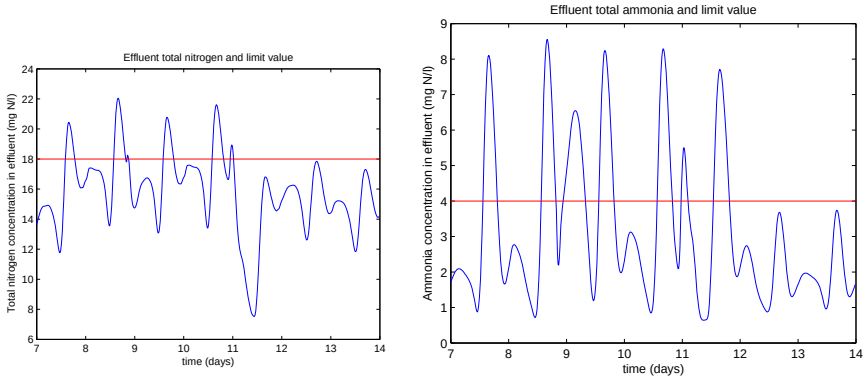

(a) Total N concentration **(b)** Ammonia concentration

Figure 5.21: Instantaneous values for the storm weather.

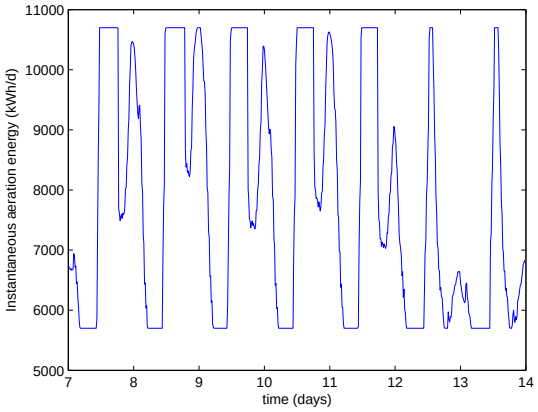

Figure 5.22: Aeration energy for the dry weather influent, using the VRFT. The controller are found to be very aggressive which in turn could lead to a high energy usage. The aeration energy was calculated as pointed out in the benchmark Alex et al. (2008)

.

5.2.3. MIMO approach to the BSM1

Four different control strategies were considered to test the viability of the MIMO version of the method for this particular WWTP. The cases are as follow:

- *Default Case* (A0): This is the default control strategy of the benchmark and consists of two control loops. The first loop controls the dissolved oxygen level in the fifth tank (S_{O5}) manipulating the oxygen transfer coefficient of the same tank ($K_L a5$). The second loop controls the nitrogen nitrate concentration in the second anoxic tank (S_{NO2}) by manipulating the internal recycle flow rate (Q_a).

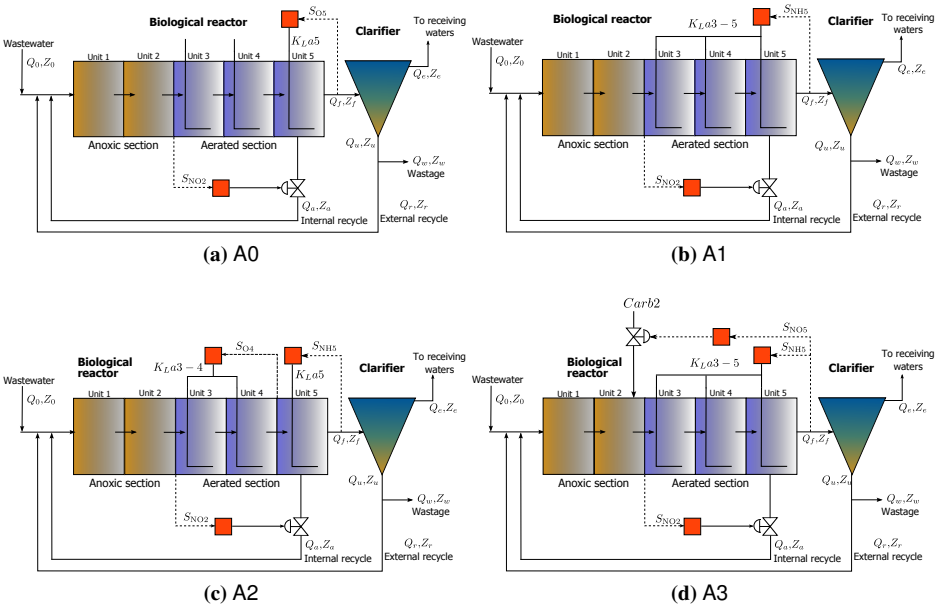

Figure 5.23: Different control strategies tested with the BSM1.

- *Direct Control of Ammonia* (A1): The second strategy involves controlling the ammonia concentration in the fifth tank (S_{NH5}) by manipulating the oxygen transfer coefficient of all the aerated tanks (K_La3-5). The nitrogen nitrate concentration of the second tank is controlled as above.
- *Parallel control of Ammonia and Oxygen* (A2): This is a 3×3 control strategy. The first loop controls the S_{NH5} by manipulating K_La5. The dissolved oxygen in the fourth tank (S_{O4}) is controlled by manipulating the oxygen transfer coefficient of the third and fourth tank (K_La3-4). Finally, the nitrogen nitrate concentration in the second tank is controlled as in A1.
- *Control of nitrogen concentration by adding carbon* (A3): This is a 3×3 strategy. The nitrogen nitrate concentration in the fifth tank (S_{NO5}) is controlled by adding carbon into the last anoxic tank ($Carb2$). The S_{NH5} is controlled as in A1, while S_{NO2} as in A0.

In Figure 5.23, the four strategies are depicted. In the diagrams, the small boxes represent the controllers. Nevertheless, only the direct controllers ($i = j$) are included in the picture for the sake of clarity of the control method (see section 4.2). The controllers in the off-diagonals are seen as compensator for the effect of the error in the other loops. The correspondence amongst the actual BSM1 variables and the control variables related with the MIMO-VRFT method is presented in Table 5.9.

In all cases, the sampling time was chosen as T_s =1 min. The chosen structure for the controllers was a discrete PI. However, it was necessary to incorporate an antiwindup system,

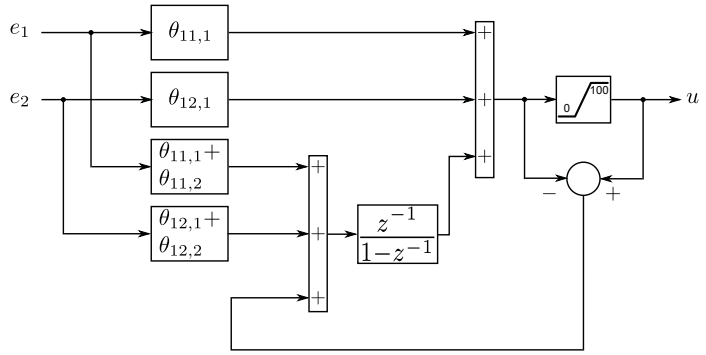

Figure 5.24: Implementation of the PI controllers for a 2×2 case with anti-windup protection.

Var	A0	A1	A2	A3
u_1	K_La5	K_La3-5	K_La5	K_La3-5
u_2	Q_a	Q_a	K_La3-4	Q_a
u_3	-	-	Q_a	$Carb2$
y_1	S_{O5}	S_{NH5}	S_{NH5}	S_{NH5}
y_2	S_{NO2}	S_{NO2}	S_{O4}	S_{NO2}
y_3	-	-	S_{NO2}	S_{NO5}

Table 5.9: Relationship between the control variables and the actual variables of the BSM1.

especially when the ammonia controllers were used. This was mainly because the variations produced by the influent are too aggressive and could saturate the integral part of the controllers.

In Fig. 5.24, the implementation of the two controllers related to input 1 is represented for a 2×2 case. Thus, e_1 and e_2 represent the error signals related to output 1 and output 2, respectively. With this configuration the "integral" part of the controller given by the term $z^{-1}/\left(1-z^{-1}\right)$ is not allowed to go beyond the saturation limits. The controller $C_{11}(z,\theta_{11})$ can be regarded as the "direct" controller that measures the error of output 1 while the controller $C_{12}(z,\theta_{12})$ is the decoupling controller that takes into account the error in loop 2. The sum of the outputs of these two controllers is the actual control signal for the manipulated variable u_1. Only one integrator is necessary for each manipulated variable. The 3×3 case is an extension of the structure in Fig. 5.24, where groups of three controllers are implemented using a single integrator.

The desired closed-loop transfer function was selected as a first-order transfer function:

$$M(z) = \frac{(1-\alpha)z^{-1}}{1-\alpha z^{-1}} \tag{5.17}$$

The value of α represents the time constant of $M(z)$ and in this work is determined based on the desired settling time for each controlled variable. The settling time represents the time that the system needs to reach a new steady state, when a step change in its manipulated variable is applied.

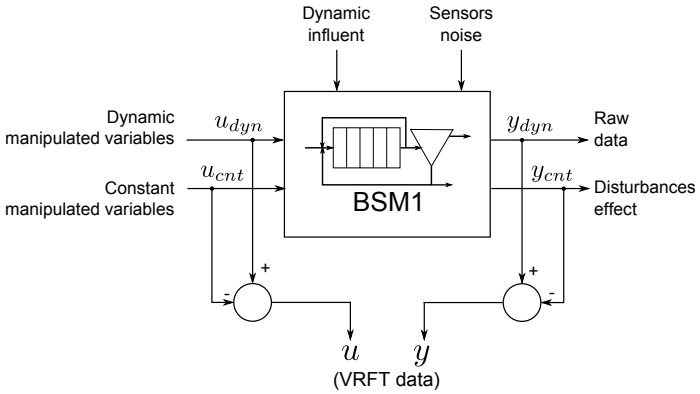

Figure 5.25: Preprocessing of data.

Training data and preprocessing step

The preprocessing strategy is depicted in Fig. 5.25. Two input data sets of 14 days are used for each control strategy. The first data set (u_{dyn}) contains the dynamic values of the manipulated variables. It should be emphasized that if two or more manipulated variables are considered, their variation must be split in different time intervals. The second (or auxiliary) data set (u_{cnt}) only contains constant values of the manipulated variables at the selected operating point. The rate of change of the input data as well as the operation points were chosen based on existing knowledge of the plant dynamics. Even if no explicit model of the plant is used, it is always necessary to have a reasonable idea of how the plant is responding to external excitation, the limit values of the variables, the time constants, etc.

Once the simulations are run, two output data sets are generated. The idea is to obtain two types of information. In the first batch (y_{dyn}), the BSM1 overall process performance is stored including dynamic influent, noise data and includes the effect of the manipulated variables. The second data set (y_{cnt}) only contains the effect on BSM1 of the dynamic influent and noise files when the manipulated variables are left at their default values. Both simulations are run under open-loop conditions.

The preprocessing step consists of calculating the difference of the inputs ($u = u_{dyn} - u_{cnt}$) and outputs files ($y = y_{dyn} - y_{cnt}$). As a result, dynamic periodicity and noisy data are subtracted, leaving only the variation due to the manipulated variables. Thus, the resulting data set will be the input (u) and the output files (y) that will be used by the VRFT algorithm. The reader should be aware that this assumptions hold as long as we consider that the effects of the different perturbations i.e. influent, noise, manipulated variable, are additive and there is no interactions amongst them.

For exemplary purposes, further details about the preprocessing step for the second control strategy (A1) are given in Fig. 5.26. The data in Fig. 5.26a shows the variation of manipulated variables K_La3-5 and Q_a (i.e. u_{dyn}) and their effect (together with the influent dynamic variability and sensor noise) on the BSM1 predictions (y_{dyn}). To obtain better results in the optimization, the manipulated variables changes were separated in time, see Fig. 5.26a.

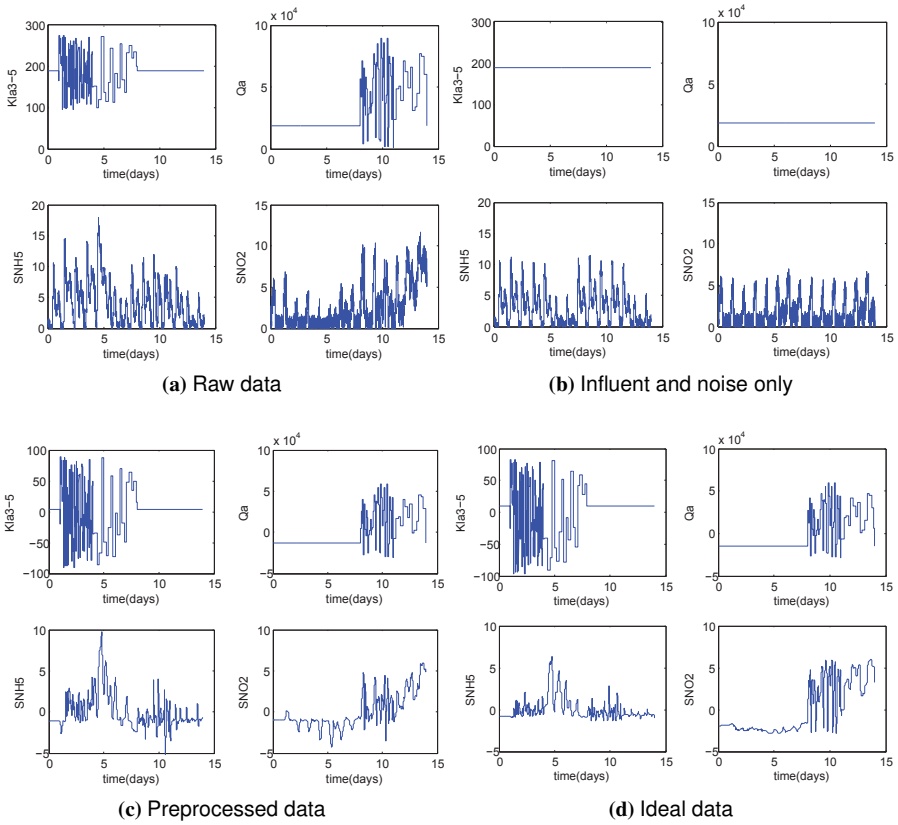

(a) Raw data **(b)** Influent and noise only

(c) Preprocessed data **(d)** Ideal data

Figure 5.26: Example of the preprocessing of the data for a TITO plant.

The same variations of the BSM1 predictions (y_{cnt}) are summarized in 5.26b, but the default values of the manipulated variables are used and only the effects of influent and noise are considered. Fig. 5.26c shows the difference between Fig. 5.26a and Fig. 5.26b, where it is possible to see how the influent periodicity (and noise) is subtracted from the effect of the manipulated variables (K_La3-5 and Q_a). Finally, in Fig. 5.26d the simulations only modifying the manipulated variables (the ideal condition without dynamics and noise) can be compared with the processed data. The trends are certainly similar although the effects of some disturbances are not completely removed.

Once the data has been preprocessed, the optimization problem is solved. All the coefficients of the controllers (4 controllers for the 2×2 cases and 9 controllers for the 3×3 cases) are computed. The selected settling times are summarized in Table 5.10.

With the computed controllers, the plant is simulated in closed-loop using the dry weather influent profile. The simulation follows an initial steady state simulation; this ensures a consistent initial point and eliminates the bias due to the selection of the initial conditions for the states of the plant (Copp, 2002). Even though the period for the dynamic simulations is 28

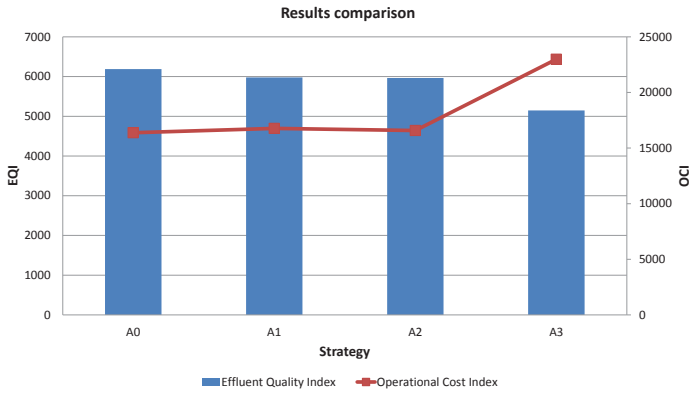

Figure 5.27: Variation of the results based on the different strategies.

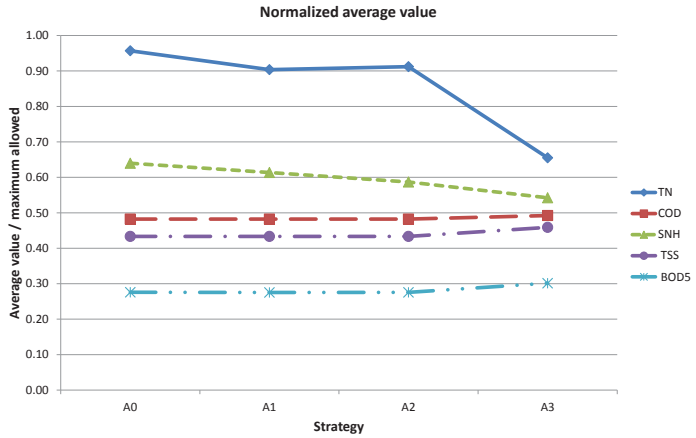

Figure 5.28: Variation of the effluent quality concentrations, normalized by their limits.

days, only the data generated during the last seven days are used to quantify the criteria. The results of the different evaluation criteria for all the strategies are summarized in Table 5.10.

In Fig. 5.27, the variations of the Effluent Quality Index (EQI) and the Operational Cost Index (OCI) are presented. The EQI improves (lower value) as the "complexity" of the control strategy increases. Thus, control strategy A2 improves the EQI by 3.62% compared to the default closed-loop strategy (A0). However, EQI substantially improves in case A3 (16.8% with respect to the default value), when an external carbon source is added to the WWTP.

In all cases, the average concentrations of Total Nitrogen (TN) and Ammonia (S_{NH}) in the effluent were always below the limit values. In Fig. 5.28, the normalized averages of the effluent quality concentration are shown i.e. the ratio between average values and maximum allowed. The S_{NH} and the TN are the most sensitive concentrations to a change of control strategy. Their absolute values are shown in Fig. 5.29 for reference. Chemical Oxygen De-

Strategy	Controlled variables	Manipulated variables	Set points (mg/l)	Settling time (hours)	IAE	EQI	OCI	% violation
A0	S_{O5}	K_La5	2	1.44	0.77	6188	16379	TN: 21.1%
	S_{NO2}	Q_a	1	7.2	2.11			S_{NH}: 18.2%
A1	S_{NH5}	K_La3-5	1.3	1.44	9.75	5978	16763	TN: 13.9%
	S_{NO2}	Q_a	1	1.44	5.19			S_{NH}: 16.82%
A2	S_{NH5}	K_La5	2	7.2	10.17	5964	16580	TN: 16.82%
	S_{O4}	K_La3-4	3	7.2	2.24			S_{NH}: 15.03%
	S_{NO2}	Q_a	2	7.2	5.70			
A3	S_{NH5}	K_La	1	7.2	9.65	5147	22986	TN: 0%
	S_{NO2}	Q_a	2	7.2	3.62			S_{NH}: 14.43%
	S_{NO5}	$Carb2$	8	7.2	4.45			

Table 5.10: Results of the different strategies, based on the last 7 days of simulation.

Figure 5.29: Average values for the total nitrogen and Ammonia concentrations for all the strategies.

mand (COD), Total Suspended Solids (TSS) and Biochemical Oxygen Demand (BOD) do not vary much. Only when there is an addition of external carbon source (A3), the values slightly increase (less than 10%). The strategy including the addition of carbon are able to reduce almost 30% of the effluent TN levels compared with the default case (see Table 5.10). TN and S_{NH} have the heaviest weights when calculating the EQI, which explains its reduction in A3.

As happened in the EQI, for the first three cases, the variation in OCI is not as large as in case A3. When alternative A2 is compared to the default A0, the additional controllers produce an increase of 1.22% of OCI. This is mainly due to the higher aeration energy required to handle the (effluent) ammonium peaks by the controller. On the other hand, when carbon is added, the OCI increases nearly 40%. Basically, this is because of the periodic purchase of external carbon source, higher aeration energy and sludge production.

The interaction between loops is shown in the IAE numbers summarized in Table 5.10. The S_{NO2} controller is heavily affected in both A1 and A2, when compared to the default A0. This fact is attributed to the S_{NH} controller. Since it is more difficult to maintain the ammonia levels around the set point, the controllers tend to aerate more (see higher OCI values). This extra quantity of oxygen is then recycled to the anoxic zone worsening the overall denitrification efficiency, and consequently the performance of the S_{NO2} controllers. When S_{NO5} is also controlled, the IAE of the S_{NO2} decreases its value thanks to the carbon provided by control of nitrate nitrogen in the fifth tank. The IAE of the S_{NH5} controller is kept almost at the same value as in A1 because of the correct tuning of the controllers. From the values of IAE it is clear that controlling the oxygen level is easier than controlling the ammonia concentration. The main reasons are that 1) the dynamics of the dissolved oxygen are faster and simpler than the ammonia dynamics, 2) the dissolved oxygen is directly related to the aeration of the tanks while the ammonia concentration is only indirectly related, 3) ammonia concentration is more strongly affected by the influent variations than oxygen and 4) the BSM1 plant is overloaded and sometimes there is not enough aerobic volume to reach the desired set-points. The results obtained in this section open the door to several discussions. Firstly, the quality of the results

entirely depends on the quality of the data, the dynamics of the plant and the control strategy. The preprocessing presented in this work was needed to obtain straightforward feasible data for the optimization given the severe condition in which the plant works. Nevertheless, this fact gives credibility to the study because these conditions are likely to be found in real plants (i.e, dynamic influent conditions, noisy sensors, etc.)

Secondly, the closed-loop response for the algorithm was chosen in order to obtain a fast response of the system. For simplicity a first order dynamics was selected. Higher order dynamics (for example a second order transfer function where the natural frequency and the damping can be used as design variables) can be useful if the dynamics of the plant are shown to be very different from a first order model.

Thirdly, in this work only discrete PI controllers were used, but the method can be used to define controllers with higher order and different parameterization. If the controllers are linear in the parameters, the optimization is still a least-squares problem, but it may also be possible to use non-linear controllers or parameterization that leads to a non-linear optimization (Campi and Savaresi, 2006). Since the BSM1 is a non-linear plant, it is difficult to totally decouple the loops.

Finally, the selected sampling times, settling times and controller parameters were based on experience using the plant. It is difficult to choose these design parameters based purely on data. This issue affects all data-driven methodologies and not only the VRFT. Most of the information needed to apply the methodology is available from the persons in charge of WWTPs (like limits on the manipulators, time constants, information about the influent dynamics, etc.). For this reason synergy between the control engineer and the personnel of the plant will always be necessary.

6. Application to a solid oxide fuel cell

In this chapter, the VRFT in its MIMO form, is applied to a Solid Oxide Fuel Cell (SOFC). As pointed by Ellis et al. (2001) and Nehrir et al. (2006), fuel cells are promissory technology to substitute the oil-based fuels to generate electricity. The range of use of fuel cell can go from portable devices to power generation, depending of the type used. Two of the most popular fuel cells are the Proton Exchange Membrane Fuel Cell (PEMFC) and the SOFC. PEMFC are low temperature fuel cells that are intended to be use in a wide range of applications, but much attention has been given to the hydrogen powered vehicle (Pukrushpan, 2003).On the other hand, SOFC are high temperature fuel cells which can be used as part of a power distribution system (Sedghisigarchi and Feliachi, 2004b, 2006).

6.1. Introduction to solid oxide fuel cells

Fuel cells (FCs) are electrochemical devices in which the free energy of a chemical reaction of fuel is converted into electrical energy (Carrette et al., 2001). A combustion process is not necessary, and therefore the CO_2 emissions are almost zero. If the fuel is hydrogen the conversion is completely emissions free. In general, the overall chemical reaction of FCs is:

$$\mathrm{H_2} + \tfrac{1}{2}\mathrm{O_2} \rightarrow \mathrm{H_2O} \tag{6.1}$$

This reaction can be divided in one subreaction for the cathode side and other for the anode side. Depending of the electrolyte, these subreactions vary. Table 1 in Carrette et al. (2001), is reproduced in Table 6.1, where different kinds of FCs are characterized.

Solid Oxide Fuel Cells (SOFC) are composed of two porous ceramic electrodes and a solid state electrolyte, made of solid metal oxides. The typical SOFC is composed of an electrolyte made of ytria-stabilized zirconia (YSZ), a porous anode made of nickel and ytria stabilized zirconia (Ni/YSZ) cermet and a porous cathode composed of doped $LaMnO_3$ (LSM) (Bove, 2007).

The anode and cathode reactions are depicted in Fig. 6.1. The oxygen reaction in the cathode is:

$$\tfrac{1}{2}\mathrm{O_2} + 2e^- \rightarrow \mathrm{O}^{2-} \tag{6.2}$$

One of the characteristics of the electrolyte is that at the operating temperature (near 1000°C), it presents very high electrical resistivity and ionic conductivity (Bove, 2007). If pure hydro-

	AFC	PEMFC	DMFC	PAFC	MCFC	SOFC
Electrolyte	Alkaline	Polymer Electrolyte Membrane	Direct Methanol	Phosphoric Acid	Molten Carbonate	Solid Oxide
Operating temperature (°C)	<100	60-120	60-120	160-220	600-800	800-1000
Anode reaction	$H_2+2OH^- \rightarrow 2H_2O+2e^-$	$H_2 \rightarrow 2H+2e^-$	$CH_3OH+H_2O \rightarrow CO_2+6H^++6e^-$	$H_2 \rightarrow 2H+2e^-$	$H_2+CO_3^{2-} \rightarrow H_2O+CO_2+2e^-$	$H_2+O^{2-} \rightarrow H_2O+2e^-$
Cathode reaction	$1/2\ O_2 + H_2O + 2e^- \rightarrow 2OH-$	$1/2\ O_2 + 2H^+ + 2e^- \rightarrow H_2O$	$3/2\ O_2+6\ H^++6e^- \rightarrow 3H_2O$	$1/2\ O_2+ 2H^++2e^- \rightarrow H_2O$	$1/2O_2+CO_2+2e^- \rightarrow CO_3^{2-}$	$1/2\ O_2+2e^- \rightarrow O^{2-}$
Charge Carrier in the electrolyte	OH^-	H^+	H^+	H^+	CO_3^{2-}	O^{2-}

Table 6.1: Different kind of fuel cells.

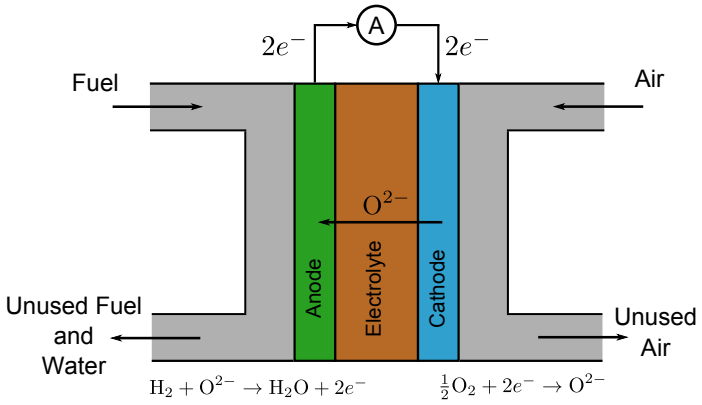

Figure 6.1: Reactions occurring on a SOFC

gen is used as fuel, the reaction that occurs in the anode is:

$$H_2 + O^{2-} \rightarrow H_2O + 2e^- \tag{6.3}$$

However, using hydrogen as fuel is expensive and dangerous. One of the advantages of SOFC is that, given its high temperatures, alternative fuels other than hydrogen can be use. For example if carbon monoxide is present, the following reaction occurs:

$$CO + H_2O \leftrightarrow H_2 + CO_2 \tag{6.4}$$

SOFCs can extract hydrogen from a variety of fuels using either an internal or external reformer Williams (2007). For the internally reformed case:

$$C_xH_y + xH_2O \rightarrow xCO + \left(x + \frac{y}{2}\right) H_2 \tag{6.5}$$

6.1.1. Voltage of SOFC fuel Cell

The "Gibbs free energy" or "Gibbs free energy of formation" (G_f or $\bar{g_f}$ if the energy is per mole) is defined as "the energy available to do external work, neglecting any work done by changes in pressure and/or volume" (Larminie and Dicks, 2003). In a fuel cell, the difference between the Gibbs free energy of the product and the reactants is equal to the energy released in a fuel cell.

Considering the overall reaction (6.1) in a typical FC, the released energy is computed as:

$$\begin{aligned} \Delta\bar{g}_f &= \bar{g}_f(\text{products}) - \bar{g}_f(\text{reactants}) \\ \Delta\bar{g}_f &= (\bar{g}_f)_{H_2O} - (\bar{g}_f)_{H_2} - \tfrac{1}{2}(\bar{g}_f)_{O_2} \end{aligned} \tag{6.6}$$

The values of the Gibbs free energy depends on temperature and state of the reactants and products, but there are tables where the empirical value can be found (Larminie and Dicks,

2003). When pure hydrogen is used as fuel , two electrons pass round the external circuit for each water molecule produced and each molecule of hydrogen used (see Fig. 6.1). Therefore for each mole of hydrogen, $2N_A$ electrons go trough the circuit ($N_A = 6.02214179(30) \times 10^2 3mol^{-1}$ is the Avogadro constant). The charge that is flowing is related to the Faraday constant F ($F = 96485.3399(24)Cmol^{-1}$) as

$$\text{Charge} = -2N_A e = -2F$$

e is the charge of an electron. The electrical work done is given by the product of charge and voltage. If there are no losses in the FC, the electrical work then is equal to the released energy and the voltage can be computed as:

$$E = \frac{-\Delta \bar{g}_f}{2F} \tag{6.7}$$

This fundamental equation gives the electromotive force (EMF) (E) or reversible open circuit voltage of the hydrogen fuel cell(Larminie and Dicks, 2003). This equation assumes pure hydrogen and oxygen at standard pressure (0.1MPa) and no irreversibilites. The real voltage will always be lower than this value. For instance, it is known that the actual value of the voltage varies depending on the temperature and the "activity" of the reactants and products, following the Nernst equation.

Following Larminie and Dicks (2003), if the following general reaction is considered

$$j\text{J} + k\text{K} \rightarrow m\text{M} \tag{6.8}$$

it can be shown that the activity (a) modify the Gibbs free energy:

$$\Delta \bar{g}_f = \Delta \bar{g}_f^0 - RT \ln \left(\frac{a_{\text{J}}^j \cdot a_{\text{K}}^k}{a_{\text{M}}^m} \right) \tag{6.9}$$

and $\Delta \bar{g}_f^0$ is the change of Gibbs free energy by molar at standard pressure. Considering the overall reaction in a hydrogen FC in (6.1), the variation of the Gibbs free energy can be written as:

$$\Delta \bar{g}_f = \Delta \bar{g}_f^0 - RT \ln \left(\frac{a_{\text{H}_2} \cdot a_{\text{O}_2}^{\frac{1}{2}}}{a_{\text{H}_2\text{O}}} \right) \tag{6.10}$$

Substituting (6.10) into (6.7):

$$E = E^0 + \frac{RT}{2F} \ln \left(\frac{a_{\text{H}_2} \cdot a_{\text{O}_2}^{\frac{1}{2}}}{a_{\text{H}_2\text{O}}} \right)$$

where E^0 is the reversible voltage at standard pressure. Activity is difficult to find (Lunelli and Scagnolari, 2009) but, according to Larminie and Dicks (2003) in the case of "ideal gases" the activity is proportional to the partial pressure P of the gas:

$$a = \frac{P}{P^0}$$

P^0 is the standard pressure. Thus:

$$E = E^0 + \frac{RT}{2F} \ln \left(\frac{\frac{P_{\mathrm{H_2}}}{P^0} \cdot \left(\frac{P_{\mathrm{O_2}}}{P^0} \right)^{\frac{1}{2}}}{\frac{P_{\mathrm{H_2O}}}{P^0}} \right)$$

And if all the pressures are given in bar, then $P^0 = 1$ and finally, the Nernst equation for the output voltage is given by

$$E = E^0 + \frac{RT}{2F} \ln \left(\frac{P_{\mathrm{H_2}} \cdot P_{\mathrm{O_2}}^{\frac{1}{2}}}{P_{\mathrm{H_2O}}} \right) \tag{6.11}$$

Other irreversibilities have to be taken into account. For example, ohmic losses due to material resistance to electric current, activation losses and concentration losses, specially in Proton Exchange Membrane FC (PEMFC) (Barbir, 2005).

6.1.2. SOFC design

According to Carrette et al. (2001) different designs has been tested for SOFC:

1. Tubular design: It was design by Siemens-Westinghouse (Hassmann, 2001). This design have a self-sealing structure which improves thermal stability and eliminates the need for good thermal-resistant sealants. The air electrode tube is generally made of doped lanthanum manganite. The other components are thin-layered on this construction by electrochemical vapor deposition.
2. Planar design: This is the typical design used in most FC. The advantage of this design is its low current resistance, but the sealing is critical in SOFC, because the material have to be resistant to its high temperatures (Bove, 2007).
3. Disk shape design: Its a planar design but with circular shape under development by Sulzer-Hexis. The interesting characteristic of this design is that the interconnection serves as heat exchanger (Carrette et al., 2001).

6.1.3. Application of SOFC

SOFC is seen as the most promising fuel cell option for the emerging distributed power market (Hassmann, 2001) given its characteristics: they can use several of fuels (either with an external o internal reforming process), works well with nickel as catalyst (which is cheaper than platinum, the catalyst for PEMFC), their efficiency is around 55% and if the produced heat is used for cogeneration or heating, the efficiency can reach 80% (Williams, 2007).

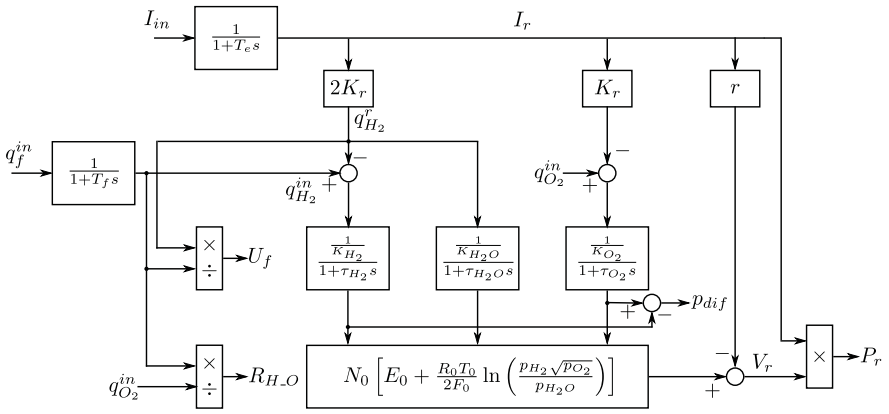

Figure 6.2: Model of the SOFC.

6.2. Application of the VRFT to a solid oxide fuel cell

The modeling and control of SOFC is treated in several papers, as for example Padullés et al. (2000) where a model for control is proposed, in Sedghisigarchi and Feliachi (2004a) the thermal aspects and voltages losses are also taken into account, in Zhang et al. (2006), a lumped non-linear model is proposed and in Murshed et al. (2007) a model for control of the fuel cell and the balance of plant (BOP) (Fuel Heat Exchanger, Reformer, Burner, Air Heat Exchanger) are also modeled.

From the control point of view, several different approaches have been tested with SOFC, for example in Wang et al. (2007) a data-driven Model Predictive Control (MPC) is used, in Fardadi et al. (2010) $\mathscr{H}_\infty$ control is used to minimize the disturbances in the variation of the spatial temperature of the fuel cell. In Murshed et al. (2010), a non-linear MPC is used and in Sendjaja and Kariwala (2011) decentralized discrete time PI controller are used based on the linearization of the model.

The aim of this section is to apply the MIMO VRFT methodology to a solid oxide fuel cell (SOFC). The simulations are made using the model presented in Padullés et al. (2000); Wang et al. (2007), depicted in Fig. 6.2. In this case, a set of input output data was obtained by simulation, and then the controllers were computed without the use of the model. The inputs to the plant are the load current I_{in} (which is considered a measurable perturbation), the input fuel flow q^{in}_f and the input oxygen flow $q^{in}_{\mathrm{O}_2}$. The outputs are the generated power P_r, the stack voltage V_r, the fuel utilization U_f, the ratio between inlet H_2 and O_2 flows $R_{\mathrm{H\_O}}$ and the fuel cell pressure difference between the anode and the cathode of the stack p_{dif}. As it can be seen, the different subsystem's effects are modeled as first order transfer functions, while the voltage of the stack is modeled using the Nernst's equation and taking into account ohmic losses considering its resistance. The parameters of the system are the same as in Wang et al. (2007) and are presented in Table 6.2 for completeness.

The operation band of the plant is presented in Table 6.3. In this case, for the test of the VRFT it will be considered that V_r and U_f are accessible and are considered as the outputs of

Parameter	Value	Concept
T_0	1273 K	Absolute Temperature
F_0	96485 C/mol	Faraday's constant
R_0	8.314 J/(mol K)	Universal gas constant
E_0	1.18 V	Ideal standard potential
N_0	384	Number of cells in series in the stack
K_r	9.96×10^{-7} kmol/(s A)	Constant, $K_r = N_0/(4F_0)$
$K_{\mathrm{H_2}}$	8.43×10^{-4} kmol/(atm s)	Valve molar constant for H_2
$K_{\mathrm{H_2O}}$	2.81×10^{-4} kmol/(atm s)	Valve molar constant for H_2O
$K_{\mathrm{O_2}}$	2.52×10^{-3} kmol/(atm s)	Valve molar constant for O_2
$\tau_{\mathrm{H_2}}$	26.1 s	Response time of hydrogen flow
$\tau_{\mathrm{H_2O}}$	78.3 s	Response time of water flow
$\tau_{\mathrm{O_2}}$	2.91 s	Response time of oxygen flow
r	0.126 Ω	Ohmic loss
T_e	0.8 s	Electrical response time
T_f	5 s	Fuel Processor response time

Table 6.2: Parameters of the SOFC model.

Variable	Band	Nominal Value	Unit
$q^{in}_{\mathrm{H_2}}$	$0 \leq q^{in}_{\mathrm{H_2}} \leq 1.7023$	0.7023	mol/s
$q^{in}_{\mathrm{O_2}}$	$0 \leq q^{in}_{\mathrm{H_2}} \leq 1.6134$	0.6134	mol/s
V_r	$328.8 \leq q^{in}_{\mathrm{H_2}} \leq 338.8$	333.8	V
I_{in}	-	300	A
U_f	$80\% \leq U_f \leq 90\%$	85%	-
$R_{\mathrm{H\_O}}$	$0 \leq R_{\mathrm{H\_O}} \leq 2\%$	1.145	-
$\lvert p_{dif}\rvert$	$0 \leq \lvert p_{dif}\rvert \leq 0.078954$	0	atm

Table 6.3: Operation band of the SOFC plant.

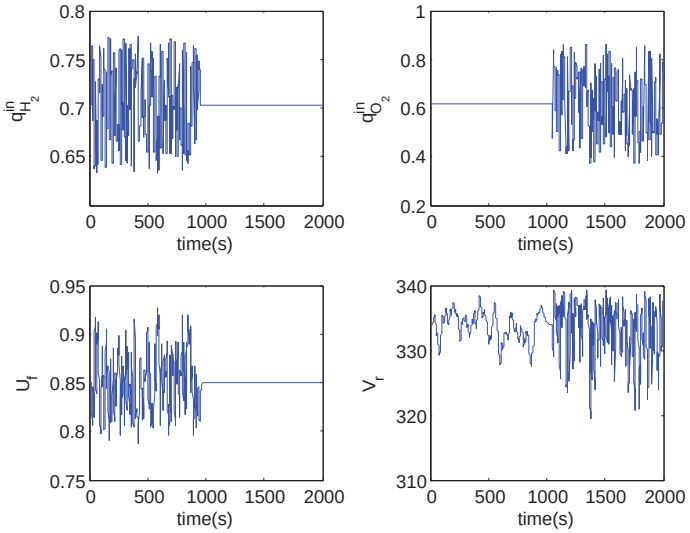

Figure 6.3: Open loop data obtained with the SOFC model.

the resulting TITO system. The input-output data taken in open-loop is depicted in Fig. 6.3. Since only two inputs are available, at most only two inputs can be effectively controlled, therefore, the output $R_{\text{H\_O}}$ is not controlled. As it can be seen in Fig. 6.2, the value of $q^{in}_{\text{O}_2}$ does not affect the value of U_f, therefore the VRFT method by itself should not select the pairing between $q^{in}_{\text{O}_2}$ and U_f. In fact, in this case using 4 controllers instead of a decentralized topology is not clear because of this fact. To check this, both the "complete" version and the "simple" version of the MIMO VRFT presented in section 4.2 are tested in the plant to see the difference between them. The results are compared with the ones given by Sendjaja and Kariwala (2011), in which discrete time PI controller are also used with a decentralized approach.

The desired closed loop transfer functions was selected as a first order response with a constant time of 0.1s for U_f and V_r. The sampling time is $T_s = 1s$. The controllers are set as discrete time PI controllers of the form:

$$C(z;\boldsymbol{\alpha}) = \frac{\alpha_0 + \alpha_1 z^{-1}}{1 - z^{-1}} \tag{6.12}$$

The VRFT is able to find a controller that gives good reference tracking and disturbance rejection, but is not able to follow exactly the desired closed-loop function. In this case, this closed-loop transfer function has to be seen as the "bandwidth" of the closed-loop system and, given the fact that the desired linear closed-loop behavior is not achievable with this linear controller over the non-linear plant, the designer is forced to enlarge the desired bandwidth to achieved good control responses, as it has been done here.

The response of the system towards a disturbance in the load current is presented in Fig. 6.4 and the response to a change in the reference is presented in 6.5. The load changes were chosen as in Wang et al. (2007), where also, in some point the voltage and the utilization go

Controller	Complete	Simple	Decentralized
C_{11}	$\frac{-4.543+3.72z^{-1}}{1-z^{-1}}$	$\frac{-4.543+3.72z^{-1}}{1-z^{-1}}$	$\frac{-4.13+3.10z^{-1}}{1-z^{-1}}$
C_{12}	$\frac{3.292\times10^{-6}-1.106\times10^{-5}z^{-1}}{1-z^{-1}}$	-	-
C_{21}	$\frac{-0.7879+1.864z^{-1}}{1-z^{-1}}$	-	-
C_{22}	$\frac{0.08186-0.06072z^{-1}}{1-z^{-1}}$	$\frac{0.0782-0.05885z^{-1}}{1-z^{-1}}$	$\frac{0.044-0.029z^{-1}}{1-z^{-1}}$
Disturbance V_r IAE	47.7315	35.2098	50.9536
Disturbance U_f IAE	0.37091	0.37058	0.44756
Disturbance $q^{in}_{\mathrm{H}_2}$ TV	1.884	1.884	1.6937
Disturbance $q^{in}_{\mathrm{O}_2}$ TV	2.1107	1.4131	0.9987
Reference V_r IAE	7.8156	9.3476	13.2976
Reference U_f IAE	0.00836	0.00828	0.0139
Reference $q^{in}_{\mathrm{H}_2}$ TV	0.14289	0.14283	0.12725
Reference $q^{in}_{\mathrm{O}_2}$ TV	0.59872	0.51194	0.28302

Table 6.4: Control parameters for the SOFC plant.

beyond the operation band, as in the case of this paper and Sendjaja and Kariwala (2011) for the selected sampling time. The values of the Integral of the Absolute Error (IAE) are presented in the figures and also summarized in Table 6.4, where the values of the parameters of the controllers are presented as well. The comparison is made by the use of IAE and the Total Variation (TV) which are calculated from $t = 101s$ up to $t = 500s$ following Wang et al. (2007). The TV is considered as a measurement of the control effort. A larger TV represents more a controller with a wider bandwidth which could yield to a "more expensive control". The TV was calculates as:

$$TV = \sum_{i=1}^{N} (u(i) - u(i-1)) \tag{6.13}$$

In the case of V_r when the load current decreases to 270A, the over voltage goes up to 340V, but rapidly returns to the operation band. The response of U_f is faster than the voltage response. When comparing the results of the simple controller and the complete controller it can be seen that the main difference is in the voltage response, where the simple controller is better than the complete one. But when controlling U_f the simple and the complete controller performs similarly thanks to the lack of effect of the $q^{in}_{\mathrm{O}_2}$ over U_f. With respect to the decentralized controllers from Sendjaja and Kariwala (2011), it can be seen that the simple VRFT controller performs better while the complete controller has a similar response. But it also has to be notice that the TV of the VRFT controller is larger than for the decentralized controllers. Since it has a lower IAE, it is logical that the controller need to use a more aggressive control signal to achieve a better performance. One of the drawbacks of the VRFT controllers is that the ratio between hydrogen and the oxygen goes out of bounds for a short time. This is because the oxygen usage is more aggressive, as can be seen in Fig. 6.4d.

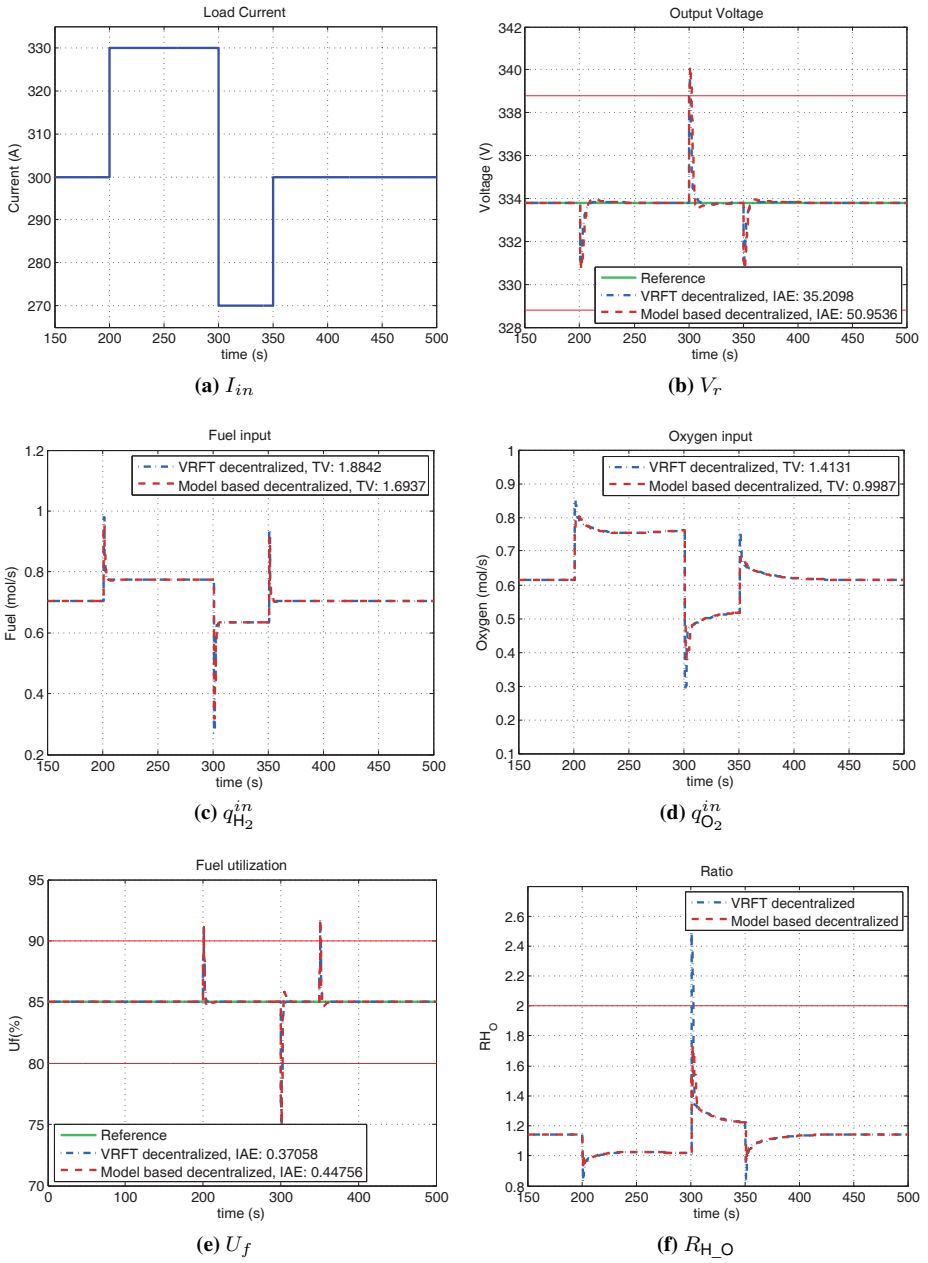

(a) I_{in} **(b)** V_r

(c) $q^{in}_{\mathrm{H}_2}$ **(d)** $q^{in}_{\mathrm{O}_2}$

(e) U_f **(f)** $R_{\mathrm{H\_O}}$

Figure 6.4: Response of the system to a disturbance in the load current.

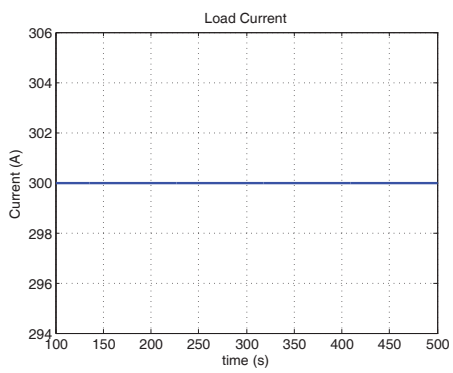

(a) I_{in}

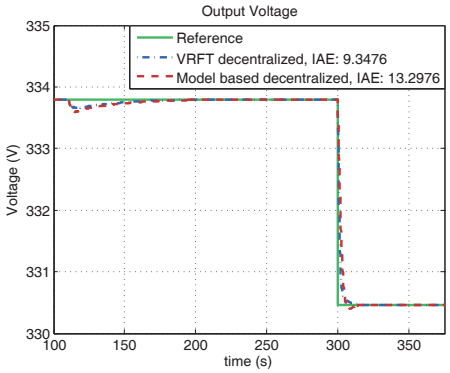

(b) V_r

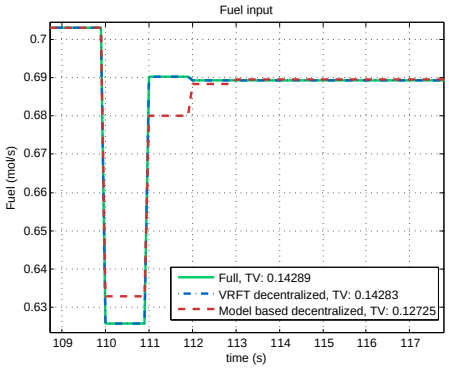

(c) $q^{in}_{\mathrm{H}_2}$

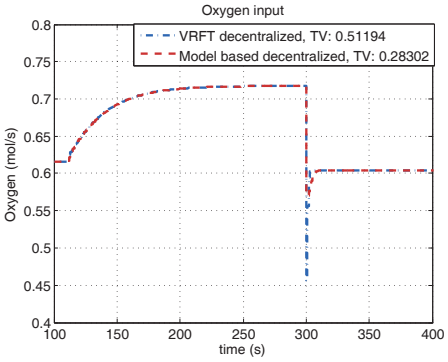

(d) $q^{in}_{\mathrm{O}_2}$

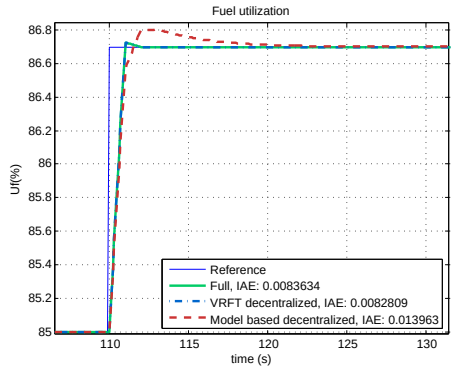

(e) U_f

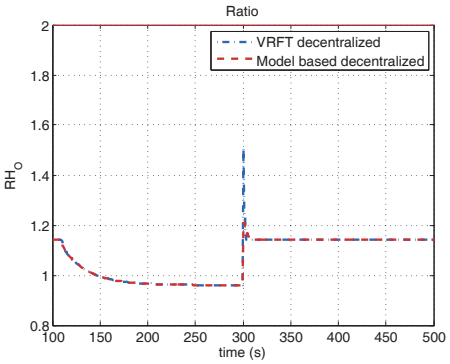

(f) $R_{\mathrm{H\_O}}$

Figure 6.5: Response of the system to a change in reference for both loops.

For the reference tracking, the complete controller is better tracking reference changes for V_r than the simple controller and the decentralized controller, but thanks to a slightly worse response for the U_f and again a more aggressive consumption of the oxygen supply. The simple controller performs also better that the decentralized controller, but at the expense of increased oxygen consumption. The selected pairing used by both the simple and the complete control is the "obvious": the U_f controlled by the fuel input flow and the V_r controlled by the the oxygen flow. It could be that, using the input fuel flow, the control of V_r could improved since the gain from the fuel flow to the output voltage is larger than the gain from the oxygen flow. But since the fuel utilization if not affected by the oxygen flow, this choice is not possible with the control topology used here.

It is important to note that, even if the control of both variables is acceptable, with the PI controllers is not possible to achieve the desired closed-loop transfer function, given the non-linearity produced by the relationship between the pressure of the gases and the output voltage (given by the Nernst equation). A different structure of the controller may lead to a better result, but without any more knowledge of the plant, but the data from the open loop experiment, it is difficult to select and appropriate structure. This issue still remains an open question for future research, not only for the VRFT approach, but for any data-driven approach.

This results confirm the use of decentralized controller for the SOFC plant, as proposed by Sendjaja and Kariwala (2011), and also, the use of VRFT in the tuning of the parameters, has been also shown to be technically sound, if U_f can be measured on line, or at least estimated.

7. Application to a pH neutralization process

The pH neutralization is an important process in different industry applications (for example in pharmaceuticals, as pointed out in Henson and Seborg (1994)) and fundamental in the prevention of corrosion, in the protection of ecological wild life and human welfare, as for example in wastewater treatment plants and water recycle (Hadjiski et al., 2002). However, it is already well known that the strong non-linearity of this neutralization is one of the points that makes this process a difficult task to control (Ali, 2001) and, at the same time, it is one of the reasons why this process have been so widely studied.

From the control area, several strategies has been applied to control this process. In Ali (2001), an auto-tuning PI Control is compared to other PI-like over a large range of set points in order to have good performance with minimum re-tuning of the controller. In Hadjiski et al. (2002), Neural Networks are applied in several different tasks as plant emulation, estimation of disturbances, gain scheduling control, feedforward control, etc. Fuzzy Control has also been applied for the pH neutralization process, for example in Fuente et al. (2002) an auxiliary fuzzy variable indicates in which of three defined different gain region is the process, and with this information a fuzzy control is implemented to control a real experimental plant, in Kwok and Wang (1993) a fuzzy PD controller is implemented along with an integrator and a Smith predictor. An example of Adaptive Control applied to the pH neutralization process can be found in Henson and Seborg (1994) in which a non-linear adaptive controller is used in conjunction with a parameter observer; and also a non-linear Model Predictive Controller is used based on non-linear prediction on the form of Wiener-Laguerre model (Mahmoodi et al., 2009).

The aim of this chapter is to find a restricted order linear controller bypassing the modeling of this highly non-linear pH plant, based only on data taken from the process itself using a Two Degrees of Freedom Controller with feedforward action which parameters are found by applying the VRFT framework. The VRFT is a straightforward, easy to implement methodology that was also found to be very flexible when trying to extend the original controller topology. Since only a simple batch of data is needed, the number of experiments on the real plant can be reduced and one set of data can be used to compute different control structures.

The methodology firstly is tested in simulation using a non-linear model of the process. In a second stage, after the data has been collected from an experiment in the plant, the controller is implemented and tested in a bench process. It was found that using this data-driven approach it was obtained good results even in the presence of noise in the measurement. The controller was implemented using Simulink and the OPC toolbox.

7.1. Introduction to pH

The pH is an intensive property that is related with the activity of effective concentration of hydrogen ions (H^+). If this activity is expressed as using molality as $a_{m,H^+} = m_{H^+}\gamma_{m,H^+}/m^\circ$, the expression for pH is (Lunelli and Scagnolari, 2009):

$$\text{pH} = -\log\left(a_{m,H^+}\right) = -\log\left(\frac{m_{H^+}\gamma_{m,H^+}}{m^\circ}\right) \tag{7.1}$$

m_{H^+} is the molality (mol kg^-) of hydrogen ions, m° is the unit molality and γ_{m,H^+} is the activity coefficient on the molality basis, a dimensionless unit. Within the extensive literature on the subject, a representative example on the modeling of the process is given in Gustafsson et al. (1995); Gustafsson and Waller (1992) where the reaction invariants are used in the modeling of the acid-base system using the Bronsted's acid-base concepts:

- An acid can release a proton (H^+).
- A base can accept a proton.
- An ampholyte can both release and accept a proton.

In this section, the model presented in Gustafsson et al. (1995) is followed. It is known that when a reaction is in equilibrium, the degree of completion of the reaction varies greatly, but there is one expression that is constant for a reaction in equilibrium at a given temperature (Day and Underwod, 1989). For a general reaction

$$a\text{A(ac)} + b\text{B(ac)} \rightleftharpoons c\text{C(ac)} + d\text{D(ac)}$$

The equilibrium constant K is

$$\frac{a_{\text{C}}^c a_{\text{D}}^d}{a_{\text{A}}^a a_{\text{D}}^d} = K \tag{7.2}$$

a is the activity, which can be seen as an *effective concentration*. The activity can be approximated using the molar concentration (c_i) multiply by an activity factor f_i for the species i:

$$a_i = f_i c_i \tag{7.3}$$

In a dissociation reaction (i.e. when a strong acid or a strong base is dissociated in water), the equilibrium constant is called dissociation constant.

In a solution, a general acid HA release a proton

$$\text{HA} = \text{A}^- + \text{H}^+$$

which in turn reacts with the water

$$\text{H}_2\text{O} + \text{H}^+ = \text{H}_3\text{O}^+$$

Thus, the overall reaction is

$$\text{HA} + \text{H}_2\text{O} = \text{H}_3\text{O}^+ + \text{A}^- \tag{7.4}$$

And the corresponding thermodynamics dissociation constant is:

$$\begin{aligned} k_{\text{acid}} &= \frac{a_{\mathrm{H_3O^+}} a_{\mathrm{A^-}}}{a_{\mathrm{HA}}} \\ &= \frac{c_{\mathrm{H_3O^+}} c_{\mathrm{A^-}}}{c_{\mathrm{HA}}} \frac{f_{\mathrm{H_3O^+}} f_{\mathrm{A^-}}}{f_{\mathrm{HA}}} \end{aligned} \tag{7.5}$$

In turn a base B reacts in water as:

$$\mathrm{B} + \mathrm{H_2O} = \mathrm{HB^+} + \mathrm{OH^-} \tag{7.6}$$

And the corresponding dissociation constant is given by

$$\begin{aligned} k_{\text{base}} &= \frac{a_{\mathrm{HB^+}} a_{\mathrm{OH^-}}}{a_{\mathrm{B}}} \\ &= \frac{c_{\mathrm{HB^+}} c_{\mathrm{OH^-}}}{c_{\mathrm{B}}} \frac{f_{\mathrm{HB^+}} f_{\mathrm{OH^-}}}{f_{\mathrm{B}}} \end{aligned} \tag{7.7}$$

As it can be seen, water can accept and release a proton:

$$2\mathrm{H_2O} = \mathrm{H_3O^+} + \mathrm{OH^-} \tag{7.8}$$

And its dissociation constant is $k_{\text{w}} = a_{\mathrm{H_3O^+}} a_{\mathrm{OH^-}}$.

Using these constants, it is possible to model fast acid-base reactions in water (Gustafsson et al., 1995). The material balance is

$$\sum a_{ki} n_i = bk \tag{7.9}$$

where a_{ki} is the index of the element number k in the species i, n_i expresses the amount of i and b_k is the total amount of elements number k. The electroneutrality condition is:

$$\sum v_i n_i = 0 \tag{7.10}$$

where v_i expresses the charge. If only monoprotic acids and bases are taken into account, the solution of a number of acids and bases give:

$$0 = \frac{k_w}{c_{\mathrm{H_3O^+}}} - c_{\mathrm{H_3O^+}} + \sum_i c_{a,i} \frac{k_{a,i}}{c_{\mathrm{H_3O^+}} + k_{a,i}} - \sum_j c_{b,j} \frac{c_{\mathrm{H_3O^+}}}{c_{\mathrm{H_3O^+}} + k_{b,j}} \tag{7.11}$$

where $k_{a,i}$ and $c_{a,i}$ are the dissociation constant and the concentration of acids i and $k_{b,j}$ and $c_{b,j}$ are the dissociation constant and concentration of base j. This equation was derived supposing $f_i = 1$. Then (7.11) is solved for $c_{\mathrm{H_3O^+}}$ and the value of pH is found using:

$$\mathrm{pH} = -\log\left(c_{\mathrm{H_3O^+}}\right) \tag{7.12}$$

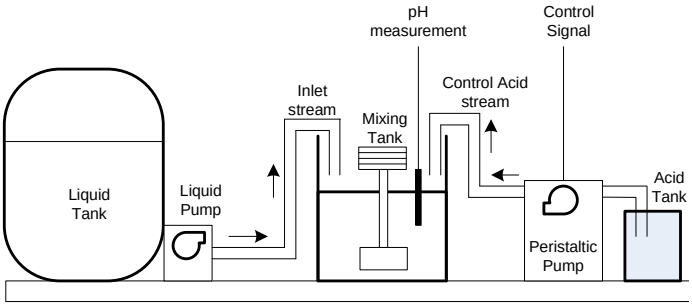

Figure 7.1: Diagram of the pH neutralization plant.

7.2. In simulation and In situ application

The process under study in this section is the neutralization of an aqueous solution with Hydrochloric Acid (HCl) in a Continuously Stirred Tank Reactor (CSTR). The experimental setup (Tadeo et al., 2000) is shown in Fig. 7.1. The aim of this experiment is to show how the VRFT methodology, and in particular the alternative 2doF structure, can be applied in a real world plant. It consists of a CSTR where a liquid of variable pH is mixed with a solution of high concentration of HCl. The liquid in the mixing tank overflows (outlet not shown), so the volume of liquid in the tank can be considered constant. The control variable u is the flow rate of the titrating stream. The output variable y is the hydrogen ion concentration in the effluent stream. The control was implemented using the OPC toolbox in MATLAB/Simulink, using discrete-time filters.

Due to the nonlinear dependence of the pH value on the amount of titrated agent, the process will be inherently nonlinear. Moreover, variations of the buffering effects could make the process time-varying. Both effects make the process difficult to control with classical process control techniques (Henson and Seborg, 1994).

The methodology was firstly tested in simulation using the following model Fuente et al. (2002), where the acid is hydrochloric acid (HCl) and the inlet is an aqueous solution of sodium acetate (CH_3COONa):

$$\begin{aligned} -x_A + 10^{-\mathrm{pH}} - 10^{\mathrm{pH}-14} + \tfrac{x_S}{1+10^{\mathrm{pKS}+\mathrm{pH}-14}} &= 0 \\ V\frac{dX_A}{dt} &= F_A C_A - (F_A + F_S)x_A \\ V\frac{dx_S}{dt} &= F_S C_S - (F_A + F_S)x_S \\ \tau\frac{dpH^*}{dt} &= pH - pH^* \end{aligned} \tag{7.13}$$

where $x_A = \left[\mathrm{Cl}^-\right]$ and $x_S = \left[\mathrm{Na}^+\right]$ are the negative and positive ion concentration within the tank respectively. F_A is the control acid stream flowrate, F_S is the inlet stream flowrate, C_S is the concentration of sodium acetate in the inlet stream, C_A the acid concentration in

Parameter	Value
F_A	1.8×10^{-4} l/s
C_A	0.0708 mol/l
F_S	7.73×10^{-3} l/s
C_S	0.0308 mol/l
V	0.63 l
τ	0.0127 s
x_A	1.63×10^{-3} mol/l
x_S	30.1×10^{-3} mol/l

Table 7.1: Steady-state operating point of the nonlinear pH model.

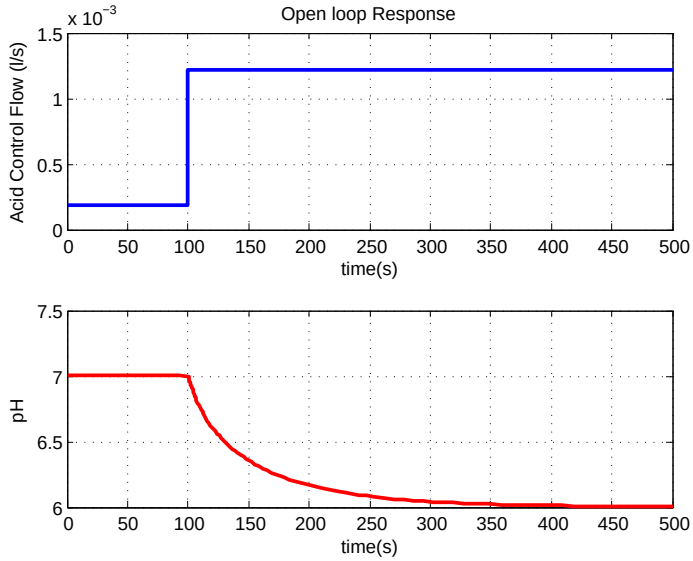

Figure 7.2: Simulation of the open loop response of the pH non-linear model.

the control acid stream, the measured pH is pH* which is supposed to have a constant time τ, pKS $= -10\log_{10} k_S$, with dissociation constants $k_w = 10^{-14}\text{mol}^2$

The purpose of the simulated model is to test the control methodology before implementing it in the real plant. The nonlinear model was excited with a pseudo random binary signal in open-loop, and the controller was calculated as pointed out in section 3.1. The target closed-loop response is set as a first order transfer function with time constant equal to 25s (which represents a settling time of approximately 150s). This value was chosen based on the prior knowledge of the settling time of the process, whose open-loop response is presented in Fig. 7.2 for completeness. The settling time of the sensitivity function was chosen as 40s. The filters W_M and W_S were set to 1.

For a linear-in-the-parameter structure for C_s, with 2 parameters in the numerator (θ_s =[-0.01237, 0.01012]), denominator $1 - z^{-1}$; and a fully parameterized C_{ff} with 3 parameters

in the numerator ($\theta_{ffnum} = [0.0001073, -0.007215, 0.006206]$) and 3 in the denominator (θ_{ffden}= [1, 0.1178, -0.6]); using a sampling time of $T_s = 1.5s$ and a saturation at the input of the controller to avoid negative values of the acid stream flowrate, the result of the controlled system is as shown in Fig. 7.3. The control signal is the sum of both the C_{ff} and the C_s outputs in Fig. 7.3b. Fig. 7.3c shows the e_0 signal.

As can be seen in Fig. 7.3a, the controller achieved a response that is close to the target one (1), but the reference tracking controller presents a non-minimum phase zero which produces an undesired oscillatory response. On the other hand, the C_s controller has a good response to (2) a step disturbance in the inlet concentration, (3) a step disturbance in the acid concentration, (4) a step disturbance in the inlet flowrate and (5) a unit step disturbance at the output of the plant. In cases (1) to (4), the disturbance step is equal to 100% of the value of the steady-state operating point given in Table 7.1. The data used for this experiment is presented in Fig. 7.4a.

Taking advantage of the separation between the controllers, new data can be found that is specifically addressed to finding the reference tracking controller without changing the feedback controller. This new data takes into account the fact that the pH cannot rise as as fast as it decreases, since it is impossible to actively withdraw acid from the tank. For this reason, the new data was made to change more slowly, and is presented in Fig. 7.4b. With this new data, the C_{ff} controller's parameters became ($\theta_{ffnum} = [-0.001424, 0.000263, 0.0009215]$) and ($\theta_{ffden}$= [1, -0.6911, -0.07566]). With this controller, the results are as given in Fig 7.5. As can be seen, the response is better without altering the disturbance rejection. The reference tracking was set faster than the open-loop response, since being able to take the system to a new operating point faster than in open loop (compared with Fig. 7.2) is an important control task, which can be achieved independently from the disturbance rejection thanks to the extra degree of freedom of the controller. Another test where only changes in the reference signal are applied is presented in Fig. 7.6. The error signal depicted in Fig. 7.6b shows that there is an error in the transient part of the response due to imperfections in the structure of the C_{ff} controller, but the C_s controller is able to cope with these errors. The saturation of the input signal is responsible for the overshoot at the end of the test, when a higher pH is required.

For the real plant in Fig. 7.7, instead of sodium acetate, the inlet is just liquid water with variable pH around the value of 7. In order to have the data with the correct magnitude, a new batch of data was taken using the OPC server connected to the system. This input to the real plant cannot be a pseudo random signal as in the simulation example, because the peristaltic pump cannot act as quickly as the data changes. The data collected from the experiment in open-loop is shown in Fig. 7.8: a series of step changes were performed in order to excite the plant at several operation points. It is well known that, from a system identification point of view, the data has to be persistently exciting (Ljung, 1999), which is why, under the physical restriction of the plant, this input signal was selected. When performing the optimization, the data was filtered with a third order Butterworth filter with cut frequency equal to 0.25 times the sampling frequency. It was decided to have a settling time of 150s in the response between the reference and the output. The C_s controller is a PI-like controller with two parameters in the numerator.

The resulting closed-loop, using the same sampling period of the simulation, is shown in

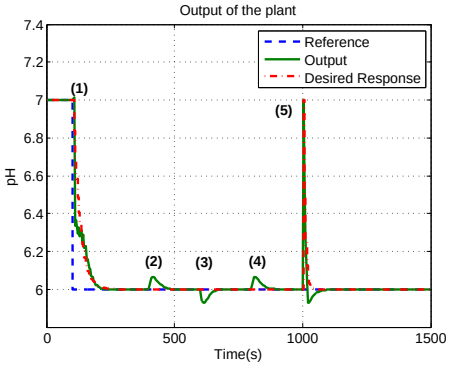

(a) Output

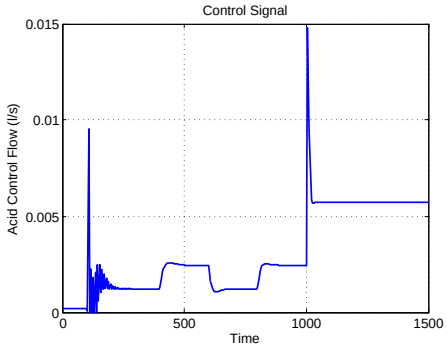

(b) Control Signal

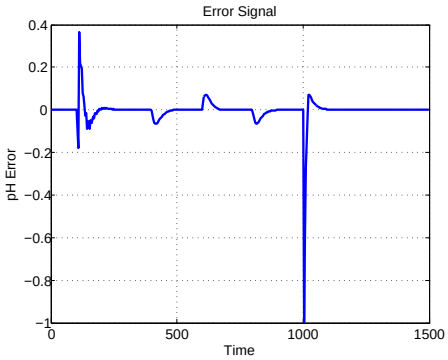

(c) e_0 signal

Figure 7.3: Results from simulation of the nonlinear model, controlled with the VRFT controllers with several disturbances.

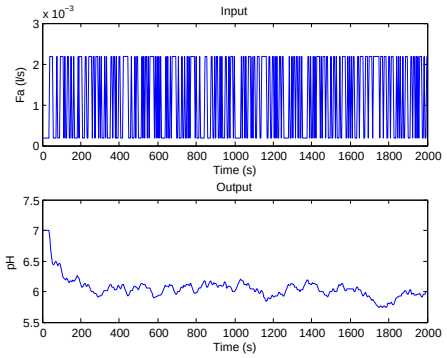

(a) First data

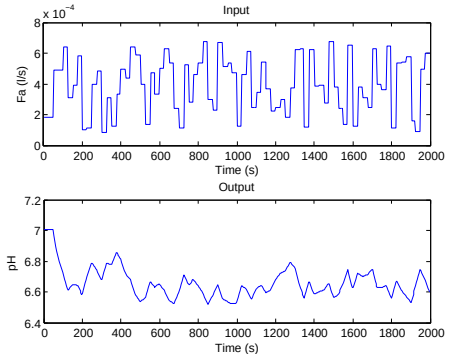

(b) Second data

Figure 7.4: Open-loop data used to find the VRFT controllers for the simulated case.

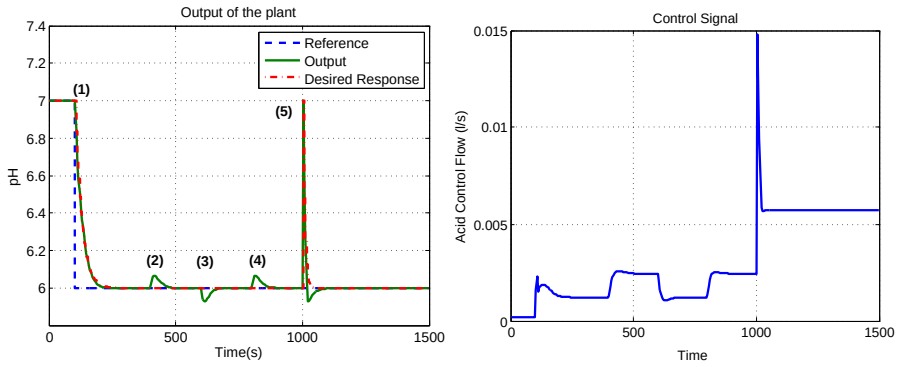

(a) Output **(b)** Control signal

Figure 7.5: Change in the C_{ff} controller to avoid oscillation in the value of pH.

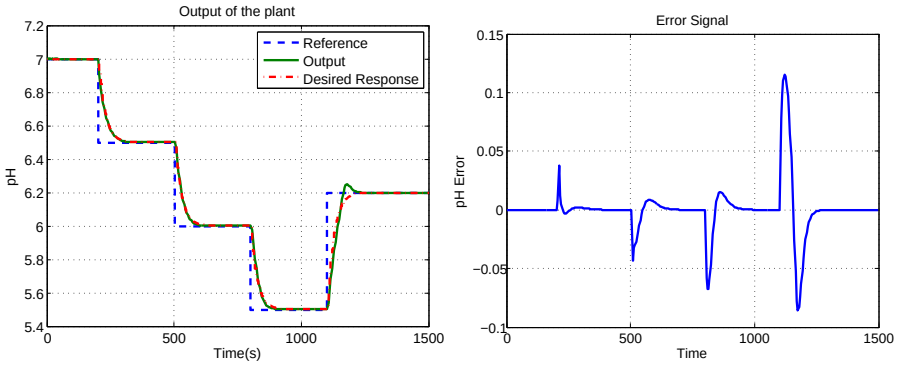

(a) Response to step changes in the reference **(b)** Error signal

Figure 7.6: Test of the C_{ff} controller for different changes in the reference signal.

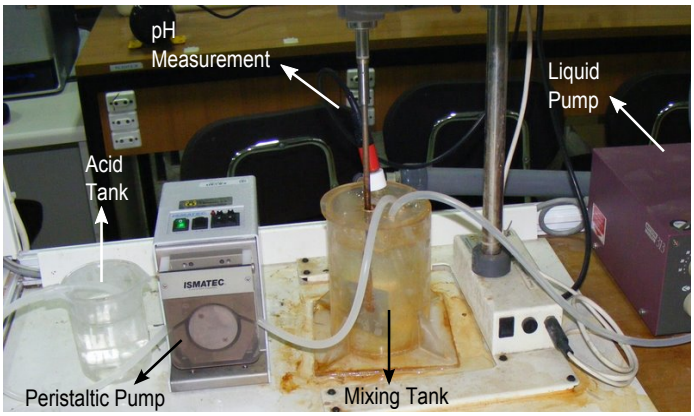

Figure 7.7: Photograph of the real pH neutralization process.

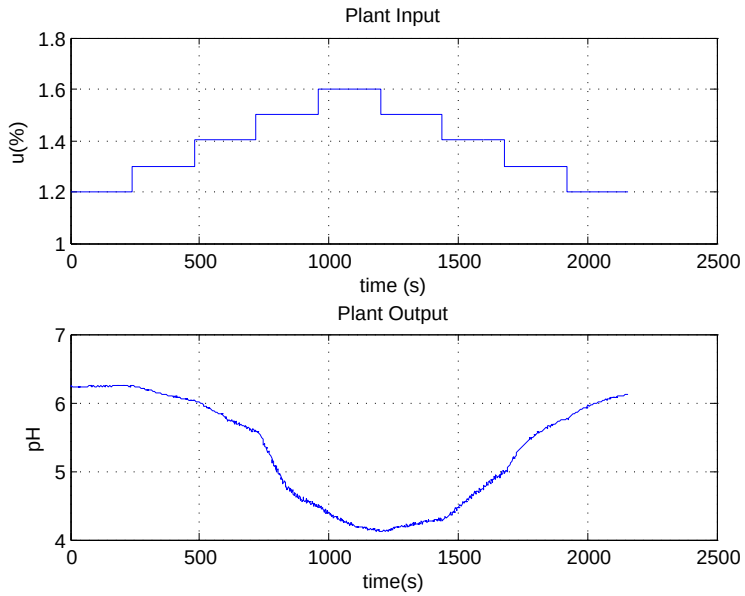

Figure 7.8: Batch of data used for computing the controllers in the real plant.

Fig. 7.9. In Fig. 7.9 b), $u_{OpPoint}$ is the output of the controller at the operation point, $u_{C_{ff}}$ is the output of the feedforward controller, u_{C_s} is the output of the feedback controller and u is the sum of all the control signals. It was decided not to go beyond a pH of 6.24 to ensure good functioning of the peristaltic pump. It was found that for higher values of the pH, the response is not as desired, but the constant time is very similar. For lower values of pH, the response is very close to the desired one (neglecting the noise). The controllers and the design transfer functions are as follows:

$$\begin{aligned} M(z) &= \frac{0.05824z^{-1}}{1-0.9418z^{-1}} \\ S(z) &= \frac{1-z^{-1}}{1-0.9418z^{-1}} \\ C_s(z) &= \frac{-0.8235+0.8201z^{-1}}{1-z^{-1}} \\ C_{ff}(z) &= \frac{\begin{pmatrix} -0.04827+0.1322z^{-1} \\ -0.1203z^{-2}+0.03634z^{-3} \end{pmatrix}}{\begin{pmatrix} 1-2.871z^{-1}+2.748z^{-2} \\ -0.8762z^{-3}-0.0001912z^{-4} \end{pmatrix}} \end{aligned} \tag{7.14}$$

It was found that the sampling time for this application was too high: the controller had poles very near to the unit circle and therefore, having the exact values of the parameters became critical. Because of this, it was decided to use a larger sampling time ($T_s = 4.5s$). The same batch of data was used, but decimated by 3. In this case, the response is as given in Fig. 7.10.

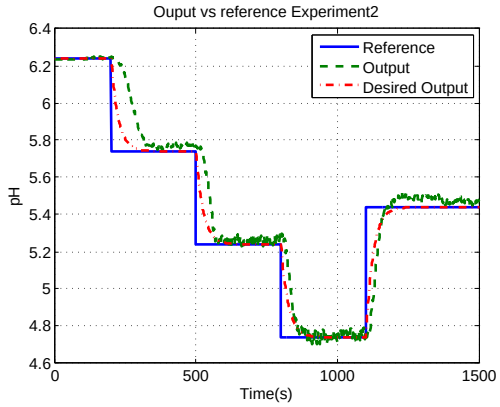

(a) Output

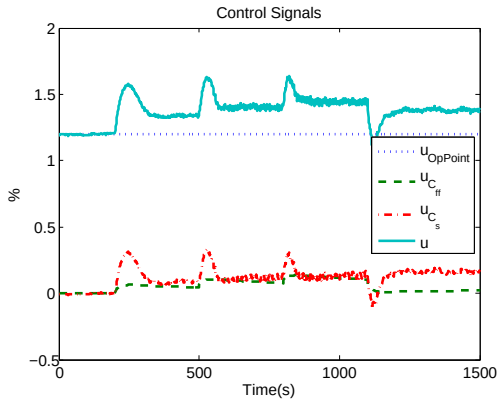

(b) Control Signals

Figure 7.9: Response of the closed-loop system in the real plant.

As expected, the system degrades its performance, but the controller poles are farther from the unit circle. With this sampling time, an oscillatory behavior affects the response, and overshoot is found as the reference changes. A lower sampling frequency made the entire system oscillate. The response of the system with $T_s = 7.5s$ is shown in Fig. 7.11. It is interesting to note that both the C_s and the C_{ff} controllers have the same output when a stationary point is reached. This is because the C_{ff} controller is not equal to the ideal C_{ff0}, as expected, given the non-linearity of the plant. That is why the C_s controller has to act when the reference is changed. Otherwise, the output of the feedback controller should only act when a disturbance is present in the plant. Also, it is interesting to note that the controller is able to cope with the noise in the measurements and keep the system near the reference points.

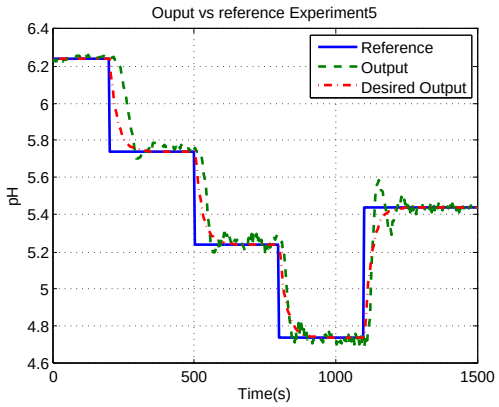

(a) Output

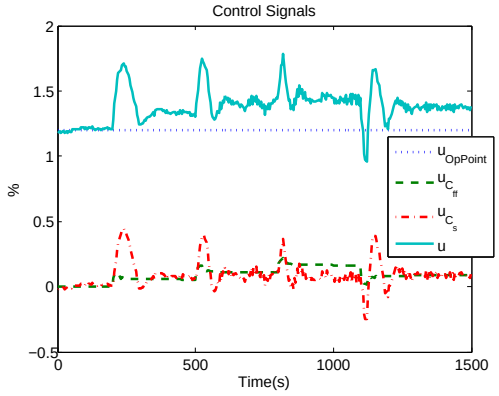

(b) Control Signals

Figure 7.10: Response of the closed-loop system in the real plant for a sampling time of $T_s = 4.5s$.

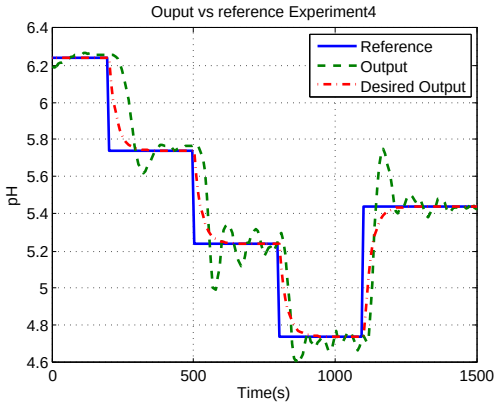

Figure 7.11: Response of the system with a sampling period of $T_s = 7.5$. The response became oscillatory.

Conclusions and Bibliography

Conclusions

In this work new extensions to the Virtual Reference Feedback Tuning method has been proposed for the two-degrees of freedom, feedforward control, multiple-inputs multiple-outputs and internal model control cases. Even more, these extensions have been applied to several complex plants.

First, an alternative two degrees of freedom controller was proposed. The main characteristic of the alternative topology is that, it is possible to separate the design of the reference tracking controller and the disturbance rejection controller. In fact it was found that the filters needed to approximate the control problem using the identification problem are exactly the same that in the original two degrees of freedom structure. That is, no extra computational effort is needed to find the parameters of this alternative controller.

It was found that for the two degrees of freedom PI controller, a constraint has to be added to the optimization in order to guarantee zero stationary error. If this constraint is not introduced, different integral action from the feedback signal and from the reference produce an undesirable offset in the closed-loop response. It is widely known that PI controllers are the most used controllers in industry. Thus, having a condition that allows the VRFT to re-tune an existing PI controller is a desirable characteristic.

Sometimes, information from the disturbances of the plant is available. Adding a feedforward path from the measurable disturbances can improve the performance of a two degrees of freedom controller. This was also accomplished with the VRFT. In this case the computation of the virtual reference has to taken into account the effect of the disturbance. To guarantee independence between the signals, it was proposed to use an arbitrary "fictitious" signal instead of a virtual signal. The approach is valid if all the equations of the optimization are written accordingly with this condition.

The MIMO case has been also investigated. It is proposed to use a non-linear optimization to find the pairing of the loops at the same time that the controller tuning. This approach is useful for the decentralized case where the pairing is not decided a priori. Also a full strategy (with decoupling controllers) was presented. The difference of this approach is that it is not necessary to use the same closed-loop specification for each loop. This is very useful for the case where the constant times of each loop are different and a single specification would not fit for all loops.

The stability of the system is addressed using an internal model control approach. Using this structure, a robust test is proposed in order to guarantee stability. When the IMC controller is computed, an instrumental model of the plant is included in closed-loop. This instrumental model is the best approximation of the model plant, from the computed controller. It was found that by having the control divided in two blocks (the IMC controller and the instru-

mental model), a better performance is accomplished than in the case of a single block for control. The reason of this is that, more information can be included in the control algorithm and also, a less restrictive parameterization of the IMC controller can be used. Also, using the IMC structure, integral action is guarantee even if it is not explicitly defined during the optimization.

The application of all these extension to complex system is the other contribution of this thesis. The most studied case is the application to wastewater treatment plants. The dynamics of this kind of plants are not difficult to control by themselves, but the effect of the disturbance on the process is very important. It was decided to apply the methodology to the control of the Benchmark Simulation Model 1. This benchmark is important among the wastewater community and allows the control researches to have a common platform to compare different control strategies. The models used within the benchmark have high complexity and are not directly suitable for model-based control. That is the reason why, the VRFT was considered as a good option to control the plant.

The first attempts to control the plant were made under rather unrealistic conditions. The data that was used for the tuning of the control parameters did not contained the effect of the influent variation and was noise-free. Under this conditions, the two degrees of freedom and the feedforward approaches were tested and compared with other techniques. The problem of the influent and noise were considered when a full MIMO approach were implemented for the BSM1. To remove the effect of the influent from the system two different batch of data were needed. One of them contains only the effect of the disturbances on the plant while the other contains also the effect of the manipulated variables in an open-loop experiment. Several configuration were considered to check the effect on the quality indexes of the plant. It was confirmed that, an auxiliary carbon source is needed to stimulate the nitrogen removal from the effluent.

Along with a better water treatment, it is necessary to find more environmental friendly sources of energy. In this sense, the VRFT was applied to the control of solid oxide fuel cells. The advantage of SOFC is that they are able to work, not only with hydrogen, but also with other fuels as methane. Even using fossil fuels, fuel cells pollute less than the counterpart combustion-based generators. The controlled variables were the voltage and the fuel utilization, manipulating the fuel and the air flow rate. It was found that VRFT was able to find a better tuning in a decentralized approach than other method that also uses discrete time PI controllers.

The two degrees of freedom controller was applied to a real laboratory bench plant. The process is a pH neutralization in a laboratory in Universidad de Valladolid in Valladolid, Spain. The method was applied with real data taken directly from an open loop experiment. The sensor noise was first filtered and then used to compute discrete time controllers. These controllers were implemented in Simulink using the OPC toolbox for the communication with the pumps. It was only possible to set the pH value of the solution under pH=0.7, since the "basic" solution was simply water. However, it was found that the VRFT was able to control correctly the reference tracking. The dynamics are different depending if the pH is increasing or decreasing. If the setpoint makes the pH to increase from its current operating point, the only control action that can be taken is to stop the pumps, and wait until the pH reaches

the desired value to start regulating. In the other case, if the pH have to be decreased, the dynamics are fast. The same controller needs to coupe with both cases. A test was performed to check how the sampling time affects the control system for this particular plant. Heavy oscillations were found where the sampling time was not chosen adequately.

Future Research In the last decade, the number of research publication on data-driven control has been increasing. In fact, in the 18th IFAC World Congress, a pair of sessions dedicated to data-driven control has been programmed. However there are still some aspects that need to be considered.

Guidelines to choose the correct number of parameters for the controllers are still needed. In the cases where the ideal controller is in the set of possible controllers, the optimization will converge to the ideal one, even without any filtering. However the performance of the method is heavily degraded if the controller is not the ideal. One may thing that allowing enough freedom to the controller (free tuning parameters in both numerator and denominator with a rather high number of parameters) the performance of the controller would improve incrementing the number of parameters. However, empirical test made during this work have shown that, for non-linear, continuous time plants, this is not always the case. An increase in the complexity of the controller have to be done in the right direction, according to the characteristics of the plant. But it is necessary to obtain this information only from the data itself. In one of the works derived from this thesis, a test was proposed for the alternative two degrees of freedom case. However, it is desirable to have a more general guidelines that can help to select the controller before any optimization is done.

The problem of stability has been addressed here in the form of a robustness test, while in other publications has been addressed as a nonlinear constraint during the optimization, by an approximation of the $\mathscr{H}_\infty$ norm. However these approaches are just approximation that either need an infinity number of samples or is just an approximation in the frequency domain given the available data. A more robust method is desirable to guarantee the best performance with enough robustness.

Data-driven control is connected with direct adaptive control, in the sense that the tuning of the parameters is computed directly from data. It may be interesting to check if the virtual reference concept can be translated to the adaptive world. In, fact, it could be interesting to try to find a way to apply it to a predictive control scheme, in order to cope with the constraints in signals values.

It is clear that data-driven control opens the door to a new set of paradigm, where the information is considered to be implicit in the data and the final objective is to take the most from it as directly as possible.

However, it has been learned trough all the extensions and applications that has been done in this work, that a deep knowledge of the system to control is always fundamental for any control engineer. The fact that no model is needed to find this controller should not be confused with a blind test over the plant. Knowledge should never be traded for easiness, whatever control methodology have been decided to apply.

Bibliography

J. Alex, L. Benedetti, J. Copp, K.V. Gernaey, U. Jeppsson, I. Nopens, M.-N. Pons, L. Rieger, C. Rosen, J.P. Steyer, P. Vanrolleghem and S. Winkler (2008). Benchmark Simulation Model no. 1 (BSM1). Technical report, Industrial Electrical Engineering and Automation, Lund University, Lund, Sweeden.

E. Ali (2001). pH control using PI control algorithms with automatic tuning method. *Chemical Engineering Research and Design*, 79(5):611 – 620. doi:10.1205/02638760152424398.

K. J. Aström and T. Hägglund (2001). The future of PID control. *Control Engineering Practice*, 9(11):1163 – 1175. doi:10.1016/S0967-0661(01)00062-4.

Frano Barbir (2005). *PEM Fuel Cells: Theory and Practice*. Sustainable World. Elsevier Academic Press, London, 1 edition. ISBN 978-0-12-078142-3.

Roberto Bove (2007). Solid oxide fuel cells: principles, designs and state-of-the-art in industries. In Suddhasatwa Basu, editor, *Recent Trends in Fuel Cell Science and Technology*, chapter 11, pages 267–285. Anamaya Publishers, New Delhi, India. ISBN 0-387-35537-5.

F. De Bruyne (2003). Iterative feedback tuning for internal model controllers. *Control Engineering Practice*, 11(9):1043 – 1048. doi:10.1016/S0967-0661(02)00237-X.

L. Campestrini, D. Eckhard, M. Gevers and A.S. Bazanella (2011). Virtual reference feedback tuning for non-minimum phase plants. *Automatica*, In Press, Corrected Proof:–. doi:10.1016/j.automatica.2011.04.002.

M. C. Campi, A. Lecchini and S. M. Savaresi (2002). Virtual reference feedback tuning: a direct method for the design of feedback controllers. *Automatica*, 38(8):1337 – 1346. doi:10.1016/S0005-1098(02)00032-8.

M.C. Campi and S.M. Savaresi (2006). Direct nonlinear control design: the virtual reference feedback tuning (VRFT) approach. *Automatic Control, IEEE Transactions on*, 51(1):14 – 27. doi:10.1109/TAC.2005.861689.

L. Carrette, K. A. Friedrich and U. Stimming (2001). Fuel cells - fundamentals and applications. *Fuel Cells*, 1(1):5–39. doi:10.1002/1615-6854(200105)1:1<5::AID-FUCE5>3.0.CO;2-G.

John B Copp (2002). *The COST Simulation Benchmark: Description and Simulator Manual*. Office for Official Publications of the European Communities, Luxemburg.

R. A. Day and A. L. Underwod (1989). *Química analítica cuantitativa*. Prentice Hall, Mexico, 5th edition. ISBN 968-880-124-0.

M.W. Ellis, M.R. Von Spakovsky and D.J. Nelson (2001). Fuel cell systems: efficient, flexible energy conversion for the 21st century. *Proceedings of the IEEE*, 89(12):1808 –1818. doi:10.1109/5.975914.

Alicia Esparza, Antonio Sala and Pedro Albertos (2011). Neural networks in virtual reference tuning. *Engineering Applications of Artificial Intelligence*, 24(6):983 – 995. doi:10.1016/j.engappai.2011.04.003.

Mahshid Fardadi, Fabian Mueller and Faryar Jabbari (2010). Feedback control of solid oxide fuel cell spatial temperature variation. *Journal of Power Sources*, 195(13):4222 – 4233. doi:10.1016/j.jpowsour.2009.12.111.

Simone Formentin, Matteo Corno, Sergio M. Savaresi and Luigi Del Re (2010). Virtual reference feedback tuning of internal model controllers. In *Decision and Control (CDC), 2010 49th IEEE Conference on*, pages 5542 –5547. Atlanta, GA, USA. doi:10.1109/CDC.2010.5718027.

M.J. Fuente, C. Robles, O. Casado and R. Tadeo (2002). Fuzzy control of a neutralization process. In *Control Applications, 2002. Proceedings of the 2002 International Conference on*, volume 2, pages 1032–1037 vol.2. doi:10.1109/CCA.2002.1038746.

Krist V. Gernaey, Mark C. M. van Loosdrecht, Mogens Henze, Morten Lind and Sten B. Jørgensen (2004). Activated sludge wastewater treatment plant modelling and simulation: state of the art. *Environmental Modelling & Software*, 19(9):763 – 783. doi:10.1016/j.envsoft.2003.03.005.

Michel Gevers (2002). A decade of progress in iterative process control design: from theory to practice. *Journal of Process Control*, 12(4):519 – 531. doi:10.1016/S0959-1524(01)00018-X.

G.O. Guardabassi and S.M. Savaresi (1997). Data-based simultaneous design of composite feedback-feedforward controllers: a virtual input direct design approach. In *4th European Control Conference (ECC97)*. Brussels, Belgium.

G.O. Guardabassi and S.M. Savaresi (2000). Virtual reference direct design method: an off-line approach to data-based control system design. *Automatic Control, IEEE Transactions on*, 45(5):954–959. doi:10.1109/9.855559.

Svante Gunnarsson, Vincent Collignon and Olivier Rousseaux (2003). Tuning of a decoupling controller for a 2x2 system using iterative feedback tuning. *Control Engineering Practice*, 11(9):1035 – 1041. doi:10.1016/S0967-0661(02)00288-5.

Tore K. Gustafsson, Bengt O. Skrifvars, Katarina V. Sandstroem and Kurt V. Waller (1995). Modeling of pH for control. *Industrial & Engineering Chemistry Research*, 34(3):820–847. doi:10.1021/ie00042a014.

Tore K. Gustafsson and Kurt V. Waller (1992). Nonlinear and adaptive control of pH. *Industrial & Engineering Chemistry Research*, 31(12):2681–2693. doi:10.1021/ie00012a009.

M. Hadjiski, K. Boshnakov and M. Galibova (2002). Neural networks based control of pH neutralization plant. In *Intelligent Systems, 2002. Proceedings. 2002 First International IEEE Symposium*, volume 2, pages 7–12 vol.2. doi:10.1109/IS.2002.1042565.

K. Hamamoto, T. Fukuda and T. Sugie (2003). Iterative feedback tuning of controllers for a two-mass-spring system with friction. *Control Engineering Practice*, 11(9):1061 – 1068. doi:10.1016/S0967-0661(02)00229-0.

Klaus Hassmann (2001). SOFC power plants, the Siemens-Westinghouse approach. *Fuel Cells*, 1(1):78–84. doi:10.1002/1615-6854(200105)1:1<78::AID-FUCE78>3.0.CO;2-Q.

M.A. Henson and D.E. Seborg (1994). Adaptive nonlinear control of a pH neutralization process. *Control Systems Technology, IEEE Transactions on*, 2(3):169–182. doi:10.1109/87.317975.

Mogens Henze, Willi Gujer, Takashi Mino and Mark van Loosdrecht (2002). *Activated sludge models ASM1, ASM2, ASM2d and ASM3*. Scientific and Technical Report. IWA Publishing, London, UK, 1 edition. ISBN 978-1900222242.

Mogens Henze, Poul Harremoës, Erik Arvin and Jes la Cour Jansen (1997). *Wastewater treatment, biological and chemical process*. Enviromental Engineering. Springer Verlag, New York, USA., 2 edition. ISBN 3-540-62702-2. Series Editors: Förstner, U. and Murphy, Robert J. and Rulkens, W.H.

H. Hjalmarsson, M. Gevers, S. Gunnarsson and O. Lequin (1998). Iterative feedback tuning: theory and applications. *Control Systems Magazine, IEEE*, 18(4):26–41. doi:10.1109/37.710876.

Hakan Hjalmarsson (1999). Efficient tuning of linear multivariable controllers using iterative feedback tuning. *International Journal of Adaptive Control and Signal Processing*, 13(7):553–572. doi:10.1002/(SICI)1099-1115(199911)13:7<553::AID-ACS572>3.0.CO;2-B.

P. Ingildsen, U. Jeppsson and G. Olsson (2002). Dissolved oxygen controller based on online measurements of ammonium combining feed-forward and feedback. *Water Science and Technology*, 45(4-5):453–460.

Ulf Jeppsson (1996). *Modelling Aspects of Wastewater Treatment Processes*. Ph.D. thesis, Department of Industrial Electrical Engineering and Automation (IEA) Lund Institute of Technology (LTH), Department of Industrial Electrical Engineering and Automation (IEA) Lund Institute of Technology (LTH) P.O. Box 118 S-221 00 Lund Sweden.

Osamu Kaneko, Tomohiko Muroyama and Takao Fujii (2006). A synthesis of linear canonical controllers based on the direct use of the experimental data. In *SICE-ICASE International Joint Conference*, pages 4038 –4041. Bexco, Busan, Korea. doi:10.1109/SICE.2006.315004.

Osamu Kaneko, Shotaro Soma and Takao Fujii (2005). A Fictitious Reference Iterative Tuning (FRIT) in the two-degree of freedom control scheme and its application to closed loop system identification. In *Proceedings of the 16th IFAC World Congress*. Prague, Czech Republic. doi:10.3182/20050703-6-CZ-1902.00105.

Yasuki Kansha, Yoshihiro Hashimoto and Min-Sen Chiu (2008). New results on VRFT design of PID controller. *Chemical Engineering Research and Design*, 86(8):925 – 931. doi:10.1016/j.cherd.2008.02.018.

A. Karimi, L. Miskovic and D. Bonvin (2003). Iterative correlation-based controller tuning with application to a magnetic suspension system. *Control Engineering Practice*, 11(9):1069 – 1078. doi:10.1016/S0967-0661(02)00191-0.

Alireza Karimi, Mark Butcher and Roland Longchamp (2005). Model-free precompensator and feedforward tuning based on the correlation approach. In *Joint IEEE CDC and ECC*. Seville, Spain. doi:10.1109/CDC.2005.1582870.

Alireza Karimi, Klaske van Heusden and Dominique Bonvin (2007). Noniterative data-driven controller tuning using the correlationapproach. In *European Control Conference*. Kos Island, Greece.

S. Kissling, Ph. Blanc, P. Myszkorowski and I. Vaclavik (2009). Application of iterative feedback tuning (IFT) to speed and position control of a servo drive. *Control Engineering Practice*, 17(7):834 – 840. doi:10.1016/j.conengprac.2009.02.005.

D.P. Kwok and P. Wang (1993). Enhanced fuzzy control of pH neutralization processes. In *Industrial Electronics, Control, and Instrumentation, 1993. Proceedings of the IECON '93., International Conference on*, pages 285–288 vol.1. doi:10.1109/IECON.1993.339066.

James Larminie and Andrew Dicks (2003). *Fuel Cell Systems Explained*. Wiley, West Sussex, England, second edition. ISBN 0-470-84857-X.

A. Lecchini, M.C. Campi and S.M. Savaresi (2001). Sensitivity shaping via virtual reference feedback tuning. In *Decision and Control, 2001. Proceedings of the 40th IEEE Conference on*, volume 1, pages 750–755 vol.1. doi:10.1109/.2001.980196.

A. Lecchini, M.C. Campi and S.M. Savaressi (2002). Virtual reference feedback tuning for two degree of freedom controllers. *International Journal of Adaptative control and Signal Processing*, 16(5):355–371. doi:10.1002/acs.711.

Olivier Lequin, Michel Gevers, Magnus Mossberg, Emmanuel Bosmans and Lionel Triest (2003). Iterative feedback tuning of PID parameters: comparison with classical tuning rules. *Control Engineering Practice*, 11(9):1023 – 1033. doi:10.1016/S0967-0661(02)00303-9.

J. Löfberg (2004). YALMIP: A Toolbox for Modeling and Optimization in MATLAB. In *Proceedings of the CACSD Conference*. Taipei, Taiwan.

L. Ljung (1999). *System Identification, Theory for the User*. Prentice Hall, second edition. ISBN 0136566952.

Bruno Lunelli and Francesco Scagnolari (2009). pH Basics. *Journal of Chemical Education*, 86(2):246. doi:10.1021/ed086p246.

Sanaz Mahmoodi, Javad Poshtan, Mohammad Reza Jahed-Motlagh and Allahyar Montazeri (2009). Nonlinear model predictive control of a pH neutralization process based on Wiener-Laguerre model. *Chemical Engineering Journal*, 146(3):328 – 337. doi:10.1016/j.cej.2008.06.010.

L. Miskovic, A. Karimi, D. Bonvin and M. Gevers (2005). Correlation-based tuning of linear multivariable decoupling controllers. In *Decision and Control, 2005 and 2005 European Control Conference. CDC-ECC '05. 44th IEEE Conference on*, pages 7144 – 7149. doi:10.1109/CDC.2005.1583313.

L. Miskovic, A. Karimi, D. Bonvin and M. Gevers (2007). Correlation-based tuning of decoupling multivariable controllers. *Automatica*, 43(9):1481 – 1494. doi:10.1016/j.automatica.2007.02.006.

M. Miyachi, O. Kaneko and T. Fujii (2006). A parameter identification based on tuning of a controller with one-shot experimental data. In *SICE-ICASE, 2006. International Joint Conference*, pages 5619–5623. doi:10.1109/SICE.2006.315100.

J Monod (1949). The growth of bacterial cultures. *Annual Review of Microbiology*, 3(1):371–394. doi:10.1146/annurev.mi.03.100149.002103.

M. Morari and E. Zafirou (1989). *Robust Process Control*. Prentice-Hall International, New Jersey. ISBN 9780137821532.

AKM M. Murshed, Biao Huang and K. Nandakumar (2007). Control relevant modeling of planer solid oxide fuel cell system. *Journal of Power Sources*, 163(2):830 – 845. doi:10.1016/j.jpowsour.2006.09.080.

AKM M. Murshed, Biao Huang and K. Nandakumar (2010). Estimation and control of solid oxide fuel cell system. *Computers & Chemical Engineering*, 34(1):96 – 111. doi:10.1016/j.compchemeng.2009.06.018.

M. Nakamoto (2004). An application of the virtual reference feedback tuning for a MIMO process. In *SICE 2004 Annual Conference*, volume 3, pages 2208–2213. Sapporo, Japan.

M. Nakano, N. Matsunaga, H. Okajima and S. Kawaji (2009). Tuning of feedback type decoupling controller for two-dimensional thermal process based on VRFT method. In *ICCAS-SICE, 2009*, pages 925 –930.

H. Nehrir, Caisheng Wang and S.R. Shaw (2006). Fuel cells: promising devices for distributed generation. *Power and Energy Magazine, IEEE*, 4(1):47 – 53. doi:10.1109/MPAE.2006.1578531.

Gustaf Olsson and Bob Newell (1999). *Wastewater Treatment Systems. Modelling, Diagnosis and Control*. IWA Publishing, London, UK, 1 edition. ISBN 1-900222-15-9.

J. Padullés, G. W. Ault and J. R. McDonald (2000). An integrated SOFC plant dynamic model for power systems simulation. *Journal of Power Sources*, 86(1-2):495 – 500. doi: 10.1016/S0378-7753(99)00430-9.

R.E. Precup, I. Mosincat, M.B. Radac, S. Preitl, S. Kilyeni, E.M. Petriu and C.A. Dragos (2010). Experiments in iterative feedback tuning for level control of three-tank system. In *MELECON 2010 - 2010 15th IEEE Mediterranean Electrotechnical Conference*, pages 564 –569. doi:10.1109/MELCON.2010.5476027.

Stefan Preitl and Radu-Emil Precup (2006). Iterative feedback tuning in fuzzy control systems. theory and applications. *Acta Polytechnica Hungarica*, 3(3):81–96.

F. Previdi, T. Schauer, S.M. Savaresi and K.J. Hunt (2004). Data-driven control design for neuroprotheses: a virtual reference feedback tuning (VRFT) approach. *Control Systems Technology, IEEE Transactions on*, 12(1):176–182. doi:10.1109/TCST.2003.821967.

Fabio Previdi, Maurizio Ferrarin, Sergio M. Savaresi and Sergio Bittanti (2005). Closed-loop control of FES supported standing up and sitting down using virtual reference feedback tuning. *Control Engineering Practice*, 13(9):1173 – 1182. doi:10.1016/j.conengprac.2004.10.007.

Jay Tawee Pukrushpan (2003). *Modelling and control of Fuel Cell Systems and Fuel Processors*. Ph.D. thesis, Department of Mechanical Engineering. The University of Michigan, Ann Arbor, Michigan.

Antonio Sala and Alicia Esparza (2005a). Extensions to "virtual reference feedback tuning: A direct method for the design of feedback, controllers". *Automatica*, 41(8):1473 – 1476. doi:10.1016/j.automatica.2005.02.008.

Antonio Sala and Alicia Esparza (2005b). Virtual reference feedback tuning in restricted complexity controllers design of non-minimum phase systems. In *Proc. 16th IFAC world congress*, pages 235 – 340. Prague, Czech Republic.

K. Sedghisigarchi and A. Feliachi (2004a). Dynamic and transient analysis of power distribution systems with fuel cells-part i: fuel-cell dynamic model. *Energy Conversion, IEEE Transactions on*, 19(2):423 – 428. doi:10.1109/TEC.2004.827039.

K. Sedghisigarchi and A. Feliachi (2004b). Dynamic and transient analysis of power distribution systems with fuel cells-part ii: control and stability enhancement. *Energy Conversion, IEEE Transactions on*, 19(2):429 – 434. doi:10.1109/TEC.2003.822302.

K. Sedghisigarchi and A. Feliachi (2006). Impact of fuel cells on load-frequency control in power distribution systems. *Energy Conversion, IEEE Transactions on*, 21(1):250 – 256. doi:10.1109/TEC.2005.847962.

A.Y. Sendjaja and V. Kariwala (2011). Decentralized control of solid oxide fuel cells. *Industrial Informatics, IEEE Transactions on*, 7(2):163 –170. doi:10.1109/TII.2010.2097601.

S. Skogestad and I. Postlethwaite (2007). *Multivariable Feedback Control, Analysis and Design*. John Wiley & Sons, West Sussex, England, second edition. ISBN 13-978-0-470-01167-6.

J. F. Sturm (1999). Using SeDuMi 1.02, a MATLAB toolbox for optimization over symmetric cones. *Optimization Methods and Software*, 11-12:625–653.

F. Tadeo, O.P. Lopez and T. Alvarez (2000). Control of neutralization processes by robust loop shaping. *Control Systems Technology, IEEE Transactions on*, 8(2):236–246. doi: 10.1109/87.826795.

I. Takács, G.G. Patry and D. Nolasco (1991). A dynamic model of the clarification-thickening process. *Water Research*, 25(10):1263 – 1271. doi:10.1016/0043-1354(91)90066-Y.

Arthur Tay, Weng Khuen Ho, Jiewen Deng and Boon Keng Lok (2006). Control of photoresist film thickness: Iterative feedback tuning approach. *Computers and Chemical Engineering*, 30(3):572 – 579. doi:10.1016/j.compchemeng.2005.10.004.

K. van Heusden, A. Karimi, D. Bonvin, A. den Hamer and M. Steinbuch (2010). Non-iterative data-driven controller tuning with guaranteed stability: Application to direct-drive pick-and-place robot. In *Control Applications (CCA), 2010 IEEE International Conference on*, pages 1005 –1010. Yokohama, Japan. doi:10.1109/CCA.2010.5611118.

Klaske van Heusden, Alireza Karimi and Dominique Bonvin (2011). Data-driven model reference control with asymptotically guaranteed stability. *International Journal of Adaptive Control and Signal Processing*, 25(4):331–351. doi:10.1002/acs.1212.

Peter A. Vanrolleghem, Ulf Jeppsson, Jacob Carstensen, Bengt Carlsson and Gustaf Olsson (1996). Integration of wastewater treatment plant design and operation - a systematic approach using cost functions. *Water Science and Technology*, 34(3-4):159–171. doi: 10.1016/0273-1223(96)00568-9.

R. Vilanova, R. Katebi and V. Alfaro (2009). Multi-loop PI-based control strategies for the Activated Sludge Process. In *Emerging Technologies and Factory Automation, 2009. ETFA 2009. IEEE International Conference on*. doi:10.1109/ETFA.2009.5347062.

D. Vrecko, N. Hvala and B. Carlsson (2003). Feedforward-feedback control of an activated sludge process: a simulation study. *Water Science and Technology*, 47(12):19–26. doi: 10.3182/20050703-6-CZ-1902.00105.

Xiaorui Wang, Biao Huang and Tongwen Chen (2007). Data-driven predictive control for solid oxide fuel cells. *Journal of Process Control*, 17(2):103 – 114. doi:10.1016/j.jprocont.2006.09.004.

M. C. Williams (2007). Solid oxide fuel cells: Fundamentals to systems. *Fuel Cells*, 7(1):78–85. doi:10.1002/fuce.200500219.

Ma Yong, Peng Yongzhen and Wang Shuying (2005). Feedforward-feedback control of dissolved oxygen concentration in a predenitrification system. *Bioprocess and Biosystems Engineering*, 27(4):223–228. doi:10.1007/s00449-004-0390-0.

Xi Zhang and K.A. Hoo (2007). Control of an integrated biological wastewater treatment system. In *Control Applications, 2007. IEEE International Conference on*, pages 503–508. Singapore. doi:10.1109/CCA.2007.4389281.

Xiongwen Zhang, Jun Li, Guojun Li and Zhenping Feng (2006). Development of a control-oriented model for the solid oxide fuel cell. *Journal of Power Sources*, 160(1):258 – 267. doi:10.1016/j.jpowsour.2006.01.024.